Performance of DS-CDMA over millimetre wave indoor radio channels

van Workum, A.C.J.

Award date:
1994

Faculty of Electrical Engineering

Eindhoven University of Technology

Telecommunications Division

Performance of DS-CDMA over millimetre wave indoor radio channels.

By

A.C.J. van Workum

Graduation thesis.

period : November 1993 till December 1994

Mentor : Ir. P.F.M. Smulders

Supervisor : Prof. Dr. Ir. G. Brussaard

Summary

Wireless communications is a fast growing area in tele communications. The demand for wireless communication exists for voice as well as for data communications. Wireless data communications provides portability to the terminals and easy installation and relocation of the network. This wireless network can be used to transport high speed services, such as those supported by Broadband ISDN (B-ISDN). These services, with bit rates in excess of 2 Mb/s, require a large bandwidth allocation. This large bandwidth can be accomodated in millimetre wave frequency bands from about 25 GHz.

Measurements in frequency bands around 42 GHz and 58 GHz at the Eindhoven University of Technology (EUT) have been performed in order to examine the propagation characteristics [37] and showed the multipath and fading properties of the channel. Spreading of the signal bandwidth is achieved by code division multiple access (CDMA), which multiplying the signal with codes of length N. Having a multipath channel with a multipath spread T_m larger than the chip time of the CDMA signal, results in diversity. This diversity can be resolved by using special receiver techniques.

This report describes the performance of a CDMA spread spectrum system in an indoor radio environment. Besides the diversity, the CDMA system also provides multiple-access capabilities. By using these two features, a wireless network with multiple users and broadband communication can be accomodated.

First the indoor radio environment is described. Then the application of CDMA on this environment is considered. Several code sets can be used for the DS-CDMA system and a selection is made by considering the code set size and the correlation properties. The code set size is considered for the possibilities of a multiple-access system. The correlation properties are considered, because the received signal is afflicted by cross-correlation from all users. The Gold code set offers the best possibilites, with respect to the code set size and the correlation properties.

A special receiver structure can resolve the multipath, by combining the received rays, and thus increasing the performance of CDMA in a radio environment. The receiver commonly used for spread-spectrum in multipath environments is the RAKE receiver, which combines the multipath.

Simulations have been performed for all the signals from the transmitted to the received and

demodulated signal. These simulations use a Gold code set with sequence length of 511, which can be generated by two shift registers. The performance of CDMA in the indoor radio environment is described analytically and has also been implemented in simulations. These simulations are based on a model for the multipath environment, which is on its turn based on the measurements. Parameters describing the measured impulse response can be used in the simulations. These simulations can be used for determining the influence of parameters as the amount of users, the data rate, the signal power level, etc. on the average probability of error or the probability of outage of the system.

Contents

List of acronyms

ACF	Autocorrelation function
B-ISDN	Broadband ISDN
BER	Bit Error Rate
BFSK	Binary frequency-shift keying
BPSK	Binary phase-shift keying
CCF	Cross-correlation function
CDMA	Code Division Multiple Access
CMF	Code-matched filter
DCS-1800	Digital Cellular system
DECT	Digital European Cordless Telecommunications
DFE	Decision feedback equalizer
DPSK	Differential Phase-shift keying
DQPSK	Differential Quadrature Phase Shift Keying
EUT	Eindhoven University of Technology
FDMA	Frequency division multiple access
FM	Frequency Modulation
GSM	Global System for Mobile communication
HDTV	High Definition Television
IC	Interference Cancellation
ISDN	Integrated Services Digital Network
ISI	Intersymbol interference
ITU	International Telecommunication Union
JD	Joint Detection
LAN	local area network
LPI	low probability of intercept
OOK	Sequence on-off keying
PCM	Pulse Code Modulation
PDP	Power Delay Profile
PN	Pseudo-noise
PSK	Phase-shift keying
RMS	Root Mean Square
SIK	Sequence inversion keying
SNR	Signal to noise ratio
TDMA	Time division multiple access

TETRA	Trans-European Trunked Radio
WLAN	Wireless local area network
WLB	Welch lower bound
LOS	Line of sight

Chapter 1 Introduction

The modern workplace requires data communication between a variety of data processing equipment. Such interconnections are achieved through local area networks (LAN's). Wireless LAN (WLAN) is interesting in providing portability to the terminals and in avoiding installation and relocation costs. The demand for wireless communications, i.e. cordless phones, pagers, and cellular telephones, has increased enormously. This need for mobile communications includes voice-services as well as non-voice services. The wireless information networks are evolving around either voice-oriented applications (digital cellular, cordless telephone and wireless PBX) or around data-oriented networks (wireless LAN's and mobile data networks). The same separation is noticed in the major standards, such as several voice-communications based implementations DECT, GSM and DCS-1800, and data-communications based implementations TETRA, IEEE 802.11 and HIPERLAN.

The voice and non-voice services are both supported by the ISDN network, which will probably be widely used in future. The demand for mobility exists for all the applications of ISDN. An interesting issue is thus the connection of wireless networks to the high speed Broadband ISDN (B-ISDN). Existing radio-based networks for wireless indoor communication, as WaveLan [34], use relatively low data rates (2 Mb/s) and cannot provide the high data rates needed to support B-ISDN. "Broadband" services (bit rates > 2 Mb/s) require wideband communication, which can be accommodated in millimetre wave frequency bands from about 25 GHz.

Millimetre wave propagation has favourable properties for indoor radio communication. The radio waves in millimetre frequency bands will remain mostly inside the rooms, due to the highly attenuating walls at these frequencies. The reflection properties prevent interference between systems operating in adjacent rooms. The millimetre waves however might still propagate through windows. To avoid interference from systems outside the building, the frequency band around 60 GHz is of special interest. Frequencies around 60 GHz exhibit high loss due to the attenuation of atmospheric oxygen of about 15 dB/km. Measurements have been performed in frequency bands around 42 GHz and 58 GHz at the Eindhoven University of Technology (EUT) to examine the propagation characteristics at these frequencies [37].

Due to the highly reflective walls, the indoor radio channel exhibits multipath dispersion and fading. A signal-to-noise advantage could be gained by utilising a transmission bandwidth in excess of the actual signal bandwidth. The support of multiple subscribers requires increased transmission bandwidth. A wideband coding technique, based on orthogonal signalling

achieving both the bandwidth expansion and the multiple-access capabilities, is Code Division Multiple Access (CDMA). CDMA is an example of spread spectrum modulation, which is by definition the transmission of digital information with a signal bandwidth W much greater than the information rate R. In CDMA, each user transmits a specific code, which either identifies the user to the central station in a star network, or addresses another user directly in a peer-to-peer network.

A CDMA system using spread spectrum codes is based on the use of a code set. Several code sets exist, distinguished by the correlation properties and the set size. Due to the multipath propagation properties of the channel, the auto and cross-correlation of the codes have a large influence on the maximum amount of simultaneous users. A special receiver structure resolving the multipath by combining the received rays, can be used to increase the performance of CDMA in a multipath environment.

This report describes the use of CDMA in an indoor radio environment and studies the optimal code set, the optimal receiver structure and the performance of this CDMA based system. Chapter 2 describes the properties of the indoor radio environment and gives a statistical model for describing these properties. Chapter 3 describes the principles of CDMA and considers several code sets. Chapter 4 deals with the optimal CDMA receiver. Chapter 5 starts with an analytic presentation of the performance of CDMA in an multipath environment, next the measurements of the propagation properties are considered. The simulations dealing with generating the CDMA signals and simulations determining the performance are in the last part of Chapter 5. Finally, the conclusions and recommendations of this report are given in Chapter 6.

Chapter 2 Indoor radio environment

The indoor radio communication system considered for ISDN services can be represented by a central station connected to the ISDN network. This central station delivers information to and receives information from all the users in a specific room. CDMA is most interesting for upstream traffic, because of its interesting uncoordinated multiple-access possibilities. CDMA used for i.e. communication at data rates in excess of 2 Mbps, requires large spectral space, which is only available in the millimetre wave frequency band. The selection of modulation frequency is restricted by ITU. The reflection and propagation properties in a room are related to the carrier frequency used.

2.1 Global configuration of the system

The indoor radio communication environment can be used for wireless LAN systems, with moving remote stations (further referred to as "remotes") and a steady central station. A wireless LAN supports a limited amount of users in a private indoor area and has no limitations due to interference with users of the same frequency band outside the indoor area. The achievable data rate is an important parameter for the usability of the wireless network, which depends on the channel characteristics and receiving techniques. The wireless network has several advantages above conventional cable systems. The users become mobile without changing the hardware configuration and second, installing a system (or reorganising) is much less expensive and easier. Connections among the central stations, using wireless LAN, are often provided by conventional cables. A schematical presentation of a configuration with mobile stations and a central station is given in figure 2.1.

2.1.1 Using spread spectrum in an indoor radio environment

Spread spectrum communication includes the transmission of a signal with a much wider bandwidth than the message bandwidth. The transmission bandwidth is determined by a spreading function, which is independent of the message and is known to the receiver [6].
The two main spread spectrum techniques are direct-sequence spectrum spreading and frequency hopping. Both techniques spread the transmitted power over a wide frequency band with the result that the power per unit bandwidth (watts per Hertz) is very small. This additional bandwidth can of benefit for rejecting multipath and jamming, which will be explained in Paragraph 3.2. Phase modulation is used in direct-sequence systems and

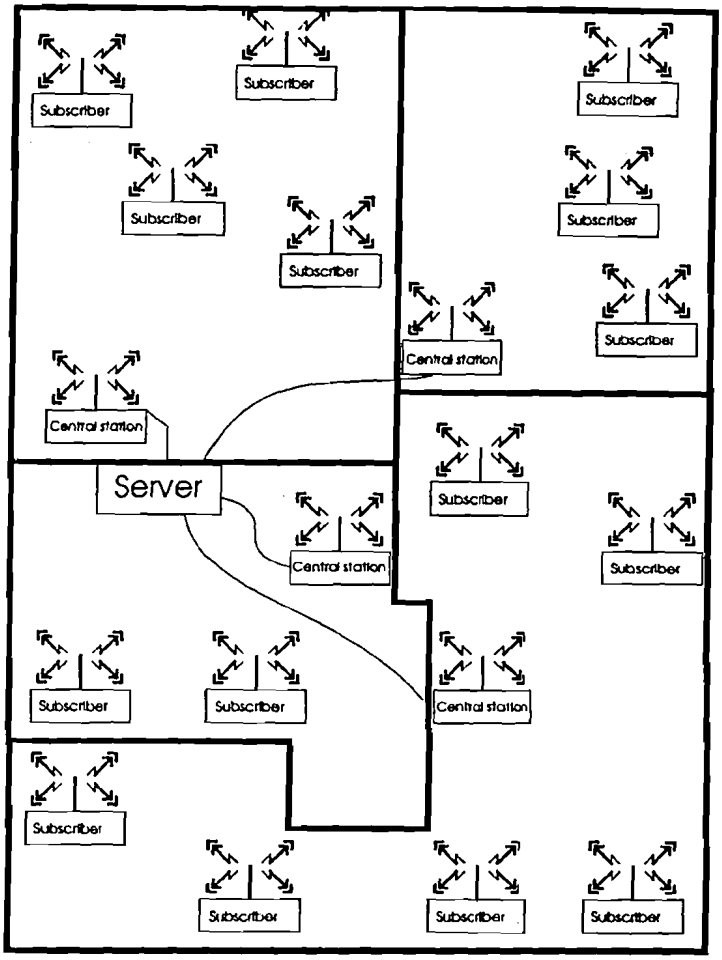

Figure 2.1: Schematical presentation of the system.

frequency modulation in frequency hopping systems. Direct-sequence systems occupy all of the bandwidth at a fraction of the original power level, whereas frequency hopping systems occupy a fraction of the bandwidth for a fraction of the time at the original power level. Direct sequence is superior to frequency hopping, because of its resolving capabilities when exhibiting multipath. However, this increased performance is accompanied by increased receiver complexity.

The receiver compresses the signal into its original narrow band. The key to success in this operation is that the signal meant for a given user is coded with a direct-sequence or frequency hopping pattern that only that user's receiver recognizes. Subcribers from outside the network are prevented from intercepting messages.

CDMA is used to support simultaneous digital communications among a group of relatively uncoordinated users. CDMA can be used in indoor radio communication systems, where each user spread the information signal with a specific code or multiple codes (as in M-ary

signalling), which identifies the user to the central station in a star network. All users are transmitting in the same spectrum and have their own spreading sequence or sequence set. Interference from other users in multiple-access systems or self-interference, which is caused by multipath propagation, can be rejected by the correct receiver structure. The advantages of CDMA therefore enclose the offered privacy, the increased security, the flexibility in supporting multiple services and multiple data rates.

CDMA is interference limited in contrast with Frequency Division Multiple Access (FDMA) and Time Division Multiple Access (TDMA), which are primarily bandwidth limited [9]. In CDMA, any reduction in interference or lowering the Bit Error Rate (BER) requirements converts directly and linearly into an increase in capacity. The capacity of the CDMA system can be increased by making use of diversity techniques. In TDMA and FDMA instead, a predefined amount of channels can be used without interference, but an extra user will be blocked [35].

2.2 Services and their requirements

Broadband services will be provided to customers by broadband ISDN (B-ISDN) and Broadband Local Area Networks (B-LAN). Typical services are multimedia teleconferencing, distribution of high resolution graphics, document distribution and video entertainment. The maximum estimated peak rate for broadband wireless systems is approximately 150 Mb/s for video entertainment using High Definition Television (HDTV) as shown in table 2.1 [8]. The available bandwidth for millimetre waves is large and is promising for supporting the broadband ISDN services in indoor radio systems.

Table 2.1: Broadband wireless services.

Service	Average rate (Mb/s)	Peak rate (Mb/s)	Typical session duration	Max. packet loss rate
Video teleconferencing	0.3 - 2	10	30 min.	10^{-5}
Video telephony	0.06 - 2	6	3 min.	10^{-5}
High volume transfer	1 - 20	1 - 20	10-100Mb	10^{-9}

Service	Average rate (Mb/s)	Peak rate (Mb/s)	Typical session duration	Max. packet loss rate
High resolution image retrieval	4 - 45	4 - 45	8 Mb	10^{-9}
Video entertainment	3 - 32	150	15 min.-2 hrs.	10^{-7}
Manufacturing (Robotics)	0.01 - 3	0.01 - 3	continuous	10^{-9}

The services video conferencing, video telephony and video entertainment have variable bit rates.

2.3 Properties of indoor radio

Information about the propagation characteristics in an indoor radio environment has been obtained at the Telecommunications Division of EUT. Wideband frequency domain measurements of the propagation characteristics in several rooms in different buildings at the university have been done [37]. Also a simulation program for calculating impulse responses in a room configuration has been developed [25].

The electromagnetic waves are reflected by walls. Besides the direct path, several indirect paths exist from transmitter to receiver, due to the reflections against walls, with various received path strength. The transmit time of the signal along any of the various paths is proportional to the length of the path, which is in turn determined by the size of the indoor area and the objects in that area. The indoor radio propagation channel is therefore a multipath channel which exhibits time dispersion and frequency selective fading as will be explained in 2.3.4.

2.3.1 Channel impulse response

The radio waves with sufficiently small wavelengths (millimetre waves) act as rays, running along discrete paths. In the time domain, a single transmitted pulse will be received as a train of successive pulses with varying amplitudes and phases. This spreading of the impulse response (time dispersion) affects the quality of the radio channel. The system performance

will not proportionally improve by increasing the transmit power, since this will not eliminate the self-interference. A more viable solution for combatting multipath losses is to use diversity combining techniques as described in Chapter 4.

An analysis for the discrete received signal in the time domain can be done using the transmitted wave and the channel impulse response. The transmitted wave $x(t)$, with carrier frequency ω_c and a lowpass signal $u(t)$, can be formulated as

$$x(t)=Re[u(t)e^{j(\omega_c t+\phi)}] \ . \tag{2.1}$$

The discrete received signal for the kth user can be formulated as

$$r_k(t)=\sum_l \beta_{lk}(t)e^{j(\omega_c t-\omega_c \tau_{lk}(t)+\phi-\theta_{lk})}u(t-\tau_{lk}(t)) \ . \tag{2.2}$$

β_{lk}, τ_{lk} and θ_{lk} are slowly randomly time-varying functions, due to the motion of people and objects in the environment. The factors β_{lk}, τ_{lk} and θ_{lk} also depend on the positioning of transmitter and receiver in the room.

The complex equivalent low-pass channel impulse response $h_k(\tau;t)$ can be derived by comparing the two preceding equations (2.1) and (2.2), because the received signal of formula (2.2) is the convolution of the transmitted wave (2.1) and the impulse response, thus

$$h_k(\tau;t)=\sum_l \beta_{lk}(t)e^{j\theta_{lk}(t)}\delta(\tau-\tau_{lk}(t)) \ , \tag{2.3}$$

where δ is the Kronecker delta function, β_{lk} is a Rayleigh distributed random ray amplitude of the l th path of the kth user [28], τ_{lk} is a Poisson distributed random path delay and θ_{lk} is the uniformly distributed random path phase including $\omega_c\tau_{lk}$.

The rate of the variations in β_{lk}, τ_{lk} and θ_{lk} is very slow compared to the signal rates that are likely to be considered and the channel is therefore assumed to be quasi-static. Thus, these parameters can be treated as time-invariant random variables. The channel is thus represented by

$$h_k(\tau)=\sum_l \beta_{lk}e^{j\theta_{lk}}\delta(\tau-\tau_{lk}) \ . \tag{2.4}$$

The multiple paths or rays have time-invariant real positive amplitudes β_{lk}, propagation delays τ_{lk} and associated phase shifts θ_{lk}, where l is the path index and k is the user index. These statistically distributed variables will be implemented by the statistical model in paragraph 2.5. This statistical model has been found by measurements described in paragraph 2.4.

The path amplitudes β_{lk} are related to the free space loss, the configuration of the environment and antenna pattern weighting, which is described by the radio equation in free space situation

$$P_r = P \cdot G_t \cdot G_r \cdot \left(\frac{\lambda}{4\pi d}\right)^2 , \tag{2.5}$$

where P_r and P are the received and transmitted power, respectively. G_r and G_t represent the receive and transmit antenna gain, the distance between transmitter and receiver is denoted by d and λ denotes the wavelength of the carrier. In general, the total received power P_r is inversely proportional to d^m, where m denotes the power decay rate. For free-space radio propagation, the power decay rate equals 2, which means the received power decays with inverse of the square of the distance between transmitter and receiver. For indoor radio channels the power decay rate will change with the room as well as the construction material and shows values between 2 and 6. The total sum of the path amplitudes is determined by the radio equation and a Rayleigh distribution has been found for the path amplitudes [28].

This impulse response function is schematically presented in Figure 2.2

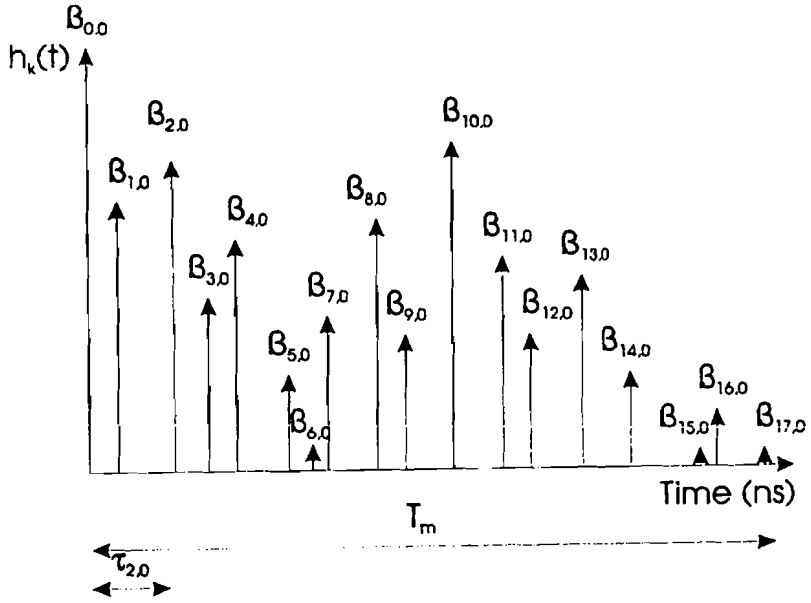

Figure 2.2: Schematical presentation of the impulse reponse.

This impulse response consists of the individual rays, with the first discrete ray corresponding to the line-of-sight ray. The received multipath signals do not show any clustering of the paths [28].

2.3.2 Correlation function of the channel

The autocorrelation of the lowpass impulse response, given in equation (2.3), is given by [23]

$$\phi_h(\tau_1,\tau_2;\Delta t) = \frac{1}{2}\overline{h^*(\tau_1;t)h(\tau_2;t+\Delta t)} = \phi_h(\tau_1;\Delta t)\delta(\tau_1-\tau_2) , \tag{2.6}$$

using the assumption that the phase shift and attenuation of the channel at two different path delays τ_1 and τ_2 are uncorrelated (uncorrelated scattering). The autocorrelation function equals the average power output of the channel as a function of the time delay τ for $\Delta t = 0$. Thus, $\phi_h(\tau)$ is called the multipath intensity profile of the channel. The range of values of τ over which $\phi_h(\tau)$ is non-zero is called the multipath spread of the channel T_m.

The time-variant transfer function $H(f;t)$ can be retrieved from $h(\tau;t)$ by taking the Fourier transform, thus

$$H(f;t) = \int_{-\infty}^{\infty} h(\tau;t)e^{-j2\pi f\tau}d\tau . \tag{2.7}$$

Both $h(\tau;t)$ and $H(f;t)$ are complex-valued zero mean Gaussian random processes in the t variable. Since $H(f;t)$ is the Fourier transform of $h(\tau;t)$, the autocorrelation function $\phi_H(f_1,f_2;\Delta t)$ $(= \phi_H(\Delta f;\Delta t))$ is the Fourier transform of $\phi_h(\tau;\Delta t)$. The assumption of uncorrelated scattering implies that the autocorrelation function of $H(f;t)$ in frequency is only a function of the frequency difference $\Delta f = f_2 - f_1$. Therefore, $\phi_H(\Delta f;\Delta t)$ is called the spaced-frequency spaced-time correlation function of the channel. Having $\Delta t = 0$ results in the transform relationship

$$\phi_H(\Delta f) = \int_{-\infty}^{\infty} \phi_h(\tau)e^{-j2\pi\Delta f\tau}d\tau . \tag{2.8}$$

This relationship is illustrated in Figure 2.3 [23].

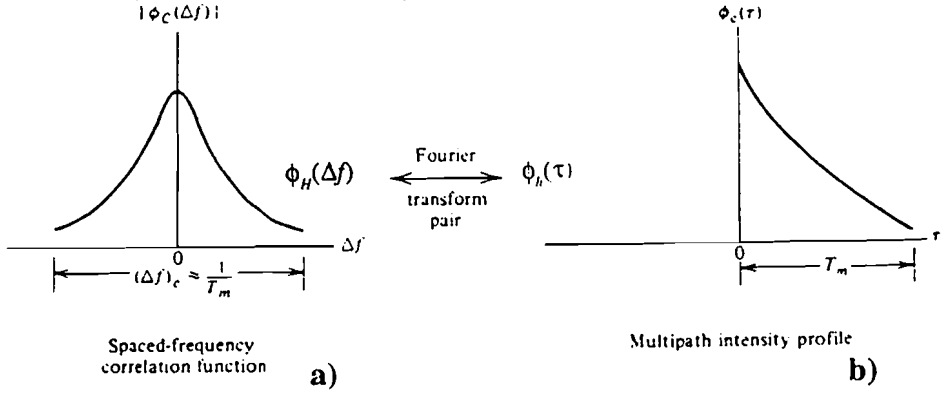

Figure 2.3: Relationship between spaced-frequency correlation function and multipath intensity profile. a) Spaced-frequency correlation function, b) Multipath intensity profile.

2.3.3 Features of fading multipath channels

Time dispersion causes intersymbol interference and multipath fading. This multipath fading results for narrowband signals to flat fading. The multipath fading results for broadband signals to frequency-selective fading, which results in distortion of the signal with less fluctuation.

A transmitted pulse is received by a train of pulses (time spread) as shown in Paragraph 2.3.1. For a large number of paths, the central limit theorem can be applied. This theorem concerns the probability distribution function of a sum of random variables in the limit as the number of terms m in the sum approaches infinity [23]. The sum of statistically independent and identically distributed random variables with finite mean and variance, approaches a Gaussian probability distribution function as $m \to \infty$. Thus, the received signal $r(t)$ can be modeled as a complex-valued Gaussian random process.

As a result of the Fourier transform relationship between $\phi_H(\Delta f)$ and $\phi_h(\tau)$, the coherence bandwidth of the channel can be given as the reciprocal of the multipath spread, thus

$$(\Delta f)_c \approx \frac{1}{T_m} . \tag{2.9}$$

Two signals with a frequency separation larger than $(\Delta f)_c$ are not equally affected by the multipath channel. For a transmitted signal with a bandwidth larger than the coherence bandwidth of the channel, the channel is a frequency-selective channel.

For a signalling interval $T > T_m$, the channel introduces negligible amount of intersymbol interference (ISI). If the bandwidth of the signal is $W \approx 1/T$ and $T < T_m$ shows that

$$W > \frac{1}{T_m} \approx (\Delta f)_c , \tag{2.10}$$

which proves that the channel is frequency-selective. Thus, a transmitted lowpass signal is distorted by this channel, because the frequency content of the signal is subject to different gains and phase shifts across the band. For frequency-nonselective channel, the received signal equals the transmitted signal multiplied by a complex-valued gaussian random process $H(0;t)$ [23]. For a frequency-selective channel, the channel can be characterized by $H(f;t)$.

Proakis [23] showed that the random time variations of the channel parameters (path amplitude, propagation delay and phase shift), result in either constructive or destructive combining of the received multipath signal components. The received signal, given by formula (2.2), possesses these multipath fading characteristics. The amplitude variations in the received signal (signal fading) are due to the time-variant multipath characteristics of the channel. For

slowly fading channels (quasi-static) channels, the signalling interval T (=1/W) satisfies the condition $T<(\Delta t)_c$, which is valid for spread-spectrum communication using millimetre waves. Since the signalling interval is smaller than the coherence time, the channel attenuation and phase shift are fixed for the duration of at least one signalling period.

For spread spectrum communication in an indoor radio environment using millimetre waves, the channel can be characterised as frequency-selective and slowly fading.

2.3.4 Diversity in the system

Supplying to the receiver several replicas of the same information signal transmitted over independently channels, reduces the probability that all the signal components fade simultaneously. Having L independent fading replicas of the signal shows that a probability p that any one signal fade below some critical value decreases to the probability p^L that all L independently fading replicas will fade below the critical value.

Several methods for diversity are known:

- *Frequency diversity:* the signal is transmitted on L carriers, with a separation larger than the coherence bandwidth $(\Delta f)_c$ of the channel.
- *Time diversity:* the signal is transmitted in L different time slots.
- *Antenna diversity:* combining the received signals of multiple receiving antennas.
- *Bandwidth diversity:* diversity can be obtained by using a signal with bandwidth W much greater than the coherence bandwidth $(\Delta f)_c$ of the channel as in paragraph 2.3.2. Such a signal will resolve the multipath components and provide the receiver with several independent fading signal paths. With a time resolution of $1/W$ and a multipath spread of T_m seconds, $T_m W \approx W/(\Delta f)_c$ resolvable signal components exists. The use of a wideband signal may be viewed as a method comparable to frequency diversity of order $L \approx W/(\Delta f)_c$. The optimum receiver will be explained in Chapter 4 and is called a RAKE correlator or a RAKE matched filter with delay taps spaced at $1/W$.
- Other methods of diversity are *angle-of-arrival diversity* or *polarization diversity*.

2.3.5 The normalised received power and RMS delay spread

Instead of deducing the statistics of τ_{lk} and β_{lk}, two simple parameters are mostly used to

describe the features of the channel [26]. These parameters are useful in describing the overall characteristics of the multipath profile.

The total received power normalised on transmitted power for user k as a function of the path amplitudes is given by

$$G_k = \sum_l \beta_{lk}^2 \ . \tag{2.11}$$

The normalised received power is usually less than unity and is useful in estimating the signal-to-noise ratio of a communications system. The received signal power is proportional to the inverse of the distance between transmitter and receiver, raised to a certain power, which is called the power-decay rate. This power-decay rate has been treated in paragraph 2.3.

The power delay profile of a multipath channel is given by

$$p_k(t) = |h_k(t)|^2 = [Im(h_k(t))]^2 + [Re(h_k(t))]^2 \ , \tag{2.12}$$

using

$$h(t) = Re[h(t)] + i \cdot Im[h(t)] \tag{2.13}$$

and the average power delay profile for user k is

$$P_{k,av}(t) \triangleq \frac{1}{N} \sum_{n=1}^{N} \frac{p_{k,n}(t)}{G_k(n)} \ , \tag{2.14}$$

with N the number of measured profiles in the considered room. The average power delay profile is calculated by weighting each individual profile by its own normalized received power.

The Root Mean Square (RMS) delay spread for user k is another useful parameter, given by

$$\sigma_{\tau_k} = \sqrt{\overline{\tau_k^2} - (\overline{\tau_k})^2} \ , \tag{2.15}$$

where

$$\overline{\tau_k^u} = \frac{\sum_l \tau_{lk}^u \beta_{lk}^2}{\sum_l \beta_{lk}^2} \qquad u = 1, 2 \ . \tag{2.16}$$

The RMS delay spread is a measure of the width of the multipath delay profile, which relates to performance degradation caused by interference and indicates the feasable bit rate when no sophisticated techniques as channel equalization are used.

2.3.6 Maximum symbol rate

The maximum achievable symbol rate is bounded by the RMS delay spread of the channel. When the symbol time is comparable or smaller than to the delay spread, the discrete rays along multiple paths belonging to one symbol interval will interfere with rays of neighboring symbol intervals, resulting in irreducible ISI. This ISI is almost independent of the delay profile shape and depends only on the RMS delay spread and limits the maximum transmission rate attainable with a chosen modulation technique. Glance [10] showed that for a system with phase-shift keying (PSK) using cosine roll-off pulses and space diversity with maximal ratio combining, the maximum symbol rate is limited by the relation

$$\frac{\sigma_\tau}{T_{s,\max}} = 0.2 \; . \tag{2.17}$$

The maximum symbol rate without using spread spectrum is 2 Msymbol/s for a RMS delay spread of 100 ns for binary transmission. The bit rate, which is for binary signalling equal to the symbol rate of 2 Msymbol/s is not sufficient for services as shown in paragraph 2.2. An higher bit rate can be achieved by using a modulation technique with a ratio bit per symbol larger than one, such as 4-PSK instead of 2-PSK, thus $r_{b,\max} = 0.2 \cdot k/\sigma$. Besides the modulation technique also using channel equalization or diversity techniques offers increased information rates.

2.3.7 The near-far effect

The near-far effect (additional path loss for longer antenna distances) is a problem in asynchronous multiple-access systems, where the signal from a near transmitter overwhelms that from a far transmitter at the receiver. This effect is severe in CDMA systems, since interference by cross correlation is continuous for non-orthogonal codes. This near-far effect can be reduced by monitoring the received power at either end of the link and controlling power to a maximum quality of reception [39]. This average power control will continuously equalize all user's received powers. Without average power control of each transmitter decreases the performance of direct-sequence CDMA, due to near-far, fading and shadowing effects. Only the slow varying effects can be compensated for by average power control, due to its limitations [35].

Unlike the average power control, which compensate for propagation losses and slow channel fading, a fast power control tries, in addition, to compensate for the fast channel fading. Diaz [5] analyses a model using fast power control with coherent BPSK in a multipath Rayleigh channel using conventional block and coding schemes. When the central station has been a

ble to estimate the received powers from every user, it sends a power command to the mobiles to change their powers appropriately.

A special design of receive and transmit antenna can be used to overcome the near-far problem. Smulders [32] configured a millimetre wave biconical horn at the transmitter as well as at the receiver site to have the same received power everywhere in the picocell. The principle of rejecting the near-far effect is compensation of free space losses by antenna gain. The used biconical horn antennas have an omnidirectional radiation pattern in the azimuth plane and an approximately figure-eight-shaped beam in the elevation plane. Low path loss for near remotes is compensated by a small antenna gain. High path loss for far remotes is combined with large antenna gain. This layout results in a more uniform coverage. This near-far effect compensation is illustrated in Figure 2.4.

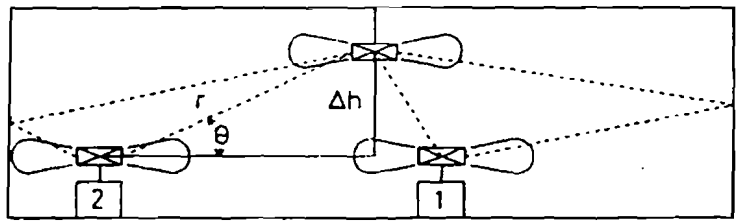

Figure 2.4: Layout of indoor radio network.

2.4 Measurements of power delay profiles

Extensive wide-band measurements of the indoor propagation characteristics at millimetre-wave frequencies have been carried out in eight different indoor areas at the Eindhoven University of Technology [28], [30] to determine impulse resonses of millimetre wave indoor radio links. The measurements have been accomplished with a measurement resolution of 1 ns, which was sufficient to resolve most of the received rays.

2.4.1 Measurement setup

A frequency step sounding technique has been used for the measurements. The complex equivalent low-pass impulse response can be calculated via Inverse Fourier Transform of the frequency data. It is easier for millimetre wave frequencies to measure in the frequency domain instead of measuring in the time domain with very narrow strong pulses. The Doppler effects cannot be measured, because the channel must be fixed during a complete measurement sweep.

The network analyzer is capable of taking a maximum of 801 frequency samples. The aliasing-free range in the time domain is determined by the maximum number of frequency samples N and the measurement bandwidth B as

$$Range = \frac{(N-1)}{B} . \tag{2.18}$$

Finally, the impulse response can be determined by assuming a maximum impulse response excess delay of 400 ns. The measurement bandwidth for measuring the impulse responses is 2 GHz. This results in intervals of $1/B$ = 0.5 ns for the time domain data points. This interval of 0.5 ns limits the detection of rays that are close to each other. This minimum interval can be taken into account when simulating the model of the power delay profile.

The identical biconical horn antennas applied are designed to give near-uniform coverage. The measurements use the line-of-sight (LOS) conditions at 20 randomly chosen positions for the remote in eight areas with different dimensions and dominant wall materials.

2.4.2 Measurements results

The network analyzer is used to determine the S_{21} parameters [16]. The channel transfer function $H(f)$ is related to the S_{21} parameters. After measuring in the frequency band from f_{min}=57 GHz to f_{max}=59 GHz, $H(f)$ can be used to determine the received power P_r normalised to the transmitted power P by [31]

$$\frac{P_r(r)}{P} = \frac{1}{f_{max} - f_{min}} \int_{f_{min}}^{f_{max}} |H(f)|^2 df . \tag{2.19}$$

The average power delay profile shows that for large t (>350ns) all profiles converge to the system noise floor and for t > 50ns the received power in dB decays linearly. For small t (<50ns) the power in the average profiles remain more or less constant, which is caused by compensating of the free-space losses with antenna gain in elevation [32]. A measured average power delay profile in room 008 in the computer centre, with omnidirectional antennas and the basestation at the low position of 1.60 meter, is shown in Figure 2.5 and is conform the model described in paragraph 2.5.

The RMS delay spread has been analytically given in paragraph 2.3.5. Values for the RMS delay spread of 13-98 ns have been found, which would limit the symbol rate to 2 Msymbol/s without channel equalization or diversity techniques.

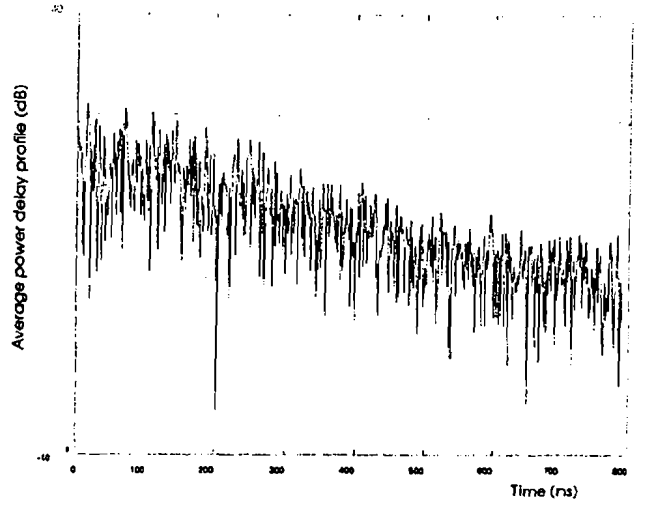

Figure 2.5: Measured average power delay profiles in computer centre room 008.

2.5 Statistical model for power delay profile

The system performance simulations and signal generating simulations, which will be explained in Chapter 5, can be based on the measured impulse responses or on a channel model. Such channel model could be a statistical model or a deterministic model. A statistical model describes the channel characteristics in terms of statistical distributions and moments of the various channel parameters (which are derived from the measurement results). A deterministic model describes the channel properties according to a predefined environment based on geometrical optics, as has been used in [25]. Especially, the statistical model allows to generate numerous individual channel responses to calculate the performance by means of average as well as outage probability.

Therefore, a statistical model has been developed for purpose of simulating the signals and their performance and will be described in following paragraphs.

2.5.1 Distribution of ray amplitudes

At cross sections at a certain excess time, the rays are identically distributed and mutually independent. The rays are mutually independent, because they arrive via independent ray paths. The real as well as the imaginary part of the ray phasor is built up of many random components and are thus according to the Central Limit Theorem (Paragraph 2.3.3) Gaussian distributed. Combining this feature with the fact that the ray phases are uniformly distributed over [-180°,180°] [28] results in a Rayleigh distribution for the path amplitudes. The path amplitudes are at a certain place and time Rayleigh distributed, due to the large amount of

rays, which are added complex and due to the limited resolution used for the received rays, the rays will coincide. The Rayleigh distribution for path amplitudes can be expressed as

$$f(\beta(\tau)) = \frac{2\beta(\tau)}{\overline{\beta^2(\tau)}} e^{-\frac{\beta^2(\tau)}{\overline{\beta^2(\tau)}}} . \tag{2.20}$$

The variance can be given by

$$\theta^2 = \frac{\overline{\beta^2(\tau)}}{2} . \tag{2.21}$$

The cumulative distribution function of the Rayleigh distribution function is given by

$$F(\beta) = 1 - e^{-\frac{\beta^2}{\overline{\beta^2}}} \tag{2.22}$$

for $\beta > 0$.

The function $\overline{\beta^2(\tau)}$, the average power delay profile (averaged over measured profiles), can be determined as an average over the several measurements done in one environment. The power delay profile can be modeled as done by Smulders [28], using the line of sight (LOS) ray followed by a constant level up to $\tau = \tau_1$. The constant level results from $\Delta_{LOS} \triangleq \overline{\beta^2(0)} - \overline{\beta^2(\tau_1)}$, which depends on the configuration of the environment. The part of the power delay profile for τ larger than τ_1 is characterised by a linear decreasing part (in dB value) down to the noise floor. This linear decreasing part can be given by

$$10 * \log(\overline{\beta^2(\tau)}) = 10 * \log(\overline{\beta^2(\tau_1)}) + A * (\tau - \tau_1) \tag{2.23}$$

with A in dB/ns, dependent on reflection coefficients and the dimensions of the environment.

The influence of free space loss, the configuration of the environment and antenna pattern weighting, as considered in paragraph 2.3, can be included in the power level of the LOS ray. Including path and antenna losses in the first path lowers all the received multipath components, resulting in the correct total path gain and power delay profile.

This model of the power delay profile (PDP) is illustrated in Figure 2.6.

2.5.2 Distribution of ray interarrival times

As a result of the measurement configuration (paragraph 2.4), the spacing between detected rays is a multiple of the spacing between datapoints of 0.5 ns. The likelihood of receiving a ray in a certain time span around excess delay τ is independent on τ. Interarrival times of 0.5ns and overlap of rays cannot be detected, due to the limited time domain resolution of the

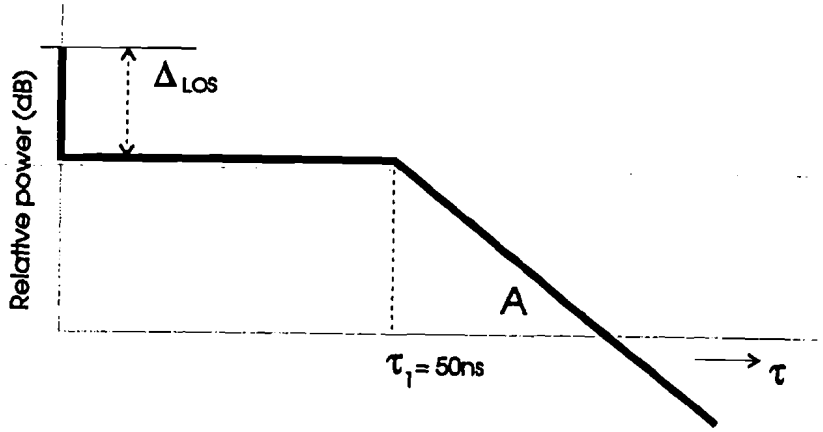

Figure 2.6: Model for the PDP.

measurement setup.

The interarrival times between rays $\Delta\tau$ are statistical distributed as a Poisson process. The statistical distribution found by the measurements, fits to the Poisson process for $\Delta\tau \geq 1.5$ ns, due to the time resolution of the measurements. The probability distribution function for a Poisson process is given by

$$f(\Delta\tau) = \lambda e^{-\lambda\Delta\tau}, \tag{2.24}$$

where λ is known as the mean arrival rate and its reciprocal as the mean time between two consecutive arrivals. The cumulative distribution function of the Rayleigh process is given by

$$F(\Delta\tau) = 1 - e^{-\lambda\Delta\tau}. \tag{2.25}$$

The determination of λ is influenced by the threshold considered for detecting rays.

Chapter 3 Principles of CDMA

CDMA provides resistance to multipath caused by walls, ceilings and other objects between the transmitter and the receiver. In addition CDMA can overlay existing systems, because of the low spectral power density level.

3.1 The CDMA system

CDMA is an application of a spread spectrum technique. Spread spectrum signals have the property that the bandwidth W used for the transmission of digital information is much wider than the information rate at the input of the encoder R in bits per second. The time duration of the chip T_c is the reciprocal of the signal bandwidth W. The duration of an information bit equals $T_b = 1/R$ and can be used to describe the bandwidth expansion [18]

$$B_e = \frac{W}{R} = \frac{T_b}{T_c} . \tag{3.1}$$

This bandwidth expansion is a figure for the number of chips per information bit and the processing gain G_p is this ratio expressed in dB. This bandwidth expansion is used to reduce the interference.

Figure 3.1 shows the block diagram of spread spectrum digital communications systems [23]. The pseudo-random pattern generators are used by the modulators and generate a pseudo-random or pseudo-noise (PN) binary-valued sequence for encoding the datasignal. At the transmitter the PN generator performs the spreading function, i.e. increasing the bandwidth. At the receiver the PN generator performs the despreading function, i.e. decreasing the bandwidth of the received message into its original size.

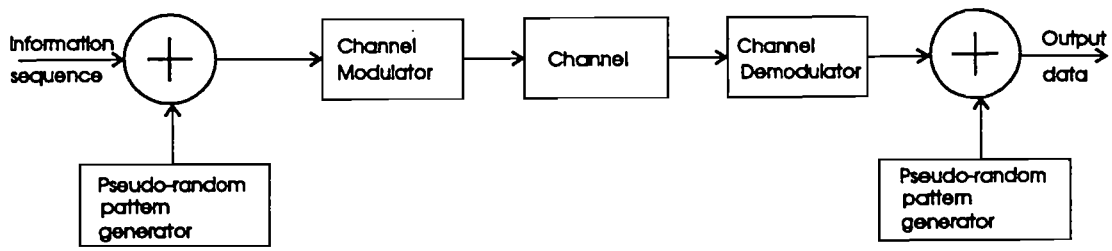

Figure 3.1: Block diagram of spread spectrum digital communication system.

The transmitted information signal travelling through the channel is interfered. The kind of interference, which can be broadband or narrowband and continuous or pulsed, depends on

the environment (e.g. amount of users and other users employing radio frequencies).

3.2 Bandwidth spreading with CDMA

The bandwidth expansion is achieved by multiplying the information signal with a pseudo-random sequence with pseudo noise (PN) properties, thus spreading the spectrum. All spread spectrum users transmit at the same frequency [7]. The spreading feature of CDMA is shown in Figure 3.2 and Figure 3.3 shows the CDMA spectrum allocation [23].

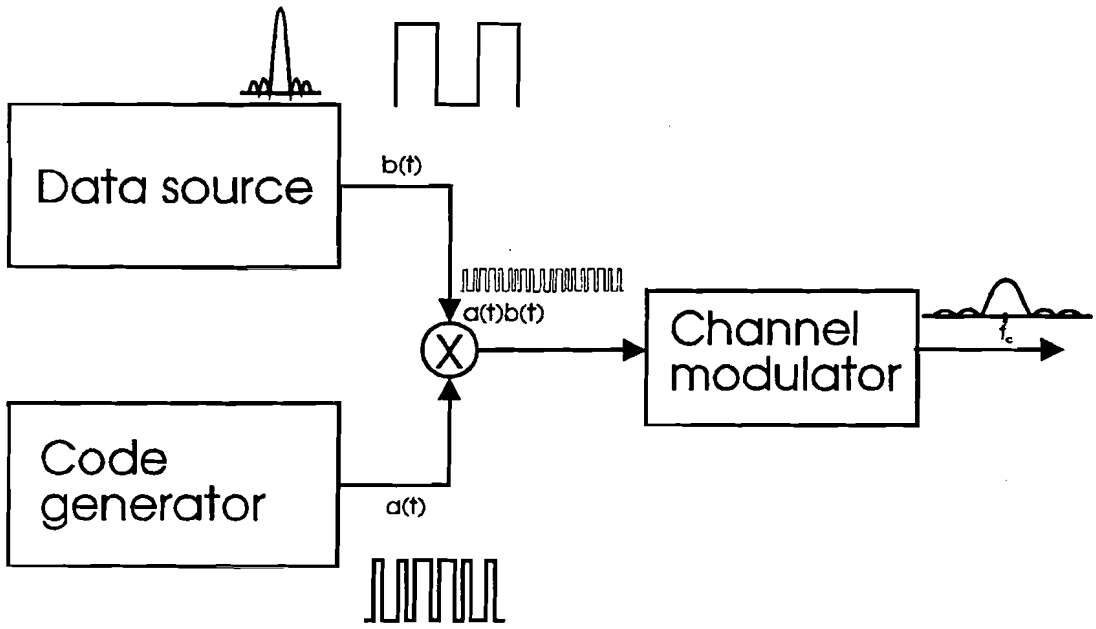

Figure 3.2: DSSS using pseudo random noise chips.

The autocorrelation function (ACF) peak contains the maximum possible signal to noise ratio (*SNR*) [18]. The output *SNR* of the code-matched filter (CMF) correlation peak compared with the input *SNR* prior to matched filtering equals SNR_{out} / SNR_{in}, which is equal to the processing gain

$$G_p = 10^{10} log N \; dB \;, \tag{3.2}$$

with N the code length. The processing gain is effectively the signal power gain over all the interference present in the communication channel, including that from CDMA co-channel self interference.

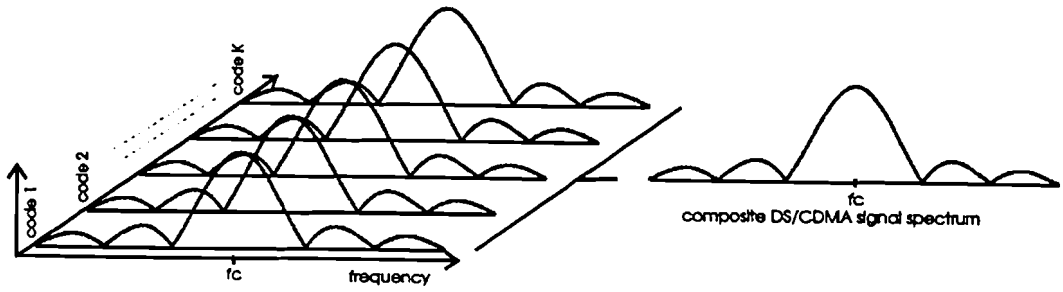

Figure 3.3: DS-CDMA spectrum allocation.

For a spread spectrum signal with bandwidth B_{ss} and a power of P watt, suppose that a jammer tries to jam this signal by transmitting a noise-like signal within the bandwidth B_{ss}, with power of this signal at the receiver of J watt. The spectral power density N_0 of this signal is then [14]

$$N_0 = \frac{J}{B_{ss}} \quad W/Hz \tag{3.3}$$

and the received signal-to-noise ratio, SNR, is

$$SNR = \frac{P}{J} . \tag{3.4}$$

The received signal is returned to its original bandwidth B_D by despreading. The jamming signal, which is not despread, now has a power of $J \cdot B_D / B_{ss}$ watt in the bandwidth B_D. This results in an improvement of SNR with the processing gain G_P [9],

$$SNR = \frac{P}{\frac{J}{B_{ss}} B_D} = \frac{P}{J} \frac{B_{ss}}{B_D} = \frac{P}{J} G_P .$$

An unsophisticated jammer, who does not have access to the subscriber PN coding scheme, thus must increase his transmitter power level by G_p in order to cause the same level of signal degradation as the original jammer power used on an uncoded transmission scheme.

As a result of the spreading of the spectrum the bandwidth efficiency has been decreased, but can be improved by implementing special coding or diversity combining techniques. Also M-ary orthogonal sequences could be used by the users to improve the bandwidth efficiency

significantly compared to binary signalling. The users transmit $\log_2 M$ bits of information/sequence [7], [20]. This choice trades increased bandwidth efficiency for increased signal complexity and is well suited for radio systems using the low frequency and the medium frequency band, because bandwidth is scarce in these bands.

3.3 CDMA in multipath environment

In conventional systems intersymbol interference (ISI) is either avoided by keeping the information rate low and hence reducing the bandwidth to below the minimum coherence bandwidth or corrected by using equaliser techniques [39]. In order not to have ISI, the symbol time must be larger than channel multipath delay spread T_m. Assuming M-ary transmission and an information rate of r_b (bits/sec), we have a limit on r_b due to the multipath spread, $r_b < (\log_2 M)/T_m$. The effects of fading are reduced by using space, frequency or time diversity.

In CDMA systems, an additional approach is necessary, due to the much higher chip rate when compared to the bit rate [39]. With the bandwidth expansion, paths arrive dispersed in time at the receiver at different delays, which may be distinguished in the signal. The extra arriving paths with information is made use of with different diversity strategies such as selection combining, equal gain combining and maximum ratio combining.

To ensure that bandwidth diversity exists and to ensure that there is significant power in the resolved components, the chip period of the direct sequence system must be less than or equal to the differential path delay [36]. The time resolution of the measurements must be less than or equal to the differential path delay to detect the rays. The increased performance with diversity receivers will be accompanied by increased system complexity. Neither of these techniques (selection, equal gain or maximum rate combining) can be used to combat strong multipath. The maximum symbol rate is still limited by the maximum delay spread in the channel. High gain antennas can be used to reduce the delay spread, by reducing the number of paths that are received by the antenna.

3.4 Sequence keying

One property of the autocorrelation function (ACF) is the fact that the correlation function between code-matched filter (CMF) and an inverted representation of the matched sequence results in a negative ACF peak with identical amplitude. The polarity of the ACF peak can

be used as the basis for the data transmission, known as sequence inversion keying (SIK) [18]. The data can be recovered from the output signal from the CMF by having a threshold at zero volt to detect the polarity of the ACF peak.

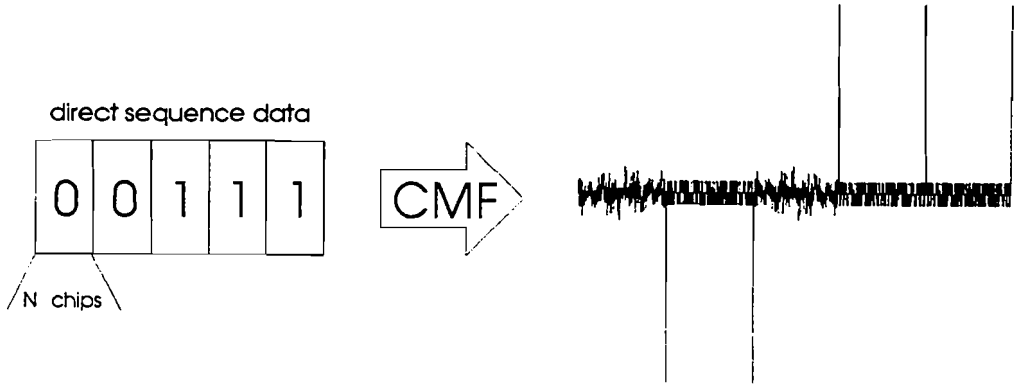

Figure 3.4: Schematical presentation of sequence inversion keying.

The output from the code-matched filter in the transitional areas, the change from one sequence to its inverted sequence, are generally referred to as odd correlation functions and those of the non-transitional areas of the sequence train are referred to as even correlation functions.

However, other less efficient direct sequence spreading schemes, such as sequence on-off keying (OOK) also exist [18].

3.5 Schematical presentation of the signals in CDMA systems

The information signal suffers from interference due to jamming, interference arising from other users of the spread spectrum system and self-interference due to multipath propagation.

As is shown in Figure 3.5 and Figure 3.6, the main part of the direct sequence transmitter output power is contained within the main lobe. Demodulation of the typical sequence signal is performed by a code-matched filter. To any narrowband signal coexisting with the spread spectrum subscriber, the direct sequence signal will appear as Gaussian noise since its power spectral density is essentially flat over the narrowband channel.

Other direct sequence subscribers can also be overlaid in the same spreading bandwidth, since the orthogonal or pseudo orthogonal sequences utilised by each subscriber are independent and can be decoded as such by the spread spectrum receivers. The effects of narrowband and

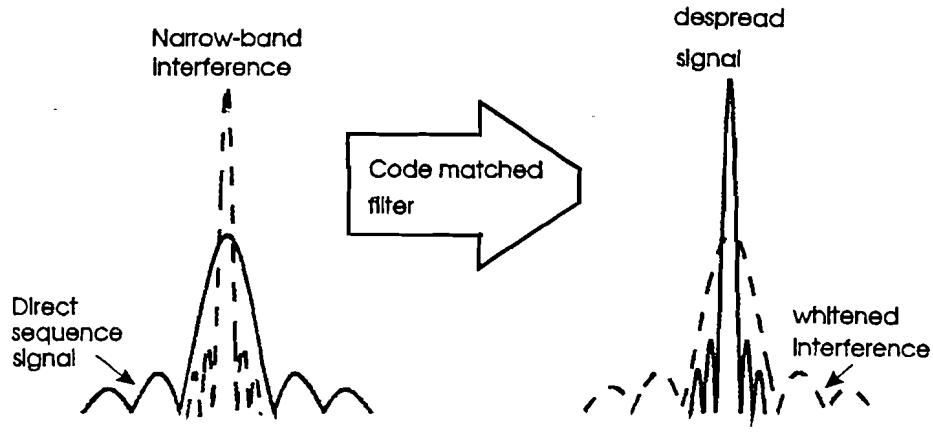

Figure 3.5: Despreading with narrow-band interference.

broadband interference are reduced by the code-matched filter as is shown in Figure 3.5 and Figure 3.6.

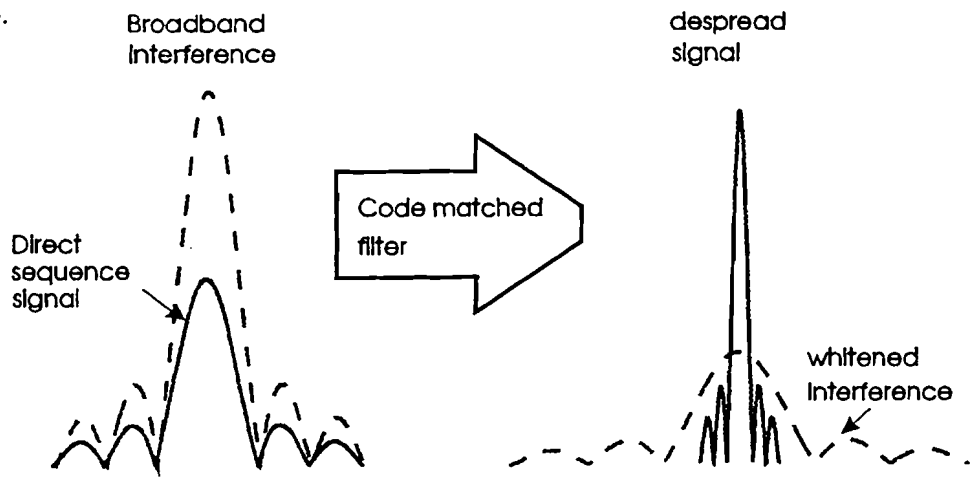

Figure 3.6: Despreading with broadband interference.

The code-matched filter contains the bit pattern corresponding to the addressed user. The spreading by the code-matched filter of unwanted signals applies to coexisting CDMA subscribers, which are coded by other sequences in the set [18]. Co-channel interference arising from subscribers utilising an identical spreading sequence will also be whitened by the digital matched filter, provided that the two competing coded waveforms are not in phase. When maliciously using identical sequences by two or more subscribers, the majority of collision will be prevented. In these cases, providing that the subscriber phases are not aligned, the interference apparent on the ACF peak of each contending subscriber will have the same effect as an independent sequence coded waveform.

The bandwidth allocated for DS-CDMA differs from other multiple-access systems in that there are no predefined physical slots for the concurrent active subscribers. CDMA is therefore interference limited only. The bit error performance responds to the traffic loading fluctuations, thus the bit error rate performance is degraded as the traffic loading becomes more intense [18].

3.6 Modulation scheme

If the channel fades slowly enough to allow the establishment of a phase reference, then PSK may be employed. If not, then Differential Phase-shift keying (DPSK) or FSK modulation with non-coherent detection at the receiver is appropriate.

Considering the properties of the indoor radio channel, the most common modulation scheme employs binary phase-shift keying (BPSK). Besides BPSK, r-phase modulation is optional, which means that each signature sequence is r-valued [7]. At high frequencies bi-phase of quadriphase sequences are used, because of implementation issues. There is no specific relationship between r, the amount of sequences/user M or the length of each sequence N. PSK modulation is a linear modulation so that superposition can be applied to the transmitted data sequences to retrieve the compound received signal. For linear receivers r-phase modulation gives no performance improvement over bi-phase modulation.

The simple bi-phase or quadriphase direct sequence signal has a $(\sin(x)/x)^2$ power spectrum [6], when using a rectangular pulse with duration T and amplitude A over $T \pm T/2$ and zero elsewhere. Pulse shaping can provide a significantly improved power distribution. The most efficient use of the allocated frequency spectrum is by using raised cosine pulses. In any case, the direct sequence system has a main lobe bandwidth, that is a function of the waveshape and the code rate used.

An alternative phase-modulation technique is DQPSK modulation, which stands for Differential Quadrature Phase Shift Keying modulation. In doing so, no absolute phase reference is needed for demodulation, which simplifies the receiver design.

The transmitter and receiver of a typical binary DS-BPSK system have the structure of Figure 3.7 and Figure 3.8, respectively.
This DS-BPSK system shows a PN code generator at the transmitter and a PN code generator and synchronizer at the receiver.

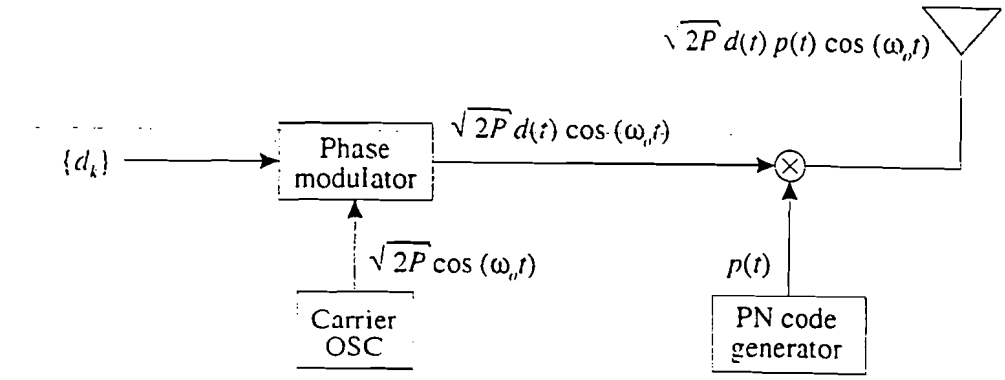

Figure 3.7: BPSK direct sequence spread-spectrum transmitter.

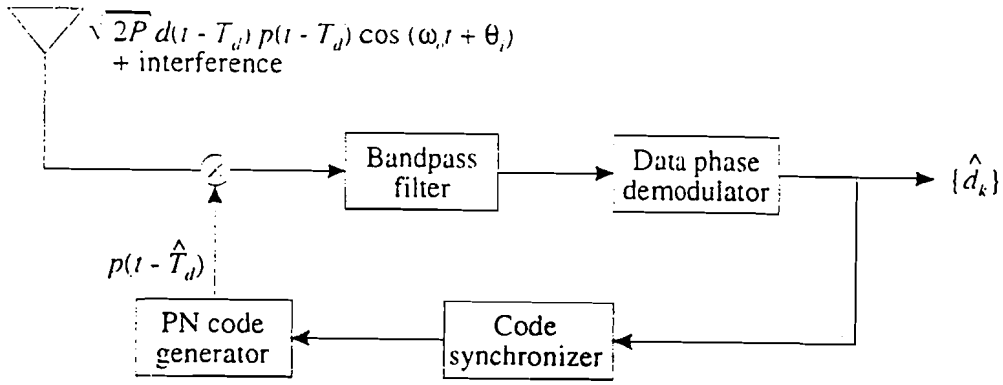

Figure 3.8: PSK direct sequence spread-spectrum receiver.

In Figure 3.7 and Figure 3.8 $p(t)$ and $p(t-\hat{T}_d)$, which take on the value ± 1, represent the output of the sequence generators, where $\hat{T}_d$ is the propagation delay estimated by the receiver. The transmitter of Figure 3.7 first modulates the binary data sequence $\{d_k\} \in \{-1, 1\}$ onto a carrier with power P and angle frequency ω_0 in the phase modulator. The BPSK modulated carrier is given by

$$v_d(t) = \sqrt{2P}\, d(t)\cos(\omega_0 t) \ , \tag{3.6}$$

where $d(t)$ is the data waveform resulting from the data sequence $\{d_k\}$. The transmitter multiplies this signal with the spreading waveform $p(t)$. Thus, the transmitted waveform is given by

$$v_s(t) = \sqrt{2P}\, d(t)p(t)\cos(\omega_0 t) \ . \tag{3.7}$$

By calculating the power spectral density [W/Hz] of the BPSK modulated carrier of equation (3.6) and the transmitted spread carrier of (3.7) shows the spreading operation.

$$V_d(f) = \frac{1}{2}PT_b\{sinc^2[(f-f_0)T_b] + sinc^2[(f+f_0)T_b]\}\ , \tag{3.8}$$

$$V_n(f) = \frac{1}{2}PT_c\{sinc^2[(f-f_0)T_c] + sinc^2[(f+f_0)T_c]\}\ . \tag{3.9}$$

In (3.8) and (3.9) T_b is the bit duration, T_c the chip duration and f_0 is the centre frequency of the carrier. The chip duration is much smaller than the bit time and therefore the spectrum of $V_n(f)$ is much lower and wider than the spectrum of $V_d(f)$. This is shown in Figure 3.9 for $T_c = T_b/10$.

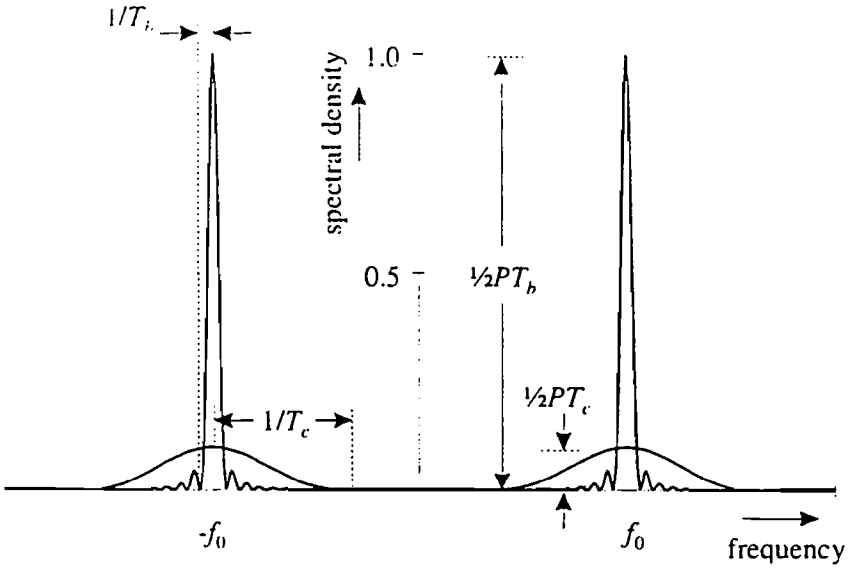

Figure 3.9: Power spectral density of BPSK signal and spread BPSK signal (T_b=10T_c).

At the receiver site, the received signal is modulo-2 added with the sequence $p(t-\hat{T}_d)$, which results in the original phase modulated signal on the condition that $T_d = \hat{T}_d$. Thus the spreaded received signal is despreaded.

3.7 Coding

The use of CDMA makes it possible for multiple users to share a common channel bandwidth and allows them to transmit information simultaneously. The transmitted signals in this common channel bandwidth are distinguished by different pseudo-random codes. Coding of the information bits results in expansion of the bandwidth and offers multiple-access capabilities. The codes should be chosen in such a way that the signals are pseudo-random, which makes the signal appear similar to random noise and thus harder to demodulate those signals by unintended users. The transmitter introduces an element of randomness in each of

the transmitted coded signal waveforms, which is known to the intended receiver but not to a jammer.

The codes to use in spread spectrum systems are designed to be quasi-orthogonal, which implies that the cross-correlation function between two codes is much smaller than their common energy [35]. This restriction in the cross-correlation for the codes applies also for the cross-correlation between mutual shifted codes. The cross-correlation function between the codes $c_i(t)$ en $c_j(t)$, $0 \le t \le T$, is given by

$$r_{ij}(\tau) \triangleq \int_0^T c_i(t)c_j(t-\tau)dt \ . \qquad |\tau| \le T \qquad (3.10)$$

Their total energy, is equal to

$$E_c \triangleq r_{ii}(0) = \int_0^T c_i^2(t)dt \ . \qquad i = 0, 1, \ldots\ldots, N \qquad (3.11)$$

A typical relation between the cross-correlation and autocorrelation is

$$|r_{ij}(\tau)| \le \frac{E_c}{\sqrt{TW}} \qquad |\tau| \le T \ , \ i \ne j \qquad (3.12)$$

where W is the common bandwidth of the code waveforms.

A selection of several most commonly used code sets for spread spectrum systems is given in the following paragraphs [18].

3.7.1 m-sequences

Binary PN sequences are generally derived from the output states of linear feedback shift register devices. A maximal length shift register, with n elements, generates all of the possible shift register states, apart from the all-zero state. The length N of these maximal length shift register sequences, or m-sequences, generated by the maximal length shift register, is $N = 2^n - 1$. The generation of m-sequences, by a binary shift registers of length n with feedback connections, is illustrated in Figure 3.10 [14].

A shift register, for generating a sequence is the practical translation of a primitive polynomial $h(x)$

$$h(x) = x^n + h_{n-1}x^{n-1} + \cdots + h_1 x + 1 \ , \qquad (3.13)$$

where h_i takes on the binary value 0 or 1. Related to the shift register, the numbers h_i

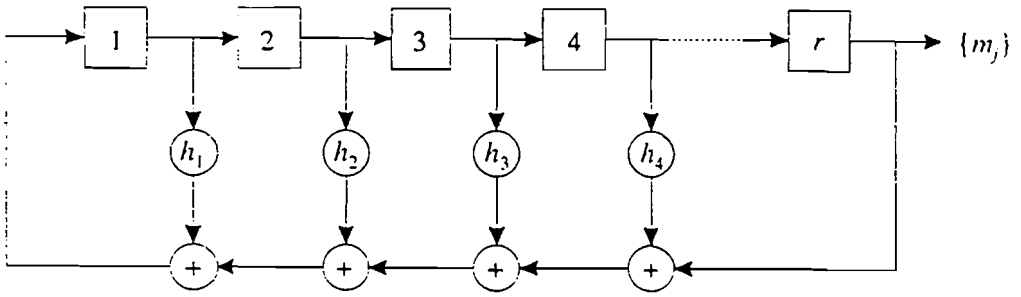

Figure 3.10: Shift register for the generation of m-seqeunces.

determine the feedback connections. Dixon [6] gives feedback connections for the generation of the sequences.

It is necessary that the feedback polynomial is selected from the set of irreducible polynomials [21]. The size of the m-sequence family is restricted by the available number of irreducible polynomials, which is defined by the Euler quotient function for the shift register order [18]. The m-sequence set size, S, for a shift register of order n is given by

$$S = \frac{1}{n} Y(2^n - 1) = \frac{1}{n} Y(N) \ , \tag{3.14}$$

where $Y(x)$ is the Euler number of x. The Euler number of x can be described as the count of numbers in the range $1..x$, which are prime to x.

The correlation properties of the m-sequence family are very interesting owing to the flat periodic autocorrelation sidelobes of level -1, which approximate the ideal situation for short spreading lengths. Shorter length coding schemes are often subject to significant autocorrelation sidelobes, which when incorporated into the channel matched filter scheme cause further interference.

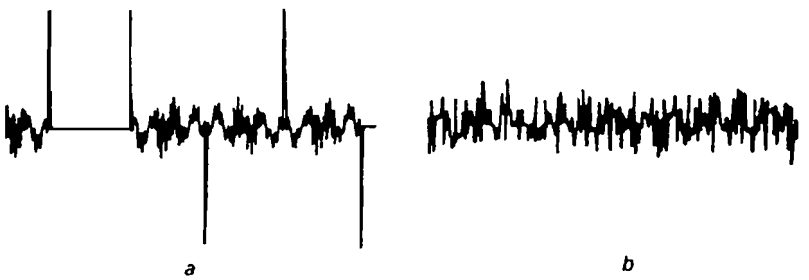

Figure 3.11: a) Autocorrelation and b) cross-correlation of m-sequences.

The available set size, S, is very much smaller than the sequence length, N, particularly in the case of the even shift register orders. Therefore as a multiple-access code set, it does not

provide adequate capability for system subscribers, each requiring their own unique sequence. Therefore, m-sequences are not favoured for practical, high traffic-capacity DS-CDMA with multiple users.

3.7.2 Gold codes.

It was noted by Gold [18] that selected pairs of m-sequences exhibit a three-valued cross-correlation function, with a reduced upper bound on the correlation levels as compared with the rest of the m-sequence set. For the preferred pair of m-sequences of order n, the periodic cross-correlation and autocorrelation sidelobe levels are restricted to the values given by

$$\{-t(n),-1,t(n)-2\}\ , \tag{3.15}$$

where $t(n)=2^{(n+1)/2}+1$ for n odd and $t(n)=2^{(n+2)/2}-1$ for n even.

Table 3.1: The parameter $t(n)$ for n = 5 .. 9.

n	N	$t(n)$
5	31	9
6	63	17
7	127	17
8	255	33
9	511	33

Hence the off-peak values of the autocorrelation function are upper-bounded by $t(n)$. The Gold codes exist for all $N = 2^n - 1$, n that are not multiples of 4 [11].

The enhanced correlation properties of the preferred pair can be noticed by similar sequences derived from the original pair. By a process of modulo-2 addition [18] of the preferred pair, the resulting derivative sequences share the same features and can be grouped with the preferred pair to the newly created family. This family of sequences are known as Gold codes. Since there are N possible cyclic shifts between the preferred pair of m-sequences of length N, the available set size , S, for the Gold code is $N + 2$.

It is clear from Figure 3.12, which uses SIK, that the even correlation areas exhibit the three valued property investigated by Gold. This property is lost as soon as the applied data modulation introduces transitional or odd correlation areas, with correlation levels outside the expected set of values.

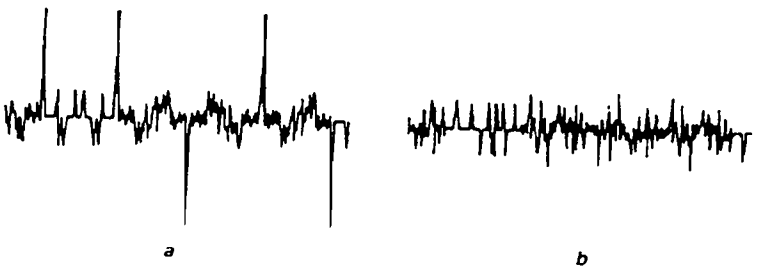

Figure 3.12: Typical Gold code family a) ACF b) CCF over a period of 5 sequences.

Generating the Goldcode set can be done according to the techniques of the Gaulois Fields Theory, described by Dixon at p. 80 of [6]. Table 3.7 in Dixon shows the taps of the shift register for the maximal polynomials for several code lengths. The all-ones vector is set into both registers as an initial condition. Proper selection of the maximal polynomials from this table is necessary to generate a Gold code set. Arbitrary selection of code pairs can result in very poor correlation performance. Gold uses "preferred" pairs of codes that give a correlation, which is bounded at $2^{(n+1)/2}+1$ for n odd and $2^{(n+2)/2}-1$ for n even. The preferred pair can be chosen using Table 3.7 in Dixon [6] and appendix D in Peterson [21]. After finding the preferred pair, the entire Gold set can be generated by combining the two output maximal codes with different initial offsets. With the two maximal sequences of length N, another 2^n-1 maximal length sequences can be generated.

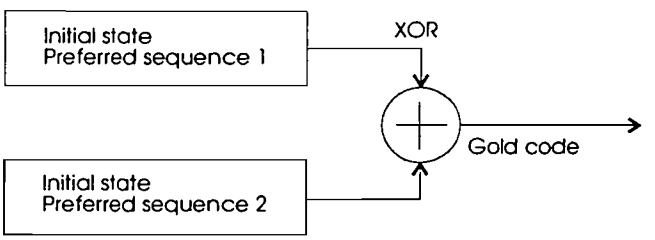

Figure 3.13: Shift register for generating a Gold code set.

Two methods of realising the Gold code set based on shift register hardware exist [18]. First by a direct approach consisting of two m-sequence generators, using the preferred pair of feedback polynomials. These two m-sequences are finally combined by an "exclusive or", which results in the Gold set codes. Alternatively, the Gold code set can be generated through

a single much larger feedback shift register with the feedback polynomial being derived from the product of the preferred pair polynomials.

3.7.3 Kasami codes (small set)

The procedure for generating the small set of Kasami sequences is similar to that of Gold codes. If the longer preferred m-sequence, produced by the generator polynomial $h_2(x)$ of order $2n$, is selected correctly, it can be decimated to give a new sequence, which is also a preferred m-sequence, produced by the generator polynomial $h_1(x)$ of order n [18]. If we take the full $2^{2n}-1$ bits from the longer sequence and perform a modulo-2 addition with the repeated short sequence over all 2^n-1 possible relative cyclic shifts of this sequence, we obtain a new family of binary sequences with length $N = 2^{2n}-1$ and sequence set size $S = 2^n$. The periodic cross-correlation and autocorrelation sidelobe levels are again restricted to the values given by (3.15), with $t(n) = 2^n+1$. Hence the maximum cross-correlation value for any pair of sequences from the set is

$$\theta_{max} = 2^n + 1 \ . \tag{3.16}$$

The autocorrelation and cross-correlation of the Kasami codes is illustrated in Figure 3.14. Comparing Figure 3.14 with Figure 3.11 and Figure 3.12 shows an improvement for Kasami codes on the maximum peak level of the sidelobes.

Figure 3.14: Typical Kasami code family a) ACF b) CCF over a period of 5 sequences.

3.7.4 Barker codes

Barker codes, have a autocorrelation peak with value N and the magnitude of the minimum peak sidelobe is 1. Only a small list of Barker codes exists having a minimum peak sidelobe of 1 and are listed by Skolnik [27] in Chapter 10. No Barker codes longer than 13 have been

found to exist.

3.8 Welch lower bound

In asynchronous CDMA systems the usefulness of a code set is therefore not its orthogonality, but its correlatedness [18]. The lower bounds on the peak levels in the correlation are related to the sequence length N and sequence set size S. This Welch lower bound (WLB), on unwanted correlation peak levels, θ_{max}, is

$$\theta_{max} \geq N\sqrt{\frac{S-1}{SN-1}}\ , \tag{3.17}$$

which, for large values of N and S, is well approximated as $\sqrt{N}$.

It is interesting to compare the peak cross-correlation value of Gold sequences $t(n)$, with the Welch lower bound on the cross-correlation between any pair of binary sequences of period N in a set of S sequences. For Gold sequences, $N = 2^n - 1$ and hence the Welch lower bound is approximately $\theta_{max} \approx 2^{n/2}$ [23]. This bound is lower by $\sqrt{2}$ for n odd and by 2 for n even, relative to $t(n)$. The maximum cross-correlation value for Kasami codes is given in (3.16) and satisfies the Welch lower bound for a set of 2^n sequences.

Comparing the correlation bounds for the types of codes indicate that the Kasami sequences are optimal, because they have lower periodic cross-correlation peaks. The frequency of occurrences of -1 cross-correlation is higher for Gold codes, than for Kasami sequences. For these two comparisons it is inconclusive to choose the better code set on base of the cross-correlation. Another parameter to compare Gold codes and Kasami codes is the set size, which is larger for Gold codes than for Kasami codes, thus Gold codes are more useful for multiple-access systems.

The bit error rate (BER) for any of the subscribers in a CDMA system is dependent of the number of competing active subscribers, m. The maximum cross-correlation peak level that could conceivably occur for m active subscribers is given by $m\theta_{max}$, and a finite error rate will occur if this value exceeds the autocorrelation peak value of N. Therefore, for zero transmission errors due to co-channel interference the condition $m\theta_{max} \leq N$ must be satisfied. This restriction implies that, for a sequence set approximated by the CDMA Welch lower bound approximation, the number of competing active subscribers with equal receiver power is limited to $m \leq N/\sqrt{N} = \sqrt{N}$. For subscriber activities above this figure, the cross-correlation statistics will tend towards Gaussian profile owing to the central limit theorem as explained

in paragraph 2.3.3 [18].

3.9 Improving the properties of the code set

Two selection criteria exist for selecting the codes with optimal properties from a code set:

- Balanced codes have better correlation properties compared to unbalanced codes.
- For synchronisation purposes and reducing the effect of multipath, it is advantageous to have a near-zero sidelobe energy of the autocorrelation peak.

A Gold code set with a set size of 513 and sequence length of 511, will be reduced to a set of 257 by selecting the balanced codes. Following the second criteria, dealing about the autocorrelation function, diminishes the set size to 125 codes with both of these properties.

3.10 Correlation properties of binary PN codes

The code sets described in paragraph 3.7 typically have well-defined cross-correlation levels, when repeated continuously. However using SIK data modulation, unintended random sequences, not contained within the sequence set, appear in the transitional regions of the sequence train [18]. The probability distribution function (PDF) of the postcorrelation noise levels, caused by correlative co-channel interference experienced by a sequence set, is useful in the determination of the performance.

The successive convolution of the generated Gold PDF for an increasing amount of subscribers quickly tends towards the Gaussian distribution. The peak-to-side lobe ratio, given by $20\log(N/\theta_{max})$, is increased as the length of the sequences is increased. The code families designed for reduced maximum correlation levels, θ_{max}, such as the small set Kasami codes, suffer from a similar level of cross-correlation variability as compared with the random code set. Table 3.2 shows the distribution variability for several acceptable sequence sets for CDMA.

Table 3.2: Cross-correlation properties for several binary sequences.

Type	Length N	Set size S	θ_{max}	$20\log(N/\theta_{max})$	PDF variance
m-sequences	31	6	19	4.25	31.696 ($1.022N$)
	63	6	31	6.16	63.426 ($1.007N$)
	255	16	99	8.22	253.660 ($0.995N$)
gold codes	31	33	21	3.38	30.403 ($0.981N$)
	63	65	31	6.16	62.551 ($0.993N$)
Kasami codes	15	4	11	2.69	13.231 ($0.882N$)
	63	8	27	7.36	59.090 ($0.934N$)
	255	16	55	13.32	244.720 ($0.960N$)
Random codes	63	unlimited	35	5.11	62.956 ($0.999N$)
	255	unlimited	73	10.86	254.350 ($0.997N$)

For typical binary PN sequence of length N, the cross-correlation noise between code x and y can be approximated by N (regardless of the sequence set and pairing) as shown in table 3.1. Proper selection of the code set for CDMA does not depend on the cross-correlation properties, but more on the set size available for each particular family. It is possible to meet the system requirements on sequence numbers by the inclusion of multiple families or randomly selected codes into the system set.

Even with very few numbers of active subscribers the correlation level distribution is approximately Gaussian, as a consequence of the central limit theorem as explained in paragraph 2.3.3 [18]. Since for CDMA system analysis it is more important to model the noise statistics in the upper regions of channel loading, it is therefore reasonable to assume Gaussian approximation for the purpose of performance analysis.

Chapter 4 Indoor radio CDMA receivers

The indoor radio propagation channel has been characterised by a multipath channel, which exhibits time dispersion and frequency-selective fading. Applying the wide signal bandwidth W in the CDMA system to a multipath channel with coherence bandwidth $(\Delta f)_c$, which is much smaller than W, results in $W/(\Delta f)_c$ resolvable signal components. The fading on the resolved components is uncorrelated and this multipath diversity can be made use of by a diversity combining technique. The structure of a multipath receiver is much more complicated than that of a single-path receiver. In the past, several adaptive receivers as means of increasing the data rates on fading multipath channels have been developed.

In conventional digital communication systems intersymbol interference, caused by a non-ideal frequency response of the channel, is avoided by keeping the information rate low or by using other techniques. On of these other techniques is increasing the data rate on a fading channel by using antenna diversity. The antenna diversity can be achieved by using multiple transmitter and/or receiving antennas or using sectored antennas. Elimination of unwanted paths reduces the delay spread. Another technique is reversing the channel frequency response by using adaptive equaliser techniques [23]. Linear equalizers are not effective on frequency-selective fading multipath channels and therefore the decision feedback equalizer (DFE) technique is typically used on these channels [29]. A DFE can isolate the arriving paths and take advantage of them.

In a CDMA system in an indoor radio environment, a number of user signals arrive at the uplink receiver simultaneously in the same frequency band, only distinguishable by different user specific signature sequences. The CDMA chip rate $1/W$ is much higher than the symbol rate, with a ratio equal to the sequence length. The most significant diversity combining technique, mostly used for spread spectrum systems, is known as a RAKE receiver. The RAKE receiver uses the correlation properties of a spread-spectrum signal to resolve the multipath signals and combine them. The RAKE receiver uses a much wider bandwidth, but has the advantage of much greater resistance to interference.

In the multipath and multi-user environment, both self-interference and multiple-access user interference occur at the receiver, which can be treated at the receiver site in different ways. Basically, two types of receivers may be distinguished, one treating self-interference and multiple-access interference as noise and the other exploiting knowledge about self-interference and multiple-access interference [2].

The first type of receiver is realized by matched filter receivers as conventional RAKE receivers. The weighting and combining of the multipath signals by a RAKE receiver bring all the multipath components back into alignment and combine them optimally in the mean correlation signal peak. Although the conventional RAKE receivers coherently add the signals received over distinguishable paths, they are not combatting the distortions introduced by the multipath radio channel. Hence ISI, which occur for a maximum delay spread T_m larger than the symbol time, and multiple-access interference are not suppressed by the RAKE receiver, but still occur as correlation self noise at the receiver output. RAKE receivers allow a non-organized, flexible multiple-access, but on the other hand they require a very tight power control or special antenna design to correct for equal power arrivals for all subscribers.

The second type of receiver exploits knowledge about ISI and multiple-access interference either by interference cancellation (IC), by applying multiple receiving antennas [2] or by other advanced techniques. These techniques improve the performance of the CDMA system and may increase the capacity, because more knowledge about the received signal is exploited.

The remaining part of this chapter describes the conventional RAKE receiver as well as receivers using interference cancellation technique and their structures. The signal despreading process, included in the receiver, involves a direct comparison between the incoming spread spectrum multipath signal and the sequence, or sequences for M-ary CDMA, used by a specific subscriber. The presence of a sequence can be detected by a large autocorrelation peak in the post-correlation signal. The correlation properties depends on the family of codes, as described in paragraph 3.7. The part of the receiver that involves the code comparison is often referred to as a correlation receiver (also called code-matched filter or digital matched filter).

4.1 Code-matched filter

Code-matched filtering can be physically realised through the use of a N-stage shift register with accumulated taps, weighted by multiplication with the vector c [18]. When the weight vector, c, is matched to the coding sequence employed in the signal sample values, the output correlation signal will contain the autocorrelation function (ACF) of the sequence and also interference arising from the cross-correlation functions (CCF) of the vector with other sequences, overlaid signals and channel noise leakage. The ACF can be characterised by an in-phase peak, corresponding to the point of phase alignment between the code-matched filter (CMF) tap weight vector and the received data.

The level of the sidelobes occurring outside the alignment depends on the properties of the

sequence set. It is desirable to have PN codes which exhibit near-zero sidelobe energy around the correlation peak over the area in which multipath energy is of interest. By using the optimal codes from a correct coding set, as was discussed in paragraph 3.9, results in low sidelobe energy. Assuming the correlation sidelobe energy to be negligible, then ISI is only a problem for a delay spread of the channel greater than the symbol period. The cross-correlation is a measure of the orthogonality and correlatedness of the interference sequence with the matched sequence.

The post-correlation signal, which equals the signal at the output of the code-matched filter can be considered as a first approximation to the impulse response of the channel [22]. A better estimation of the impulse response of the channel is possible by filtering the delay elements, by removing much of the noise. The filtering is mostly effective for a slow fading multipath signals, which give a better estimate of the channel.

4.2 RAKE or matched filter receiver structures

The optimal spread spectrum receiver consists of a code-matched filter (CMF), and a channel matched filter, hence the receiver is matched to the received signal rather than to the transmitted one by using the estimation of the multipath. The RAKE receiver is a channel matched filter. The CMF can be placed in front of the channel matched filter or in the channel matched filter at the tap signals. The channel matched filter performs optimal combining on the individual multipath responses. This channel matched filter can be implemented as a RAKE receiver [23]. A spread spectrum receiver consisting of a CMF cascaded with a RAKE receiver is given in Figure 4.1.

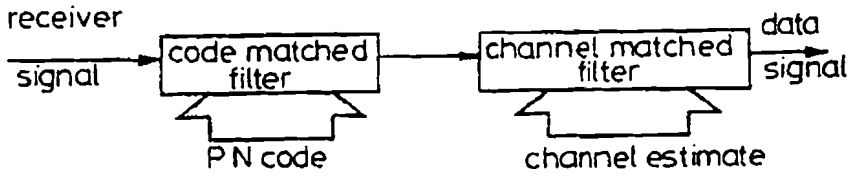

Figure 4.1: spread-spectrum receiver [17].

A RAKE receiver is built of a tapped delay line and a code-matched filter, which can be cascaded or integrated. The post-correlation signals at the taps are multiplied with matched coefficients. The relative signal power for each delay element of the received element is

related to the channel impulse response. The weighting and combining of the signals will bring multipath components back into alignment and combine them optimally, such that the main correlation signal peak is enhanced and is less prone to severe fades. The diversity of the RAKE receiver ensures that large fades are minimised and the signals instantaneous *SNR* is higher and more stable, compared to a non-RAKE type system.

As the number of taps increases, performance improves. Similarly, as the tap spacing decreases, allowing the receiver to take better advantage of the internal diversity from the multipaths, performance improves. Each ray adds to the signal energy and to the self-interference. The performance is maximized closer the taps are synchronized to the path delays.

Several types of RAKE receivers, distinguished by the way of combining the tap signals, exist, as for example:

- ***Maximal ratio combining***

  The best performance obtainable in a system with diversity is by maximum-ratio combining as was shown in [22]. The CMF is succeeded by a RAKE receiver. In maximum-ratio combining the received rays are weighted according to their perceived signal-to-noise ratios. When the rays contain the same noise power, the rays can then be weighted by their signal powers included in their channel impulse responses.

  For an enhanced RAKE receiver the post-correlation signal is convolved with the complex-conjugated of the estimated channel impulse response to obtain maximum combining.

- ***Square law combining***

  Another method of combining the outputs is a square law combiner [23], which can be implemented without any information about the channel characteristics. This type of receiver will be used when the fading is too rapid for making good channel estimations. The received signal is passed through a tapped delay line and next passed through a bank of code-matched filters, matched to the transmitted symbols. The sampled outputs of the matched filters from different taps are squared and added. The decision of the symbol is made on the largest output accumulated output. This RAKE demodulator for square-law combining of orthogonal signals is assumed to contain a signal component at each delay. If not, the performance will degrade due to the inclusion of noise-only taps.

- ***Diversity combining***
  Combining the two strongest tap signals is a form of diversity combining.

- ***Selection of the strongest***
  Selecting the strongest tap signal is a form of diversity combining.

For communication system design it is important to find an optimum relation between values of T_m, the number of RAKE-receiver taps F and the bandwidth of the communication system $W=\tau_r^{-1}$, with τ_r the time resolution [4]. The maximum delay T_m is determined by the properties of the environment. If the amount of taps F of the RAKE receiver is kept constant, then for an optimum gain by multipath diversity, τ_r should be adjusted so that $\tau_r \approx T_m/F$. The time delay for indoor environments will be about 100ns [37]. According to preceding equation, high bandwidths are necessary for utilizing multipath diversity.

If the bandwidth W is too large, only the information within F resolvable paths, on which the RAKE receiver can position a delay line, is utilized. The other resolvable paths increase only the interference floor. On the other hand, for a too small bandwidth, the delay resolution is too low to yield a multipath diversity gain by the F RAKE delay lines.

4.3 Interference cancellation techniques

In general, the spectral efficiency of CDMA systems with the commonly applied code-matched filter receiver is not favourable, when compared with other multiple-access methods [18]. Adaptive cancellation techniques may well improve the capacity problems. The hardware complexity will increase.

4.3.1 Multiple user interference cancellation

Interference by simultaneous other users in CDMA systems degrades the signal, which is caused by the cross-correlation levels between quasi-orthogonal codes. The principle of multiple-access interference cancellation is based on doing channel measurements to estimate and regenerate the cross-correlation components from interfering channels. A technique of cancellation considering the cross-correlation is described in [19].

The interference derived from cross-correlation product between the sequences in the code set

have a lower bound defined by Welch (paragraph 3.8). The co-channel interference, as the multiple-access interference is called, is deterministic and repeatable at the receiver given the symbol timing, incoming signal level and data content of the particular interfering channel. Having a receiver with a code-matched filter for each subscriber receiver link gives the option to estimate the symbol timing, incoming signal level and data content. The signals from these links can be regenerated and subtracted from the signal to improve the performance of the desired channel. An example of a single-stage co-channel CDMA interference cancellation by regeneration of the N-1 interfering channels is given in Figure 4.2

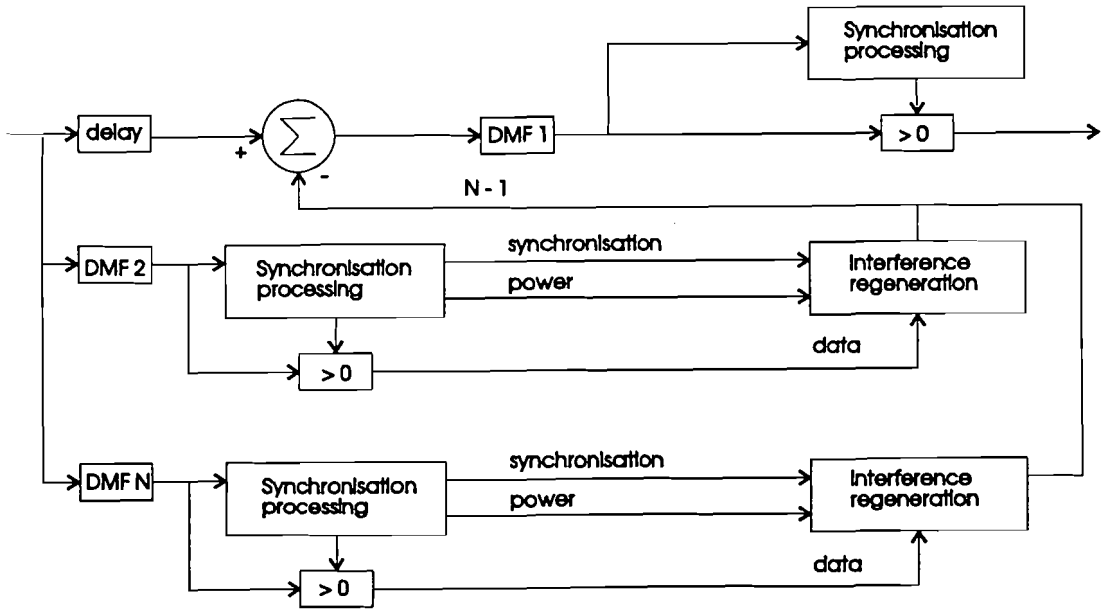

Figure 4.2: Single-stage co-channel CDMA interference cancellation.

Interference cancellation systems can also exist of more stages to further improve the signal. This increase in performance makes the system very complex.

4.3.2 Self-interference cancellation

To further improve quality, the multiple-access interference cancellation can be followed by a receiver using anti-multipath techniques. Mowbray [17] shows a modified approach to multipath recombination, which avoids the inclusion of sidelobe interference in the output main peak. These sidelobes, which occur between the data bit transitions [17], cause further interference on the channel matched RAKE main peak output, reducing the effective SNR enhancement of this process.

This technique uses an adaptive multipath cancellation matrix, which separates multipath

components in the received signal. Next an improved channel matched filter can be configured by using the estimated delay and weighting coefficients. The multipath components will be combined optimally before the correlator will be used. The main peak outputs from all significant multipath signals are aligned correctly in the code-matched filter so that none of the autocorrelation sidelobe interference from adjacent returns will reduce the output mean peak. This alternative channel matched filter design for combining resolved and separated multipath signals with Gold codes, is given in Figure 4.3

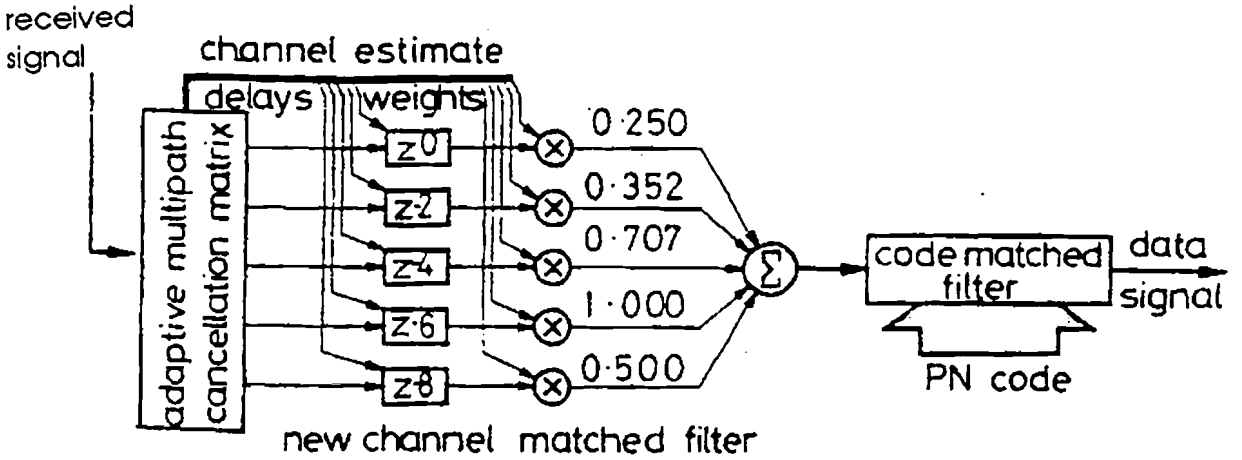

Figure 4.3: Alternative channel matched filter design.

The technique, showed by Mowbray [17], to remove the multipath interference by finding the five largest correlation peaks and weighting and combining them, such that only a single peak appeared, can be applied in short to medium spreading length (<1024) and a low amount of multipaths. Therefore, the technique of removing multipath interference fails when having strong multipath.

Chapter 5 Performance of the system

In an indoor radio network context, the geographic distributions of transmitters, multipath and fading effects lead to reception of several signals at different power levels, each via a multiplicity of fading paths. Due to the spreaded spectrum, the channel exhibits frequency-selective fading.

The performance of an asynchronous CDMA system using direct-sequence codes will be analytically considered. Since the codes cannot be exactly uniformly orthogonal, reception of code $a_{k,m}$ (with data modulated on it) suffers from cross-correlation noise caused by other codes and multipath in the channel. The codes are assumed to be quasi-orthogonal, as described in paragraph 3.7.

5.1 Subscriber capacity

The upper bound on CDMA systems performance (BER) for individual transmitting subscribers, with respect to the traffic intensity, shows that the spectral loading (active subscribers/spreading ratio) goes down considerably for better BER [18]. This is illustrated in Figure 5.1. For a tolerable BER of 10^{-5}, only $0.1N$ channels can be supported, with N the sequence length. The result is typically less than with a TDMA or FDMA system. Since the interference is proportional to the number of active subscribers and the access control is uncoordinated, CDMA is still more interesting in indoor radio systems. With the application of adaptive cancellation techniques a considerable increase in the subscriber capacity is possible [19].

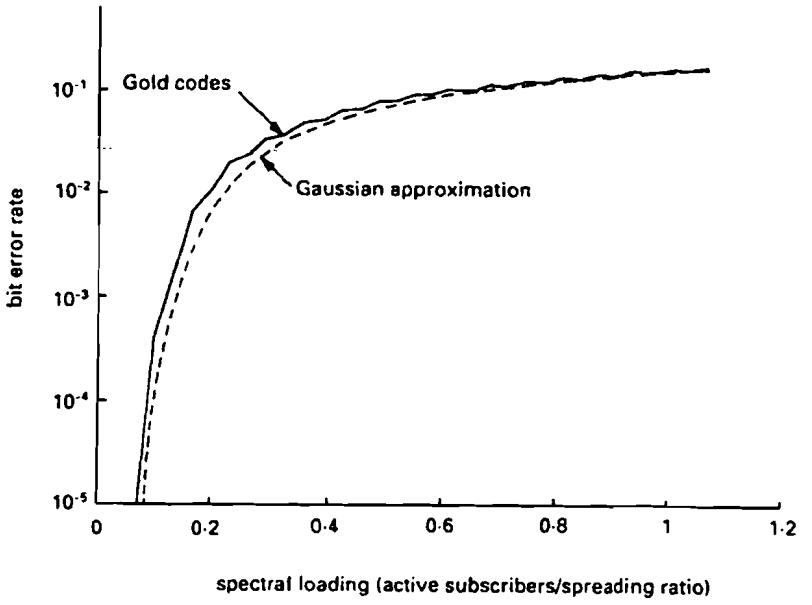

Figure 5.1: Upper bound on CDMA BER with increasing spectral loading.

5.2 Bandwidth efficiency

An important performance criteria is the bandwidth efficiency of the coding technique. The bandwidth efficiency η for spread spectrum multiple-access systems, can be defined as

$$\eta=\frac{KR_b}{W}=K\cdot\frac{\log_2 M}{N}\ , \tag{5.1}$$

where R_b is the bit rate, W the signal bandwidth, M the size of the sequence set per user, N the sequence length and K the number of users.

5.3 Analytic presentation of the performance

First a comparison of the performance for fading and non-fading channels will be given. Afterwards analyses for the fading multipath situation has been derived.

5.3.1 Performance for fading and non-fading channels using explicit and implicit diversity

An approximation for the performance of fading and non-fading paths has been made by Pahlavan [20] and Enge [7]. The relationship between SNR and the probability of error P_e

can be derived for the Gaussian assumption. The sum of statistically independent and identically distributed random variables with finite mean and variance, approaches a Gaussian probability distribution function, as explained in paragraph 2.3.3. If there are K interfering users, each of whose signals arrive via M paths, the effect is as if there would be $M \cdot K$ interfering users in the Gaussian assumption. The SNR for each path is:

$$\gamma = \left(\frac{N_o}{E_s} + \frac{2M_\Gamma (K-1)L}{NT_c^3} \right)^{-1} , \tag{5.2}$$

where M_Γ is a constant depending on the chip waveform, E_s is the energy per symbol, L is the diversity of the channel and T_c is the chip time. In fading channels γ is the average SNR. In non-fading channels γ is the SNR and $L=1$. If the chip waveform is a sine pulse, then

$$M_\Gamma = T_c^3 \frac{(15+2\pi^2)}{12\pi^2} \approx 0.293 T_c^3 . \tag{5.3}$$

The probability of error for M-ary orthogonal signalling, thus M codes per user, equals

$$Pr(\varepsilon) \approx (M-1) Q(\sqrt{\gamma}) . \tag{5.4}$$

In the flat (frequency-nonselective) fading, the only source of diversity is the explicit or antenna diversity D [20]. In frequency-selective fading channels, multipath arrival provides another source of diversity which is referred to as the implicit or internal diversity. The number of paths L by implicit diversity is $L = \lceil T_m / T_c \rceil + 1$, where T_m is the maximum delay spread, T_c is the chip time and $\lceil \cdot \rceil$ is the function that returns the largest integer less than or equal to its argument. Equations derived for the frequency-nonselective fading with explicit diversity D can be used for fading multipath channels with a diversity of LD

The implicit diversity can be exploited by resolving the multipaths with a RAKE receiver. The average probability of error, using a RAKE receiver with square law combiner, is, as given in equation (7.7.4) of [23]

$$Pr(\varepsilon) = 1 - \int_0^\infty \frac{u^{LD-1} \cdot e^{-\frac{u}{1+\gamma}}}{(1+\gamma)^{LD} (LD-1)!} \cdot \left(1 - e^{-u} \sum_{j=0}^{LD-1} \frac{u^j}{j!} \right)^{M-1} du . \tag{5.5}$$

In non-fading channels, performance improves as the length of the code increases. The performance in fading channels is almost identical for different code lengths, because the channel fades occur in one symbol time. By incorporating the implicit diversity, provided by the resolved multipaths in the indoor environment, some improvement is observed.

An increasing number of users can be accommodated at a cost of lower data rate per user

[20]. An increase in the order of implicit diversity increases the interference noise caused by other users. Explicit diversity increases the diversity of the received signal without contributing to the interference noise. The performance can surpass that found in non-fading channels at increasing orders of diversity.

The maximum bandwidth efficiency is observed for maximum number of codes M per user. Performance of the M-ary signalling system degrades considerably over the fading multipath channels when compared with the non-fading channel. In order to achieve acceptable levels of performance, a combination of implicit diversity (multipaths) and explicit (antenna) diversity is recommendable.

5.3.2 Signal description and performance analysis for fading multipath signals

This performance analysis includes the description of the data signals, using auto correlation and cross-correlation properties. A model for M-ary signalling, as a method of improving the bandwidth efficiency, has been derived with the help of Chase [7]. The model, derived by Chase, was originated for radio communication at 900 MHz and is also valid for 60 GHz, because frequency-selective fading multipath exists for both frequencies. Each user has M sequences of length N available for spreading the datasignal and the M-ary likely data symbols are transmitted at a rate of one every T seconds.

The following model is appropriate for M-ary as well as for binary signalling. Binary signalling can be implemented in the model for M-ary signalling, by having one sequence available for each user. The data symbols for binary signalling take on values from the set $\{-1,1\}$ over a T-second time interval, using sequence inversion keying (SIK). SIK is the most common data modulation technique for binary signalling and has been explained in paragraph 3.4. This SIK is implemented by modulo-2 adding the data symbols with the sequence.

After spreading the information signal with sequences of length N by modulo-2 adding, the signal is phase modulated on the carrier signal with nominal carrier frequency ω_c in rad/s. The transmitted signal of the kth user is

$$s_k(t) = Re\left[\sqrt{2P}\, b_k(t-\tau_k)e^{j(\omega_c t+\theta_k)}\right], \tag{5.6}$$

where $k = 1,2,\ldots,K$, b_k is the symbol, P is the transmitter power, τ_k represents the initial time delay due to the positions of the subscribers ($\tau_1=0$) and θ_k is the carrier phase random distributed between $[0,2\pi]$.

The spreaded information signal is included in

$$b_k(t) = \sum_{p=-\infty}^{\infty} a_{k,m}(t-pT) \ , \tag{5.7}$$

with $m=1,2,3,...,M$ and $a_{k,m}$ representing sequence m containing the kth user data at the pth timing interval. The symbol time T is related to the sequence length and the chip time by $T=N\cdot T_c$. This sequence time T contains an integer amount of carrier periods, thus $T=i\cdot 2\pi/\omega_c$, with i an integer. Each user k has M sequences available, which are used for data transmission.

The sequences and chip waveform are included in

$$a_{k,m}(t) = \sum_{j=0}^{N-1} a_{m,j}^{(k)} P_{T_c}(t-jT_c) \ , \tag{5.8}$$

where $P_{T_c}(t)$ represents the chip waveform with duration T_c. The influence of the chip waveform on the performance has been described by Anjaria [1].

The complex equivalent low-pass impulse response of the channel can be represented by

$$h_k(t) = \sum_{l=0}^{L-1} \beta_{lk} \delta(t-\tau_{lk}) e^{j\Phi_{lk}} \ , \tag{5.9}$$

equivalent to equation (2.4).

The received signal for the fading model is given by [24]

$$\begin{aligned} r(t) &= Re\left[\sum_{k=1}^{K} h_k(t) * s_k(t)\right] + n(t) = Re\left[\sum_{k=1}^{K}\left(\sum_{l=0}^{L-1} \beta_{lk}\delta(t-\tau_{lk}) e^{j\Phi_{lk}}\right) * \left(\sqrt{2P}\, b_k(t-\tau_k) e^{j(\omega_c t+\theta_k)}\right)\right] + n(t) \\ &= Re\left[\sum_{l=0}^{L-1} \sqrt{2P} \sum_{k=1}^{K} \beta_{lk} b_k(t-\tau_k-\tau_{lk}) e^{j(\omega_c t+\theta_k-\omega_c\tau_{lk}+\Phi_{lk})}\right] + n(t) \ . \end{aligned} \tag{5.10}$$

with the path delays $0 \le lT_c \le \tau_{lk} \le (l+1)T_c \le T$. The background noise $n(t)$ includes the interference from external interference and the thermal noise contained in the total spread spectrum.

A coherent RAKE matched filter with maximum ratio combining for detection of the spreaded signal has its F taps on the moments $\frac{f}{W}$ with coefficients,

$$f_k = \sum_{f=0}^{F-1} a_f \cdot e^{+j\Phi_{lk}} \ . \tag{5.11}$$

The structure of this RAKE receiver, having the received signal of equation (5.10) as input and the CMF included in the RAKE receiver ($a_{k,\lambda}(t)$), adapted for symbol λ of user k is given in Figure 5.2.

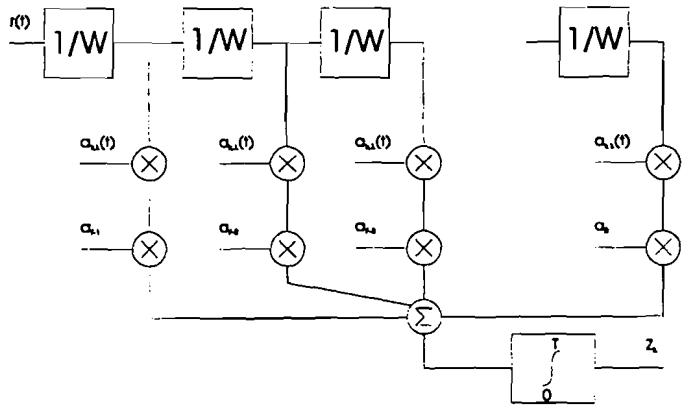

Figure 5.2: RAKE receiver with maximal ratio combining.

The decision variable Z_λ for symbol λ of the first user, using the RAKE receiver, equals

$$\begin{aligned} Z_\lambda &= Re\left\{\int_0^T r_c(t)\cdot f_1^*\cdot\sum_{f=0}^{F-1} a_{1,\lambda}(t-\frac{f}{W})\cdot e^{-j\theta_1}dt\right\} \\ &= \int_0^T\left[\sum_{l=0}^{L-1}\sqrt{2P}\sum_{k=1}^{K}\beta_{lk}b_k(t-\tau_k-\tau_{lk})e^{j(\theta_k-\omega_c\tau_{lk}+\phi_{lk})} + n(t)\right]\cdot\sum_{f=0}^{F-1} a_f a_{1,\lambda}(t-\frac{f}{W})\cdot e^{-j(\phi_f+\theta_1)}dt \\ &= \sqrt{2P}\int_0^T\sum_{l=0}^{L-1}\sum_{k=1}^{K}\sum_{f=0}^{F-1}\beta_{lk}a_f b_k(t-\tau_k-\tau_{lk})\cdot a_{1,\lambda}(t-\frac{f}{W})\cdot\cos(\theta_k-\theta_1-\omega_c\tau_{lk}+\phi_{lk}-\phi_f)dt \\ &\quad + \int_0^T\sum_{f=0}^{F-1} n(t)\cdot a_f\cdot a_{1,\lambda}(t-\frac{f}{W})\cos(\phi_f+\theta_1)dt\ , \end{aligned} \tag{5.12}$$

where $r_c(t)$ is the complex envelope of $r(t)$. The receiver for M-ary signalling is shown in Figure 5.3.

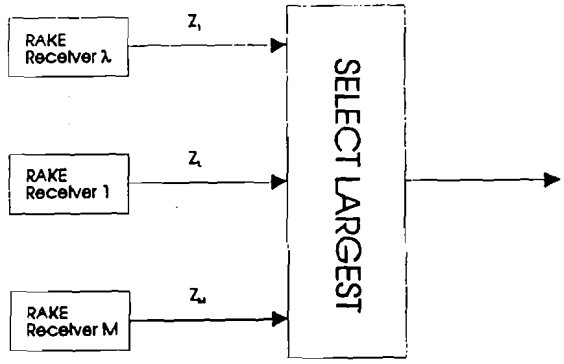

Figure 5.3: M-ary RAKE receiver structure.

Additive noise (interference) will fall into two basic categories, namely first wideband interference, characterised by thermal channel noise or overlaid spread spectrum subscribers, and second interference from narrowband communication channels. The interference power can be reduced by the narrowband data lowpass filter since the spectral density of the interference sources is reduced by the code-matched filter.

The SNR using the RAKE receiver can be calculated, using $E_b = \frac{PNT_c}{\log_2 M}$ and appendix A

$$SNR_{RAKE} = \frac{\left([Z_\zeta - Z_\lambda]\right)^2}{var\{Z_\zeta - Z_\lambda\}} = \frac{\left[\sqrt{2P}\sum_{l=0}^{L-1}\sum_{f=0}^{F-1}\beta_{ll}a_f R_{\lambda,\lambda}^{1,1}(\tau_{ll} - \frac{f}{W})\cos(\phi_{ll} - \omega_c\tau_{ll} - \phi_f)\right]^2}{N_{SI} + N_{MI} + N_I}, \tag{5.13}$$

where expressions for N_{SI}, N_{MI} and N_I are given in appendix A.

The probability of error can finally be approximated by making use of the Gaussian approximation for $R_{m,\lambda}^{k,1}(.)$ (the correlation function between code m of user k and code λ of user 1), due to the central limit theorem described in paragraph 2.3.3, as

$$P_r(\varepsilon) \approx \frac{M-1}{2} erfc\left(\sqrt{\frac{SNR_{RAKE}}{2}}\right). \tag{5.14}$$

Chapter 6 Simulation results

Two kinds of simulations have been performed, namely simulations generating the signals in the CDMA system (further referred to as "signal simulations") and simulations calculating the performance, based on a CDMA system in a multipath environment (further referred to as "performance simulations"). Simulations have been performed in the baseband using Matlab 4.2 on an UNIX machine. A number of files have been generated in Matlab for simulating the signals and the performance.

6.1 Overview of Matlab simulation programs

For simulating the codeset, the multipath channel and (de-) spreaded signals, several program files have been used.

A CDMA system with Gold sequences of length 31 has been generated by the program files:

codres.m	Applying a chip waveform to the Gold codes.
dataset.m	Applying databits by using SIK.
gold.m	Main program for calculating the transmitted and received signals.
gold0.m	Gold set containing non antipodal sequences.
goldset.m	Set of Gold codes of length 31.

The generated Gold sequences applied by multiple users and multipath are summated vectorial. Multipath profiles are generated by the program model.m and the environment configuration (amount of users, etc.) is implemented in main511.m. Several RAKE receiver types have been implemented as for example in rake.m. The post-correlation signal in the CDMA system using Gold codes can be determined by simulating spreading with Gold sequences and determining the correlation of the received signal with the originated sequence. A list of program files using Gold sequences of length 511 is:

adrake.m	Implementation of an adaptive RAKE receiver according to [3].
data511.m	Implementing the information by forming five successive sequences, used in main511.m.
fpois.m	Function for determining a statistical Poisson process, used in model.m.
frayl.m	Function for determining a statistical Rayleigh process, used in model.m.
gold511.m	Calculation of the Gold code set with sequence length 511, using shift registers, used in main511.m.

main511.m Main program for simulating the transmitted and received signals using Gold codes with length 511.

model.m Determining a statistical multipath profile for a specified user configuration using a model containing Rayleigh, Poisson and Uniform distributions, used in main511.m.

newrake.m RAKE receiver according to Mowbray [17].

norake.m Receiver without a RAKE structure, thus only a correlator, as used in main511.m.

rake.m Four types of combining the taps of a RAKE receiver according to [12], used in main511.m.

rakeherh.m Only containing the combining of the taps, not calculating the tap signals.

A selection of the most significant variables used in the programs is given in appendix B. The program files gold511.m, main511.m and model.m, using sequence length 511, are given in appendix C.

For simulating the performance in terms of bit error rate, by calculating the signal to noise ratio, the following files have been used:

c11.m Function for calculating the autocorrelation, as used in performance.m.

c12.m Function for calculating the cross-correlation, as used in performance.m.

perf511.m Generation of a profile to be used for performance calculations.

perform.m Program implementing all analytic formulas as described in paragraph 5.3.2.

The source file perform.m is given in appendix D.

A group of programs have been used for doing multiple simulations. These multiple simulations have been used for retrieving confident results for the performance estimation, by means of averaging BER curves. These programs are essential the same as the set given above, but now with invariable values for most of the parameters. These programs are:

mainperf.m Program for generating multiple profiles and calculating its performances for one configuration. This program is derived from main511.m.

profini.m Initialisation of several parameters.

profmod.m Program for generating a profile, with predefined multipath parameters. This program is similar to model.m, but now with the input parameters outside the routine.

profperf.m Performance calculation using analytic formulas as described in paragraph 5.3.2. This program is derived from model.m.

6.2 Signal simulations

Before starting simulations of the compound received signal and testing several receiver structures, several system configuration selections have to be made. Next, the implementation of the multipath model, according to paragraph 2.5, in the signal simulations is explained and several RAKE receiver structures are given attention.

6.2.1 Selection of the code set

The selection of the code set is based on consideration of the size of the available code set and the correlation levels. A consideration of the demands indicates the selection of the code set. The ability of a correlation receiver to detect the desired signal in presence of self-interference and other user interference relies to a great extent on the correlation properties of the codes. The intended indoor radio network is supposed to be used independently and simultaneously by approximately 50 users. Therefore, a code set with good performance for 50 simultaneously sequences is desirable. Considering the practical bandwidth possibilities of the radio frequecy band and equipment result in a conceivable maximum chip rate of approximately 100Mb/s.

With this background we can consider the code set and its contemplations in Mowbray [18]. An important consideration is given in paragraph 5.1, where is mentioned that for typical binary PN code sets applied to CDMA systems, only $0.1*N$ simultaneous subscribers can be supported with N the length of the code set. The Kasami sequences show a sequence set size of 32 belonging to a sequence length of 1023 and a sequence set size of 64 belonging to a sequence length of 4096. This latter sequence length, which we would need for 50 users, results in a too high chip rate demand. Gold codes have relatively larger code sets. A Gold code set of size 513 belonging to a sequence length of 511 is sufficient to support 50 users. Gold codes are also preferable compared to Kasami, because the frequency of "-1" in the cross-correlation is higher, with the drawback that the peak values of the cross-correlation are higher in the Gold codes.

For reasons given above and in paragraph 3.7, the Gold code set has been chosen as optimal for the spread spectrum system.

6.2.2 Sequence length and generation of the Gold codes

The auto and cross-correlation for a Gold code set with sequences of length 31 is bounded to the three values {-9, -1, 7}. The Gold code set with sequence length 31 can be generated with ght Matlab program "goldset.m". This program uses the two sequences given on page 81 of [6] and generates the complete set by shifting and modulo-2 adding. The multiple access capacities for this generated Gold code set is limited by its code set size. The correlation properties are illustrated in Figure 6.1.

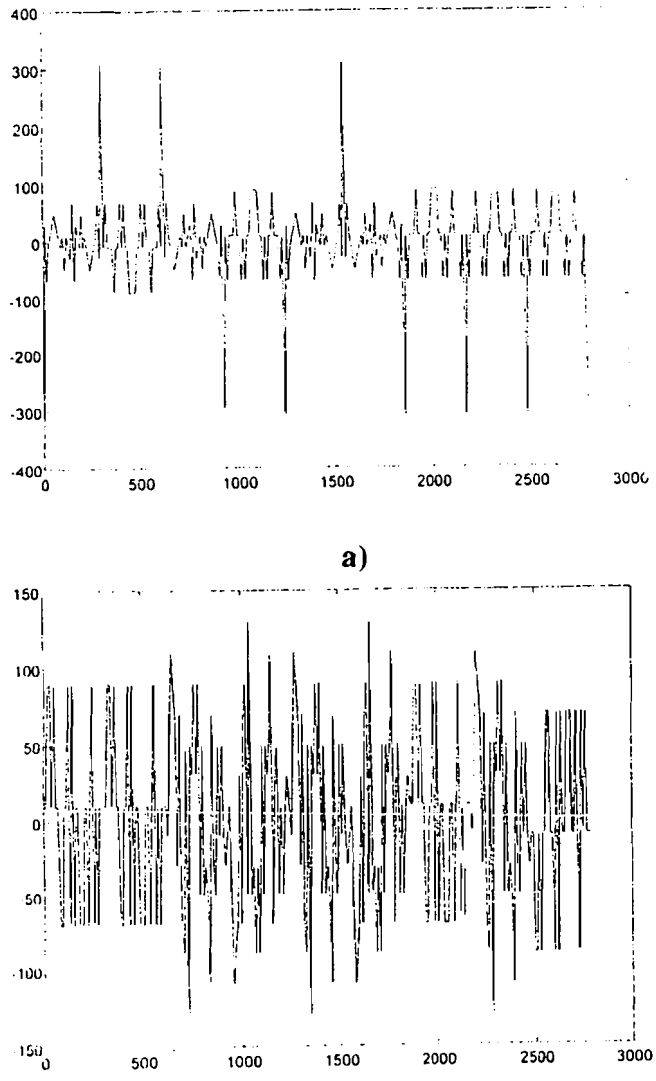

Figure 6.1: a) Auto and b) cross-correlation for Gold sequences of length 31.

Paragraph 5.1 showed a system capacity of $0.1N$ for a BER of 10^{-5}. Therefore, a long sequence is required to have sufficient performance with a sufficient amount of users. Too long spreading codes should be avoided in view of the bandwidth efficiency. No Gold sequences of length 255 (n= 8) exist [11]. Gold sequences with length 1023 are above

requirements for 50 users and unnecessarily decrease the bandwidth efficience. Therefore, Gold sequences with length 511 has been chosen for the simulations.

The Gold code set, with sequence length 511, has been generated according to paragraph 3.7.2, by using the feedback sets [9, 6, 4, 3] and [9, 5, 3, 2] in the program "gold511.m" in Matlab. These feedback sets represents the feedback taps at the stages of the register, which are modulo-2 added and fed into the first stage of the shift register. The generated Gold code set showed the three valued {-33, -1, 31} auto and cross-correlation. This correlation properties are shown in Figure 6.2.

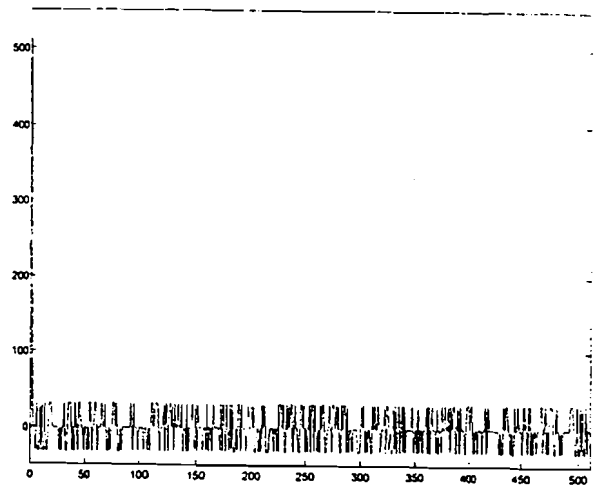

a)

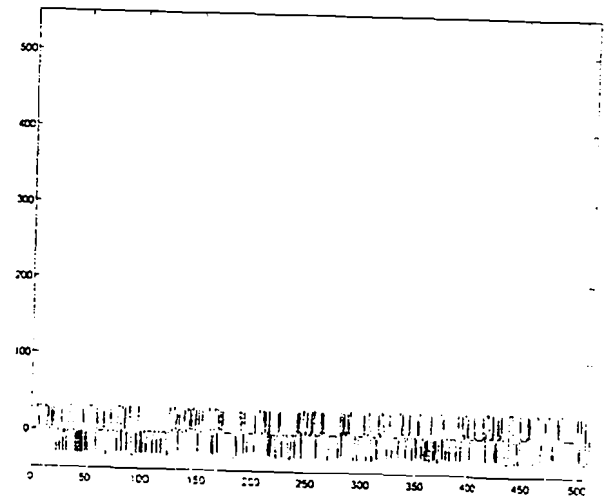

b)

Figure 6.2: a) Auto and b) cross-correlation for Gold sequences of length 511.

A selection of the optimal codes from the set, which has been described in paragraph 3.9, is

useful to obtain better correlation properties. The selection of the balanced codes results in diminishing the Gold code set from the original N+2=513 to 257. Further selection on low correlation values near the auto correlation peak, for synchronisation purpose, results in further decreasing the code set size to 125 sequences.

The bit rate for binary signalling is determined by the maximum achievable chip rate and the sequence length. This indicates the demand for techniques to increase the bit rate, to transport broadband services over the indoor radio network with bit rates of approximately 40 Mb/s. Several solutions exist for increasing the bit rate at maximum chip rate, as using M-ary DPSK modulation systems or multi-carrier modulation technique. The use of internal or external diversity can be used to increase performance in a multipath environment.

6.2.3 Implementation of the Poisson distributed path delays and Rayleigh distributed path amplitudes

The multipath model according to paragraph 2.5 has been implemented to be used for generating multipath profiles. Before starting the calculation of the Poisson and the Rayleigh distributed process, the results of the measured propagation properties in several environments [30] have to be translated into the parameters of the statistical process. These parameters are the maximum amount of rays, the power loss after the first ray Δ_{LOS}, the factor A in dB/ns, the moment t_1 and the mean arrival rate λ. From the moment t_1 the logarithm of $\overline{\beta_{lk}^2}$ starts decaying with the factor A. The transmitted power P in the measurements equals 50 mW and the normalized received power level of the first ray $\overline{\beta^2(0)}$, follows from the measured power for the first ray or from calculations with the radio equation (paragraph 2.3).

The Poisson process has been defined in Matlab by the function fpois.m, having mean arrival rate λ as input. The Poisson process has been represented by a vector of length 100, containing the cumulative distribution function of a Poisson process based on the mean arrival rate λ. The cumulative distribution function is given by

$$F_{pois} = e^{-\lambda \cdot t} \quad . \tag{6.1}$$

To have the Poisson process in a vector of length 100, requires scaling of the function F_{pois}. Scaling has been performed by a correction factor that brings back the function F_{pois} in such a way that the process up to 99.99% of the convergent value for large t is included in the vector. A Poisson distributed interarrival time is retrieved by calculating a random figure between zero and one and taking the time corresponding to this value of F_{pois}. This time need to be corrected with the correction factor.

The main program in Matlab is based on equidistant time intervals. To have a most truthful simulation, these time intervals should be as small as possible, which has the drawback that the calculations require more time. The rays have delay times according to the Poisson process, which need to be translated to the equidistant time intervals in the simulations. This has been done by rounding off the calculated times, according to the Poisson process, to fixed time intervals of $T_c/10$. Compromises have to be made between deviating from the Poisson process or having longer calculations times. Simulations with a chip rate of 100 Mchip/s and using time intervals of $T_c/10$, which is 1 ns, is not according to the Poisson model. Though it is not inferior to the measurements, which also used a time resolution of 1 ns.

The Rayleigh distributed path amplitudes have been represented by using a vector of length 100, containing the cumulative distribution function of a Rayleigh process based on the normalized received power $\overline{\beta_{lk}^2}$ at the path l for user k. The cumulative distribution of the Rayleigh function is given by

$$F(\beta_{lk}) = 1 - e^{-\frac{\beta_{lk}^2}{\overline{\beta_{lk}^2}}}. \tag{6.2}$$

The normalized received power $\overline{\beta_{lk}^2}$ has been used as the input of the function frayl.m.

To have the Rayleigh process in a vector of length 100, requires scaling of the function F_{pois}. Scaling has been performed by a correction factor that brings back the function F_{pois} in such a way that the process up to 99.99% of the convergent value for large $\overline{\beta_{lk}^2}$ is included in the vector. A Rayleigh distributed path amplitude is retrieved by calculating a random figure between zero and one and taking the value corresponding to this value of $F(\beta_{lk})$. This amplitude β_{lk} need to be corrected with the correction factor.

The multipath model is illustrated by the figures in appendix E. These figures includes the Rayleigh distributed ray amplitudes as a function of the Poisson distributed interarrival time. Also rounding off to the fixed time intervals of $T_c/10$ is shown with a chiprate of 100 Mchip/s. No obvious difference can be noticed compared to the original arrival times.

6.2.4 Receiver structure

In a time dispersive environment, effects of multipath propagation must be accounted for in the receiver. A RAKE receiver is used to combine the rays. The RAKE receiver has been implemented in the signal generating simulations as well as the performance simulations.

Several types of RAKE receivers have been implemented in the signal generating simulations with different effects on the correlation output. The goal of the RAKE receiver is to compensate the negative influence from multipath propagation and interference by controlling attenuators at the taps with respect to the power level. For low multipath with high interference, the signal will optimally be recovered by selecting the strongest signal of the RAKE receiver taps. For high multipath and low interference, the signal will optimally be recovered by summing the weighted tap signals.

Five different methods for diversity combining have been used for simulations with a tap spacing of $1/W$ [12]:

1. The strongest tap signal is selected.
2. The two strongest signals are summated (diversity combining).
3. Signals with a level > 40% of the strongest are added.
4. Normalizing the strongest signal level to one and attenuating the others in function of their levels:
   - - 3 dB for levels 0.4-0.7
   - - 6 dB for levels 0.25-0.4
   - maximum attenuation for levels < 0.25.

   This is an approximation of maximum ratio combining.

The RAKE receiver is dimensionized with taps at $1/W$, so that it can combine information from the received tap signals. Having a very high chip rate ($1/W$), due to a high bit rate combined with long code sequences, increases the effects of multipath. The RAKE receiver with stricted tap spacing, which works over a period of (the amount of taps F)* $1/W$ is not as effective for high chip rates. The optimal RAKE receiver consists of $F = T_m * W + 1$ taps, with T_m the maximum delay spread and combines the largest paths by having adaptive tap spacing ranging the F taps on the F largest paths.

Interference cancellation (IC), by detecting a users symbol and then removing its contribution from the compound data signal, increases the performance drastically. With this CDMA-IC concept the receiver becomes much more complex. The receiver requires knowledge of the sequences of all the other users to cancel them. This technique has not been implemented in the simulations.

6.2.5 Signal simulations for various amount of users and several multipath situations

Random data bits using SIK can be used for testing its correlation performance. The compound received signal can be tested by vectorial adding several sequence by superposition, which is allowed since the simulations are based on PSK modulation. Several simulations calculating the compound received signal and post-correlation signal have been performed in Matlab 4.2.

Since the maximum amount of active users is restricted indirectly to the sequence length, as shown in paragraph 6.2.2, simulations have been performed for a sequence length of 511. Simulating with an one-path and a multipath model with uniformly constant amplitudes and random path arrival times is useful to get an idea of the possibilities with this multiple-access system. These simulations included combinations of

- one-path or multipath, which were generated by uniformly constant amplitude and random distributed path arrivals and path phase shifts.
- one user or multiple simultaneous users.
- receiving with a CMF or receiving with several RAKE receiver types with F taps.

The correlation properties can be found by correlating the compound received signal with a sequence of one of the users. The first set of simulations, shown in appendix F.1, is performed with a chip time T_c of 1 ns, equidistant time intervals of $T_c/2$, a sequence length N of 511 and the amount of users varies K from 10 to 40. The post-correlation signal is retrieved by a correlation receiver, without combining techniques. Therefore, the auto correlation peak for one user has the maximum value of $2*N=1022$. This one-path simulation show increasing cross-correlation for increasing amount of users and the auto correlation peak is influenced by the cross-correlation with other users.

The second set of simulations, shown in appendix F.2, is performed under the same conditions as the first one, but now instead of varying the amount of users, the amount of received rays is varied from 2 to 16. These paths use the multipath model, consisting of random distributed arrival times (from 0 to 50ns), constant amplitudes and uniformly distributed phases. This simulation set shows that data recovery requires special combining techniques, which correct the channel characteristics.

The simulation sets of appendix F.1 and F.2 showed that data recovery is more complex for a multipath channel combined with multiple users. Benefit could be taken from the multipath profile by applying a RAKE receiver. The effect of the RAKE receiver, as it has been applied

in the signal simulations, is shown in appendix F.3 and F.4. Appendix F.3 uses a receiver technique, which combines the received rays, by using the knowledge of the exact arrival of the rays and its complex amplitude. The two rays are combined by correcting for their phase shifts and complementing the two rays. This technique was only effective for a small amount of multipath signals.

Next, simulations with the multipath model, as described in paragraph 2.5, have been performed to get an idea of the possibilities for CDMA in the multipath environment. The multipath model has the same parameter set for all five users, namely $1/\lambda$=1e-9 ns, 200 ray arrivals, B(0)=0 dB, Δ_{los}=4 dB, t_1=0 ns and A=-0.1 dB/ns. The post-correlation signals using the multipath model are illustrated in appendix F.4.

In practice heavily multipath as well as cross-correlation exists and make it harder to distinguish the multipath correlation peaks from the cross-correlation peaks. The difference between the auto correlation peak level and the cross-correlation peak levels decreases or even vanish for an increasing amount of interfering sequences. For heavily multipath, the distortion on the post-correlation signal from this multipath is big, and therefore a RAKE receiver is necessary to resolve the multipath components. RAKE combining techniques, as given in paragraph 6.2.4, are applied to the compound signal of 5 users each with 200 multipath rays. The results of the applied RAKE receiver structures are given in appendix F.4, but shows that these structures are not sufficient to resolve the multipath signals, each consisting of 200 rays.

6.3 Performance simulation

The expressions for the performance of a CDMA system using M-ary sequences, derived in paragraph 5.3.2, have been implemented in Matlab to determine the BER under several conditions. The determinations of the BER are performed by averaging the BER over a large amount of generated channel profiles.

This model contains several approximations:

- The cross-correlations of the sequences have been approximated by the Welch lower bound. No distinction has been made for the selection of a code set.
- The distribution of the correlation function $R_{\nu,\lambda}^{k,l}(\cdot)$ has been approximated to be Gaussian due to the central limit theorem. Also the difference of the decision variables are assumed to be Gaussian distributed.

6.3.1 Validation of the simulations

Before using the performance simulations, the simulations have to be validated. This validation can be done by using p. 716-728 of Proakis [23], where the theoretical performance for coherent detection of binary frequency-shift keying (BFSK) in fading channels is given. For binary signalling over a single path with transmitted signal $u(t)$, the received signal can be given by

$$r(t) = \beta e^{-j\phi} u(t) + n(t) \ , \tag{6.3}$$

with the path amplitude β Rayleigh distributed. The average received signal to noise ratio $\overline{\gamma_b}$ can be given by

$$\overline{\gamma_b} = \frac{E_b}{N_0} \cdot E(\beta^2) \ . \tag{6.4}$$

The probability of error for BFSK is given by

$$P_r(\varepsilon) = \frac{1}{2}\left[1 - \sqrt{\frac{\overline{\gamma_b}}{2+\overline{\gamma_b}}}\right] . \tag{6.5}$$

This probability of error function can be used for the validation of a multipath fading channel with a RAKE receiver with one tap [3].

The error rate performance for a binary digital communication system with diversity of order L shows for the low-pass received signals for the L channels

$$r_l(t) = \beta_l e^{-j\phi_l} u_{l,m}(t) + n_l(t) \ , \tag{6.6}$$

with $l=1,..,L$ and $m=1,2$. Proakis derived an expression for the performance, namely

$$P_r(\varepsilon) = \left(\frac{1-\mu}{2}\right)^L \cdot \sum_{l=0}^{L-1} \binom{L-1+l}{l} \cdot \left(\frac{1+\mu}{2}\right)^l \ , \tag{6.7}$$

with $\mu = \sqrt{\overline{\gamma_c}/(2+\overline{\gamma_c})}$ for BFSK and $\mu = \sqrt{\overline{\gamma_c}/(1+\overline{\gamma_c})}$ for BPSK, both using coherent detection.

For coherent detection it was assumed that the channel is time-invariant, or quasi-static, and having a receiver using noiseless estimates of the channel parameters. The average SNR per channel $\overline{\gamma_c}$ is related to the average SNR per bit by $\overline{\gamma_b} = L \cdot \overline{\gamma_c}$, assuming an identical $\overline{\gamma_c}$ for all channels. This performance curve of equation (6.7) can be compared with a simulated fading channel applying an ideal RAKE receiver, which combines optimally the largest paths by having optimally tap spacing.

One method of evaluating the performance is to give the BER as a function of the average

received signal to white Gaussian noise ratio per bit $\overline{\gamma_b}$. This $\overline{\gamma_b}$ can be given as a function of the average energy per transmitted bit to white Gaussian noise ratio $(E_b/N_0)_t$ by [15]

$$\frac{E_{b,r}}{N_0} = \frac{\overline{[\sum_{l=0}^{L} \beta_{l,R}^2]} \cdot E_{b,t}}{N_0} = \frac{L \cdot \overline{[\beta_R^2]} \cdot E_{b,t}}{N_0}, \tag{6.8}$$

where the value of the energy per bit $E_{b,t}$ equals $P*T_b = P*T_{symbol}/\log_2(M)$ and the expectation of the path amplitudes is approximated to be equal for all paths. The system is configured for M-ary signalling and shows an information rate r_b of $r_{symbol}\log_2 M$ bits/sec.

Using the spreading feature shows for the transmitted energy per bit $E_{b,t}$ the value $P*N*T_c/\log_2(M)$, with P the transmitter power, N the sequence length, M the sequence set size per subscriber and T_c the chip time. $\sum_{l=0}^{L} \beta_{l,R}^2$ represents the total path gain for user R, which is a result of losses on the path and the antenna configurations as shown in paragraph 2.3, and its value has been measured using a transmitted power P of 50 mW [30]. The thermal noise at the output, introduced by the RAKE taps has been calculated by the sum of the quadratures of the tap coefficients $\sum_{f=0} |a_f(f)|^2$.

The performance simulations have been validated by simulating a two-path model, with path spacing $1/W$ = 40ns, with one simultaneous user, and using an one-tap respectively a two-tap RAKE receiver. The amplitudes of the rays have been implemented to follow a Rayleigh distribution with $\overline{\beta_{lk}^2}$=2*0.637 equivalent to [3]. Both rays in the two-path model have a Rayleigh distribution around the average $\overline{\beta_{lk}^2}$. Due to this Rayleigh process, the simulated BER has to be averaged over a large number of profiles to approach the theory. Figure 6.3 shows the comparison of the theory for fading channels and simulations.

The validation of the simulations have been performed by averaging over 2.500 two-path profiles for curve (1) and over 17.000 for curve (4), while Chase [23] used 50.000 profiles. Considering the performance results, shows very low BER for most of the profiles and the average over the 2500 profiles is mostly determined by several worst case profiles. Therefore better fitting of the simulated curves to the theory will be obtained by averaging a larger set of profiles. The limited amount of averages combined with the influence of the machine accuracy, cause an increased deviation from the theoretical curve for low BER rates.

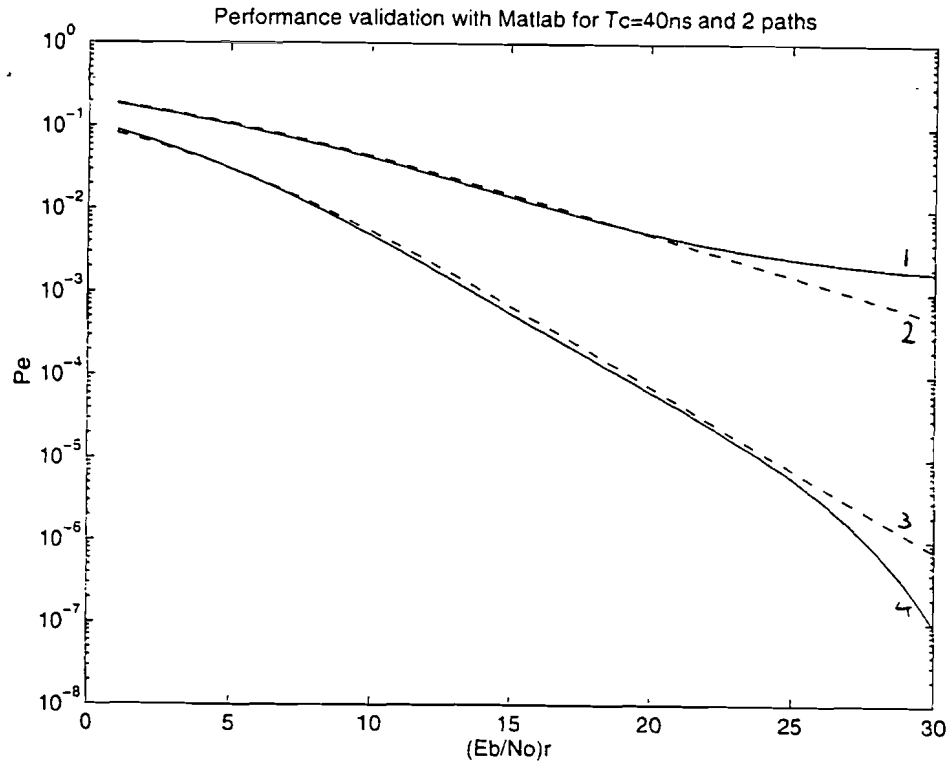

Figure 6.3: Performance validation with Matlab using two Rayleigh distributed paths with (1) simulation of one RAKE tap, (2) Proakis fading channel, (3) Proakis 2 orders of diversity and (4) simulation of two RAKE taps.

6.3.2 Translation Matlab to Fortran

As in paragraph 6.3.1, the performance simulations in a multipath environment have to be averaged over a large number of BER curves. Calculating the BER as a function of the average received SNR by averaging over 2500 profiles, seemed to be not confident enough, because variation among different averaged profile sets was present. Therefore, averaging over 25.000 profiles is necessary. Having access to these 25.000 gives the opportunity to give the performance in terms of performance outage as well.

Performing simulations for 25.000 profiles, gives an enormous rise to the simulation time. These simulations performed by Matlab often take several days, which is unbearable for generating results under varying conditions. Therefore a way of increasing the speed of the simulations is necessary. This could be done by writing some of the m-files of Matlab in the faster C language or Fortran, which could also be used by Matlab in the form of mex-files. Performing simulations on a faster hardware system, could be a feasable option too.

A critical note is placed to the simulations performed in Matlab. Matlab is an useful tool for generating fast output to relative small simulations. Extensive and large-scale simulations often result in large simulation times, due to the inefficiency of the interpreter Matlab. Programming in other languages as C++ or Fortran is more complex, but is faster in calculating more powerful expressions. Matlab is fast for implementing expressions, but slow in calculating these expressions.

To reduce the simulation time to manageable size, the performance simulations have been translated to the Fortran language. This Fortran program has the same structure as the program written in Matlab. The main differences between the two languages are firstly, the use of the variables, because the references to variables are more complex in the Fortran language than in Matlab, and secondly, the translation of special known functions in Matlab, has been written out as functions in Fortran.

Also this Fortran program has been validated to the theory, by averaging over 10.000 profiles, and is illustrated in Figure 6.4.

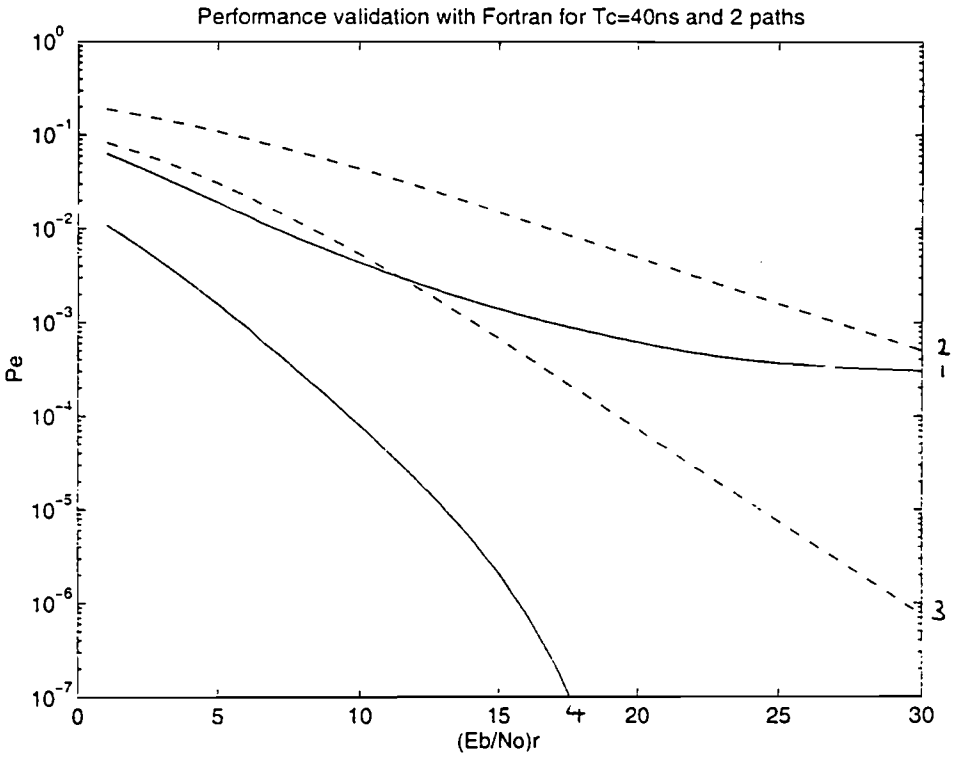

Figure 6.4: Performance validation with Fortran using two Rayleigh distributed paths with (1) simulation of one RAKE tap, (2) Proakis fading channel, (3) Proakis 2 orders of diversity and (4) simulation of two RAKE taps.

This validation shows that the average performance simulated by Fortran, does not approach the performance curves of the theory. The Fortran program is a direct translation of the programs used in Matlab for the validation. The explanation for the difference in results has not yet been found, but could be a program technical problem in Fortran, as i.e. with variables.

Another issue to consider is the accuracy of the simulations in Fortran. By comparing the results of two simulations in Fortran performed on two different systems, showed that the values of BER agreed for the first five to six digits. This comparison indicates the order of magnitude of the accuracy. The simulated averaged performance curves starts decaying relatively faster than the curves according to the theory, for $(E_b/N_0)_r$ values beyond 15 dB. The simulated curve (4) in Figure 6.4 reaches there a BER of 10^{-6}, which is beyond the proved accuracy of the simulations in Fortran and could be a reason for the relative fast decaying of (4).

6.3.3 Performance simulation results

The performance simulations can be carried out under varying conditions by giving values to parameters such as the amount of users, amount of rays and profile defining parameters. When giving values to the parameters of the profiles to be generated in the simulations, attention need to be paid to the background of the parameters. The RAKE receiver has a default tap spacing of one chip time and this receiver structure only produces valid simulations values, when the RAKE taps are within the range of the multipath profiles. This prevents having RAKE taps in the area where no received rays exist.

Since simulating the performance with the Matlab programs require too much time, these simulations should be performed with Fortran. This Fortran program is orders of magnitude faster, but has not correctly been validated to the theory. For these reasons, no results of the performance have been retrieved yet. Further research on the performance of DS-CDMA over millimetre wave indoor radio channels could start with the attempt to validate the Fortran program to the theory, with goal to use this program for the performance simulations.

Chapter 7 Conclusions and recommendations

A wireless network has several advantages above conventional cable systems. Wireless "Broadband" services (bit rates > 2 Mb/s) for this wireless network require wideband communication, which can be accommodated in millimetre wave frequency bands from about 25 GHz. The waves are reflected against walls. The indoor radio propagation channel is characterised as a multipath channel, which exhibits time dispersion and frequency selective fading. A statistical model has been implemented similar to the measurements performed at EUT.

Code Division Multiple Access (CDMA) provides bandwidth expansion by a factor N, by spreading the data signal with codes of length N. The processing gain $G_p=10^{10}logN\ dB$ is effectively the signal power gain over all the interference present in the communication channel. By assigning specific codes from a correct code set to the users, multiple-access possibilities are provided. The pseudo-random codes make the signal appear similar to random noise and thus harder to demodulate by unintended users. The Gold code set has been selected due to its attractive correlation properties combined with its relative large set size. The receiver compresses the signal into its original band.

Using a spread spectrum signal with bit time T_b, and the selection that $T_b=N\cdot T_c$ in a multipath environment with multipath spread T_m results in a diversity of order T_m/T_c. The most significant diversity combining technique, mostly used for spread spectrum systems, is known as a RAKE receiver. The RAKE receiver uses the correlation properties of a spread-spectrum signal to resolve the multipath signals and combine them.

A model for binary modulation or for M-ary modulation as a method of improving the bandwidth efficiency, has been described. Each user has M sequences of length N available for spreading the datasignal. A coherent RAKE matched filter with maximum ratio combining for detection of the spreaded signal has its F taps located on the moments $\frac{f}{W}$, where $f=f..F$. The performance has been analyzed, by using the auto and cross-correlation properties of the codes.

Two kinds of simulations have been performed in Matlab, namely simulations generating the signals in the CDMA system in a multipath environment and simulations calculating the performance. The simulations are based on a Gold code set, using a sequence length of 511 and consequently three valued {-33, -1, 31} auto and cross-correlation. This length is a

compromise between bandwidth efficiency and subscriber capacity. The statistical multipath model, based on the properties in an indoor radio environment, has been implemented in both simulations.

The maximum bit rate using binary modulation is limited by the maximum chip rate and the sequence length. A Gold sequence length of 511 combined with the maximum chip rate of 100 Mchip/s, limited by the equipment and radio spectrum, restricts the bit rate using Sequence Inversion Keying (SIK) to 200 kbit/s. Increasing the bit rate is possible by applying M-ary modulation, which increases the bit rate with $\log_2 M$, applying coding techniques, or by multi-carrier techniques, or by applying more complex receiver structures or antenna diversity.

Several simulations for calculation the compound received signal and post-correlation signal have been performed. These simulations included varying amount of users combined with a deterministic or statistical multipath model. Rounding off of the Poisson distributed arrival times to the fixed time intervals of $T_c/10$ was necessary for simulating. The Poisson properties were satisfactory for a chip rate of 100 Mchip/s, by comparing the rounded arrival times to the original arrival times. The results showed that applying multipath limits the maximum amount of users drastically. Benefit has to be taken from the multipath profile by applying a RAKE receiver.

The simulations of the performance were started with the validation of the simulation program to theoretical results. The Matlab simulation program was validated for the case of two paths, separated by one chip time, by comparing the average Bit Error Rate (BER) curves of the simulations with the theory. The validation was only successful by averaging the generated BER curves over a large amount of curves. Simulating average BER curves over such a large amount of curves (17.000), which seemed to be necessary, gave rise to the demand for faster simulations. The translation of the Matlab program to a Fortran program increased the speed of the simulations drastically, but that program has not yet been validated.

Recommendations

Simulations could be performed to determine the possibilities of the indoor radio communication network based on CDMA. The performance simulations can be done by applying the Gold coding instead of the random orthogonal codes, by inserting the auto and cross-correlation properties in the simulation model. Also the influence of the code set and the sequence length can than be determined. Several other criteria to consider the system for are the maximum amount of users, the influence of the multipath environment, the maximum transmission rate and the amount of RAKE taps

Most of these simulations require averaging of performance curves over a large set of curves. This averaging of simulated BER curves often take several days and could better be done in Fortran instead of with Matlab. Therefore, further attempts should be made to validate the results of the simulations in Fortran to the theory. Good starting points for improving the validation are considering the accuracy of the simulations, checking the variables and their types or the implemented equations.

Acknowledgements

This work has been performed at the Telecommunications Division and was supported by Ir. P.F.M. Smulders. I would like to thank Peter for this support. A special word of thanks is directed to Ad de Jong, employed at the computer centre, who translated the performance simulations from Matlab to a Fortran program.

Literature

[1] Anjaria, R. and R. Wyrwas
The effect of chip waveform on the performance of CDMA systems in multipath, fading, noisy channels.
Vehicular Technology Society 42nd VTS Conference.
New York, 10-13 May 1992, vol.2, p. 672-5.

[2] Blanz, J. et al.
Eb/No performance of a joint detection CDMA mobile radio system using coherent receiver antenna diversity
Cost 231, Limerick, TD(93) 102, September 1993, p. 1-20.

[3] Chase, M. and K. Pahlavan
Performance of DS-CDMA over measured indoor radio channels using random orthogonal codes
IEEE Transactions on vehicular technology, vol. 42, November 1993, p. 617-624.

[4] Dersch, U.
Physical modeling of macro, micro and inhouse cell mobile radio channels
PIMRC'92, The third IEEE International Symposium on personal indoor and mobile radio communications
Boston, Massachusetts, October 19-21 1992, p. 64-68.

[5] Diaz, P. and R. Agusti
Analysis of a fast CDMA power control scheme in an indoor environment
PIMRC'92, The third IEEE International Symposium on personal indoor and mobile radio communications
Boston, Massachusetts, October 19-21 1992, p. 67-70.

[6] Dixon, R.C.
Spread spectrum systems
New York: John Wiley & Sons, 1984

[7] Enge, P.K. and D.V. Sarwate
Spread-spectrum multiple access performance of orthognal codes: linear receivers
IEEE transactions on communications, com-35, Dec. 1987, p. 1309-1319

[8] Falconer, D.D. and G.M. Stamatelos
Wireless access to broadband services through mircocellular indoor systems

[9] Gilhousen, K.S. et al
On the capacity of a cellular CDMA system
IEEE transaction on Vehicular Technology, vol 40, May 1991, p. 303-312

[10] Glance, B. and L.J. Greenstein
Frequency-selective fading effects in digital mobile radio with diversity combining
IEEE Transactions on communications, vol. com-31, Sept. 1983, p. 1085-1094

[11] Gold, R.
Optimal binary sequences for spread spectrum multiplexing
IEEE Transactions on information theory, vol. IT-13, Oct. 1967, p. 619-621

[12] Grob, U. et al.
Microcellular Direct-Sequence Spread-Spectrum radio system using N-path RAKE receiver
IEEE journal on selected areas in communications, vol. 8, no. 5, june 1990, p. 772-779

[13] Ha, T. T.
Digital Satellite communications
second edition
New York: McGraw-Hill Publishing Company, 1990

[14] Kamperman, F.L.A.J.
Design study for a spread-spectrum picoterminal satellite network and the realization of a modem
Eindhoven, Technische universiteit Eindhoven, Instituut Vervolgopleidingen, 1993. Doctoral dissertation

[15] Kavehrad, M. and P.J. McLane
Performance of low-complexity channel coding and diversity for spread spectrum in indoor, wireless communication
AT&T Technical Journal, vol 64, No. 8, October 1985, p. 1927-1961

[16] S. Y. Liao
Microwave analysis and amplifier design
New Jersey: Prentice Hall inc., 1987

[17] Mowbray, R.S., Grant P.M. and R.D. Pringle
New antimultipath technique for spread spectrum receivers
IEEE Electronics letters, vol 29, March 1993, p. 456-458

[18] Mowbray, R.S. and P.M. Grant
Wideband coding for uncoordinated multiple access communication
Electronics & Communication engineering journal, Dec. 1992, p. 351-361

[19] Mowbray, M.I., Pringle, R.D. and P.M. Grant
Increased CDMA system capacity through adaptive cochannel interference regeneration and cancellation
IEE Proc.-I, vol 139, October 1992, p. 515-524

[20] Pahlavan, K. and M. Chase
Spread-spectrum multiple-Access performance of orthogonal codes for indoor radio communications
IEEE transactions on communications, vol. 38, May 1990, p. 574-577

[21] Peterson, W.W. and E.J. Weldon, Jr.
Error-correcting codes
Second edition
London: The MIT press, 1972

[22] Povey, G.J.R., Grant, P.M. and R.D. Pringle
Performance of a direct-sequence spread spectrum receiver for a UHF multipath channel
IEE colloquim vol 161, 1992, p. 5/1-4

[23] Proakis, J.G.
Digital communications
Second edition
Singapore: McGraw-Hill Book Company, 1989

[24] Pursley, M.B. et al
Error probability for Direct-Sequence Spread-Spectrum Multiple-Access communications - Part I: Upper and lower bounds
IEEE Transactions on communications, vol. com-30, May 1982, p. 975-984

[25] E.W.A.M. Ruis
An Object-Oriented Programming approach to the modelling of mm-wave Indoor Radio Channels
Eindhoven, Eindhoven University of Technology, February 1994, Graduation Th.

[26] Saleh, A.A.M. and R.A. Valenzuela
A statistical model for indoor multipath propagation
IEEE journal on selected areas in communications, vol. SAC-5, No. 2, Feb. 1987, p. 128-137

[27] Skolnik, M. I.
Radar Handbook
Second edition
New York: McGraw-Hill publishing company,

[28] Smulders, P.F.M. and A.G. Wagemans
A statistical Model for the Mm-wave indoor radio channel
PIMRC'92, The third IEEE International Symposium on personal indoor and mobile radio communications
Boston, Massachusetts, October 19-21 1992, p. 303-307

[29] Smulders, P.F.M. and H.T. Müskens
Performance of decision feedback equalization in mm-wave indoor systems
Proceedings of the ICUPC'93, Ottawa, p. 890-893

[30] Smulders, P.F.M. and A.G. Wagemans
Wideband indoor radio propagation measurements at 58 GHz
Electronic Letters, vol 28, June 1992, p. 1270-1271

[31] Smulders, P.F.M. and A.G. Wagemans
Frequency domain sounding of mm-wave indoor radio channels
Proceedings of the ICUPC'93, Ottawa, p. 636-640

[32] Smulders, P.F.M. and A.G. Wagemans
Millimetre-wave biconical horn antennas for near uniform coverage in indoor picocells
Electronics letters, vol. 28, No. 7, 1992, p. 679-680

[33] Tachikawa, S.
Spreading codes for spread spectrum communication systems.
Electronics and Communication in Japan, vol 75, no. 6, 1992, p. 41-9

[34] Tuch, B.
Development of WaveLAN, an ISM Band Wireless LAN
AT&T Technical Journal, july 1993, p. 27-37

[35] Turin, G.L.
The effects of multipath and fading on the performance of direct-sequence CDMA systems
IEEE Journal on selected areas in communications, vol. SAC-2, No. 4, July 1984, p. 597-603

[36] Turin, G.L.
Introduction to spread-spectrum antimultipath techniques and their application to urban digital radio
Proceedings of the IEEE, vol. 68, No. 3, March 1980, p. 328-353

[37] Wagemans, A.G.
Measurement and Statistical Modelling of Indoor Radio Channels in the mm-wave frequency band
Eindhoven, Eindhoven University of Technology, 1992, Graduation Th.

[38] Welch, L.R.
Lower bounds on the maximum cross-correlation of signals.
IEEE Transactions Information Theory, IT-20, May 1974, p. 397-399

[39] Wilkinson, T.A. and S.K. Barton
Spread spectrum for radio LANs
IEE colloquim, vol 104, 1992, p. 6/1-4

Appendix A

The continuous-time cross-correlation function of the mth sequence of the kth user with the λth sequence of the i th user can be represented by

$$R_{m,\lambda}^{k,i}(\tau)=\int_{0}^{\tau} a_{k,m}(t-\tau)a_{i,\lambda}(t)dt$$
$$R'^{k,i}_{m,\lambda}(\tau)=\int_{\tau}^{T} a_{k,m}(t-\tau)a_{i,\lambda}(t)dt \ , \tag{A.1}$$

with $0<\tau<T$. These two partial correlation functions can be combined together with the data information into the total correlation function. If the two adjacent data symbols, thus the two adjacent sequences, happen to be the same, the sum of the two partial correlations turns into a full correlation.

For rectangular symbol and chip waveforms the continuous-time cross-correlation of the mth sequence of the kth user with the λth sequence of the i th user can also be represented by

$$\begin{aligned} R_{m,\lambda}^{k,i}(\tau) &= C_{\xi,\lambda}^{k,i}(l-N)T_c+[C_{\xi,\lambda}^{k,i}(l+1-N)-C_{\xi,\lambda}^{k,i}(l-N)]\cdot(\tau-lT_c) \\ &\quad + C_{m,\lambda}^{k,i}(l)T_c+[C_{m,\lambda}^{k,i}(l+1)-C_{m,\lambda}^{k,i}(l)]\cdot(\tau-lT_c) \ , \end{aligned} \tag{A.2}$$

where for $\tau>0$ the value of l equals $\lfloor \tau/T_c \rfloor$ thus $\tau\in[lTc,(l+1)Tc]$ and for $\tau<0$ the value of l equals $\lceil \tau/T_c \rceil$ thus $\tau\in[(l-1)Tc,lTc]$. The discrete aperiodic cross-correlation function $C_{m,\lambda}^{k,i}$ for the sequence $a_{m,j}^{(k)}$ and $a_{\lambda,j}^{(i)}$ is defined by [24]

$$C_{m,\lambda}^{k,i}(l)=\begin{cases} \sum_{j=0}^{N-1-l} a_{m,j}^{(k)}a_{\lambda,j+l}^{(i)} & 0\le l\le N-1 \\ \sum_{j=0}^{N-1+l} a_{m,j-l}^{(k)}a_{\lambda,j}^{(i)} & 1-N\le l<0 \\ 0 & |l|\ge N \end{cases} \tag{A.3}$$

The periodic cross-correlation function $\theta_{m,\lambda}^{k,i}$ is given by

$$\theta_{m,\lambda}^{k,i}(l)=\sum_{j=0}^{N-1} a_{m,j}^{(k)}a_{\lambda,j+l}^{(i)} \tag{A.4}$$

for any integer l .

Using the equation (A.13) in equation (5.12) result in the following decision variable [3]

$$
\begin{aligned}
Z_\lambda = & \sqrt{2P}\sum_{l=0}^{L-1}\sum_{f=0}^{F-1}\beta_{ll}a_f R_{\lambda,\lambda}^{1,1}(\tau_{ll}-\frac{f}{W})\cos(\phi_{ll}-\omega_c\tau_{ll}-\phi_f) \\
& + \sqrt{2P}\sum_{l=0}^{L-1}\sum_{k=2}^{K}\sum_{f=0}^{F-1}\beta_{lk}a_f R_{m,\lambda}^{k,1}(\tau_{lk}+\tau_k-\frac{f}{W})\cos(\phi_{lk}+\theta_k-\theta_1-\omega_c\tau_{lk}-\phi_f) \\
& + \sum_{f=0}^{F-1} n(t)\cdot a_f\cdot a_{1,\lambda}(t-\frac{f}{W})\cos(\omega_c t+\phi_f+\theta_1) \ .
\end{aligned}
\tag{A.5}
$$

The tap gains are computed as follows

$$
a_f e^{j\phi_{ll}} = \sum_{l=0}^{L-1}\beta_{ll}e^{j(\phi_{ll}-\omega_c\tau_{ll})}\overline{[R_{\lambda,\lambda}^{1,1}(\tau_{ll}-\frac{f}{W})]} \ . \tag{A.6}
$$

The difference between the decision variables Z_ζ and Z_λ for the first user can be calculated using equation (A.13) and is given by

$$
\begin{aligned}
& Z_\zeta - Z_\lambda \\
& = \sqrt{2P}\sum_{f=0}^{F-1}\sum_{l=0}^{L-1}\beta_{ll}a_f\left\{R_{\lambda,\zeta}^{1,1}(\tau_{ll}-\frac{f}{W})-R_{\lambda,\lambda}^{1,1}(\tau_{ll}-\frac{f}{W})\right\}\cos(\phi_{ll}-\omega_c\tau_{ll}-\phi_f) \\
& + \sqrt{2P}\sum_{f=0}^{F-1}\sum_{k=2}^{K}\sum_{l=0}^{L-1}\beta_{lk}a_f\left\{R_{m,\zeta}^{k,1}(\tau_{lk}+\tau_k-\frac{f}{W})-R_{m,\lambda}^{k,1}(\tau_{lk}+\tau_k-\frac{f}{W})\right\}\cos(\phi_{lk}+\theta_k-\theta_1-\omega_c\tau_{lk}-\phi_f) \\
& + \sum_{f=0}^{F-1} n(t)\cdot a_f\cdot a_{1,\zeta}(t-\frac{f}{W})\cos(\omega_c t+\theta_1+\phi_f) - \sum_{f=0}^{F-1} n(t)\cdot a_f\cdot a_{1,\lambda}(t-\frac{f}{W})\cos(\omega_c t+\theta_1+\phi_f) \ .
\end{aligned}
\tag{A.7}
$$

Assuming the statistics of the difference to be Gaussian and the codes orthogonal, and the λ^{th} symbol transmitted [3], then we find for the expectation

$$
\overline{Z_\zeta - Z_\lambda} = \sqrt{2P}\sum_{l=0}^{L-1}\sum_{f=0}^{F-1}\beta_{ll}a_f\left\{-R_{\lambda,\lambda}^{1,1}(\tau_{ll}-\frac{f}{W})\right\}\cos(\phi_{ll}-\omega_c\tau_{ll}-\phi_f) \ . \tag{A.8}
$$

For x and y statistically independent gaussian random variables, the following equation is valid

$$
var(x+y) = var(x)+var(y) \ . \tag{A.9}
$$

As Z_λ and Z_ζ have the feature of (A.13) as well, the variance of $Z_\zeta - Z_\lambda$ can be written as

$$
\begin{aligned}
& Var\{Z_\zeta - Z_\lambda\} \\
& = 2P\sum_{f=0}^{F-1}\sum_{l=0}^{L-1}\left(\beta_{ll}a_f\cos(\phi_{ll}-\omega_c\tau_{ll}-\phi_f)\right)^2\cdot Var\left\{R_{\lambda,\zeta}^{1,1}(\tau_{ll}-\frac{f}{W})-R_{\lambda,\lambda}^{1,1}(\tau_{ll}-\frac{f}{W})\right\} \\
& + 2P\sum_{f=0}^{F-1}\sum_{k=2}^{K}\sum_{l=0}^{L-1}\left(\beta_{lk}a_f\cos(\phi_{lk}+\theta_k-\theta_1-\omega_c\tau_{lk}-\phi_f)\right)^2\cdot Var\left\{R_{m,\zeta}^{k,1}(\tau_{lk}+\tau_k-\frac{f}{W})-R_{m,\lambda}^{k,1}(\tau_{lk}+\tau_k-\frac{f}{W})\right\} \\
& + \sum_{f=0}^{F-1} N_0 N T_c\cdot|a_f|^2 \ .
\end{aligned}
\tag{A.10}
$$

The variance of $C_{m,\lambda}^{k,i}$ can be calculated using the general formula for statistical variables

$$var(x) = \sigma_x^2 = E(x^2) - [E(x)]^2 \ . \tag{A.11}$$

Therefore,

$$\overline{C_{m,\lambda}^{k,i}(l)} = \begin{cases} N & k=1,\ m=\lambda,\ l=0 \\ 0 & otherwise \end{cases} \ . \tag{A.12}$$

Codes have been used from a codeset as described in paragraph 3.7 and [18]. These codes will be used for the calculation of the correlation and give results, which are dependent from the chosen code set. An approximation of the lower bound of the cross-correlation peak levels was already given in the paragraph 3.8 of the Welch lower band [38].

According to equation (A.13), one needs the calculation of $Var[C_{m,\lambda}^{k,i}]$. Applying formula (A.13) to the variance of the cross-correlation $C_{m,\lambda}^{k,i}$, shows the need for the expectation of $[C_{m,\lambda}^{k,i}]^2$, which is equal to $\overline{|C_{m,\lambda}^{k,i}|^2}$. Therefore, the pseudo-randomly varying cross-correlation, with positive as well as negative values, with a maximum peak value resulting from the Welch lower band $\sqrt{N}$. The maximum of this squared cross-correlation has the maximum peak value N, when the considered codes are aligned (l=0). This results in equation (A.13)

$$\overline{|C_{m,\lambda}^{k,i}(l)|^2} = \begin{cases} N^2 & k=1,\ m=\lambda,\ l=0 \\ N-|l| & k=1,\ 0<|l|\leq N-1 \\ N-|l| & k\neq 1,\ 0\leq |l|\leq N-1 \\ 0 & otherwise \end{cases} \ . \tag{A.13}$$

The values of $\overline{|C_{m,\lambda}^{k,i}|^2}$ depend on the code set chosen, but are approximated by the Welch lower bound. The peak will linearly decrease with l to zero, when the codes are shifted next to each other. Due to the orthogonality of the sequences used by the considered user, the $\overline{|C_{m,\lambda}^{k,i}|^2}$ is zero for k=1 and l=0. The shifting of the codes is schematically shown in Figure A.1

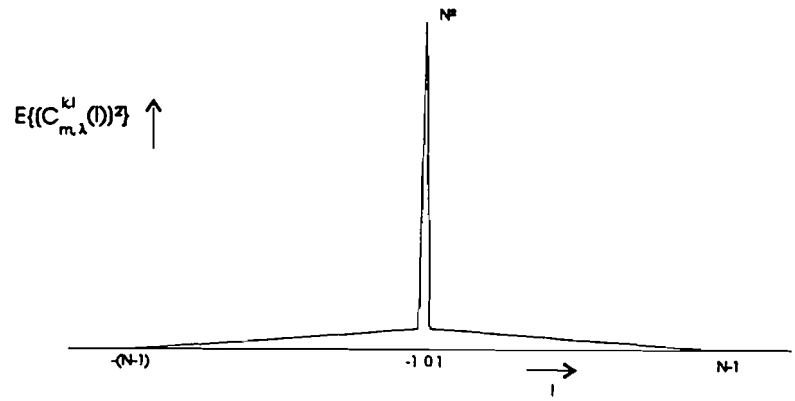

Figure A.1: Schematically presentation of correlation properties.

Now the variance can be calculated using (A.13), (A.13) and (A.13)

$$var[C_{m,\lambda}^{k,i}(l)] = \overline{(C_{m,\lambda}^{k,i}(l))^2} - (\overline{C_{m,\lambda}^{k,i}(l)})^2 \ . \tag{A.14}$$

Filling in formulas (A.13) and (A.13) give the following formulas for the variances

$$v_1 = var[C_{\lambda,\lambda}^{1,1}(l)] = \begin{cases} N-|l| & 0<|l|\le N-1 \\ 0 & otherwise \end{cases} \tag{A.15}$$

$$v_2 = var[C_{m,\lambda}^{k,1}(l)] = \begin{cases} N-|l| & 0\le|l|\le N-1 \\ 0 & otherwise \end{cases} \tag{A.16}$$

$$v_3 = var[C_{m,\lambda}^{1,1}(l)] = \begin{cases} N-|l| & 0<|l|\le N-1 \\ 0 & otherwise \end{cases} \ . \tag{A.17}$$

Expressions for the expectation and variance of the uniformly in $[0,T_c]$ distributed τ_k for $k\neq 0$, can be calculated using $E\{\tau_k\} = T_c/2$ and $E\{(\tau_k)^2\} = T_c^2/3$. Using the stastistics of τ_k and equation (A.13) of paragraph 5.3 result in an expression for the variance of $Z_\zeta - Z_\lambda$

$$\begin{aligned}
&Var\{Z_\zeta - Z_\lambda\} = \\
&= 2P\sum_{l=0}^{L-1}\sum_{f=0}^{F-1}\left(\beta_{ll}a_f\cos(\phi_{ll}-\omega_c\tau_{ll}-\phi_f)\right)^2 \\
&\quad\cdot[(\tau_{ll}-l_1T_c-\frac{f}{W})^2\cdot\{2v_3(l_1-N+1)+v_3(l+1)+v_1(l+1)\}+(T_c-\tau_{ll}+\frac{f}{W}+l_1T_c)^2\cdot\{v_3(l_1)+2v_3(l_1-N)+v_1(l_1)\}] \\
&\quad + 2P\sum_{l=0}^{L-1}\sum_{k=2}^{K}\sum_{f=0}^{F-1}\left(\beta_{lk}a_f\cos(\phi_{lk}+\theta_k-\theta_1-\omega_c\tau_{lk}-\phi_f)\right)^2 \\
&\quad\cdot[2\cdot\{(\tau_{lk}-\frac{f}{W}-l_kT_c)^2+T_c(\frac{T_c}{3}+\tau_{lk}-\frac{f}{W}-l_kT_c)\}\cdot\{v_2(l_k+1)+v_2(l_k-N+1)\} \\
&\quad + 2\cdot\{((1+l_k)T_c-\tau_{lk}-\frac{f}{W})^2+T_c(\frac{T_c}{3}+\tau_{lk}-\frac{f}{W}-(1+l_k)T_c)\}\cdot\{v_2(l_k)+v_2(l_k-N)\}] \\
&\quad +\sum_{f=0}^{F-1}N_0NT_c\cdot|a_f|^2 \ ,
\end{aligned} \tag{A.18}$$

where for $\tau_{lk}+\tau_k-\frac{f}{W}>0$

$$\begin{aligned}
&l_1T_c \le \tau_{ll}-\frac{f}{W} \le (l_1+1)T_c \le T \\
&l_2T_c \le \tau_{lk}+\tau_k-\frac{f}{W} \le (l_2+1)T_c \le T
\end{aligned} \tag{A.19}$$

and for $\tau_{lk}+\tau_k-\frac{f}{W}<0$

$$(l_1-1)T_c \le \tau_{l1} - \frac{f}{W} \le l_1 T_c \le T$$

$$(l_2-1)T_c \le \tau_{lk} + \tau_k - \frac{f}{W} \le l_2 T_c \le T \ .$$

Expressions for N_{SI}, N_{MI} and N_I as have been used in equation (5.13) in paragraph 5.3 can be given by

$$N_{SI} = Var\{Z_\zeta - Z_\lambda\} = 2P\sum_{l=0}^{L-1}\sum_{f=0}^{F-1}\left(\beta_{l1}a_f\cos(\phi_{l1}-\omega_c\tau_{l1}-\phi_f)\right)^2$$
$$\cdot[(\tau_{l1}-l_1T_c-\frac{f}{W})^2\cdot\{2v_3(l_1-N+1)+v_3(l+1)+v_1(l+1)\} + (T_c-\tau_{l1}+\frac{f}{W}+l_1T_c)^2\cdot\{v_3(l_1)+2v_3(l_1-N)+v_1(l_1)\}] \quad (A.21)$$

and

$$N_{MI} = 2P\sum_{l=0}^{L-1}\sum_{k=2}^{K}\sum_{f=0}^{F-1}\left(\beta_{lk}a_f\cos(\phi_{lk}+\theta_k-\theta_1-\omega_c\tau_{lk}-\phi_f)\right)^2$$
$$[2\cdot\{(\tau_{lk}-\frac{f}{W}-l_kT_c)^2+T_c(\frac{T_c}{3}+\tau_{lk}-\frac{f}{W}-l_kT_c)\}\cdot\{v_2(l_k+1)+v_2(l_k-N+1)\} + \quad (A.22)$$
$$2\cdot\{((1+l_k)T_c-\tau_{lk}-\frac{f}{W})^2+T_c(\frac{T_c}{3}+\tau_{lk}-\frac{f}{W}-(1+l_k)T_c)\}*\{v_2(l_k)+v_2(l_k-N)\}]$$

and

$$N_I = \sum_{f=0}^{F-1} N_0 N T_c\cdot|a_f|^2 \quad (A.23)$$

Appendix B List of significant variables in Matlab programs

A	Coefficient for decrease of Blkpow in dB per nanosecond.
Blk	Multipath ray amplitude.
Blkpow	Power level of multipath rays for all users in dB.
Btlpow	Power level of multipath rays from LOS to moment t1.
corrfact	Correction factor for scaling in statistical processes.
cros	Post-correlation signal of Gontv and G20tot using RAKE receiver.
cross	Post-correlation signal of Gontv and G20tot.
crossold	Post-correlation signal of Gontv and G20tot.
dlos	Power loss for rays compared to the LOS.
e	matrix containing five data modulated sequences.
Eii	Cross correlation between one chip shifted sequences.
fact	Normalised value of RAKE tap to the maximal tap correlation signal.
G	Matrix containing the Gold sequence set.
G20d	Matrix containing five succeeding sequences for all users.
G20dat	Matrix containing five data sequences for each K users with multipath.
G20datot	Help matrix containing five data sequences for each K users with multipath.
G20old	Matrix containing five data sequences for each K users without multipath.
G20tot	Summation of data sequences for all K users, applying multipath.
Gnew	Matrix used for sorting out the balanced codes in G.
Gontv	Sequence for correlation receiver .
Gshift	Matrix containing one chip shifted sequences.
Gsum	Vector representing the cumulative sum of the chips in the sequences in G.
k	User number.
K	Amount of users.
l	Relative shift between G20tot and Gontv used in correlators.
lambda	The mean arrival rate.
llk	Multipath delay index (=tlk*10/Tc).
M	Maximum amount of paths.
M2	Number of RAKE taps.
N	Sequence length.
p1new	New state first shift register .

p1old	Old state first shift register .
p2new	New state second shift register .
p2old	Old state second shift register .
ph	Vector containing the phases of the multipath rays.
poison	Vector of length 100 containing a poisson process.
q	Sequence to be received.
r	Sequence to be received combined with the waveform.
R	User number to be received.
RA	RAKE receiver y/n.
RAK	Type of RAKE receiver.
rayleigh	Vector of length 100 containing a Rayleigh process.
seq	Vector associating sequences with users.
seq1	First maximal length sequence.
seq2	Second maximal length sequence.
seq2old	Shifted second maximal length sequence .
seq2shift	Shifted second maximal length sequence.
t1	Moment in multipath model when Blkpow starts to diminish.
tap	Vector containing the RAKE tap positions.
Tc	Chiptime (ns).
tlk	Multipath delay times.
tt1	Delay index (=t1*10/Tc).
wc	Carrier frequency.
y	Variable defining the chip waveform.

Appendix C Signal simulation programs

C.1 Gold511.m

```
% Gold511 calculates the Gold code set, with codes of length 511,
% using two shift register sequences

for x = 1:9
        p1old(x)=1;
        p2old(x)=1;
        % initialisation of the states of the shift registers
end

for n=1:511
        seq1(n)=0;
        seq2(n)=0;
        % initialisation of the generated first two Gold code sequences
end

for g=1:511
% generation of the first two codes (preferred pair)
        for n=511:-1:2
                seq1(n)=seq1(n-1);
                seq2(n)=seq2(n-1);
                % the sequence are shifted one position
        end
        seq1(1)=p1old(9);
        seq2(1)=p2old(9);
        % the first chip of the codes equals the output of old state of the
        % shift register

        p1new(1)=p1old(9);              p2new(1)=p2old(9);
        p1new(2)=p1old(1);              p2new(2)=p2old(1);
        p1new(3)=p1old(2);              p2new(3)=xor(p2old(2),p2old(9));
        p1new(4)=xor(p1old(3),p1old(9));    p2new(4)=xor(p2old(3),p2old(9));
        p1new(5)=xor(p1old(4),p1old(9));    p2new(5)=p2old(4);
        p1new(6)=p1old(5);              p2new(6)=xor(p2old(5),p2old(9));
        p1new(7)=xor(p1old(6),p1old(9));    p2new(7)=p2old(6);
        p1new(8)=p1old(7);              p2new(8)=p2old(7);
        p1new(9)=p1old(8);              p2new(9)=p2old(8);

        % The new state of the shift register equals the shifted old state
        % including several feedback connections

        p1old(:)=p1new(:);          p2old(:)=p2new(:);
        % The new state becomes the old state and start over
g=g+1;
end

%---------- genereren overige 511 sequences----------
% The remaining 511 codes can be calculated by modulo-2 addition of the
% preferred pair
G = zeros(513,511);
% initialisation of the Gold code set G
seq2old(:)=seq2(:);
% making a copy of the seconde Gold sequence
G(1,:)=2*seq1(:)'-1;
% The first generated sequence is made bipolar and becomes the first sequence
% in the Gold code set
G(2,:)=2*seq2(:)'-1;
% The second generated sequence is made bipolar and becomes the second sequence
```

```
% in the Gold code set

for g=3:513
% the other 511 Gold codes can be generated by modulo-2 addition of the
% preferred pair, while shifting them mutually
        for n=511:-1:2
                seq2shift(n)=seq2old(n-1);
                % shift the second preferred code one position
        end
        seq2shift(1)=seq2old(511);
G(g,:) = 2*xor(seq1(:)',seq2shift(:)') -1;
% The bipolar modulo-2 addited preferred pair is added in the Gold code set
seq2old(:)=seq2shift(:);
end
%-------------------------------------------------------------------------

%---------------------- Take only balanced sequences----------------------------
% To have optimum correlation properties, only the balanced sequences will be
% selected from the Gold code set.
Gsum=sum(G');
% A vector representing the cumulative sum of the chips in the sequences of G
s=1;
for g=1:513
        if Gsum(1,g)==1
                Gnew(s,:)=G(g,:);
                s=s+1;
                % A new matrix only containing 257 balanced sequences is
                % determined
        end
end
clear G
G=Gnew;
clear seq1 seq2 seq2old seq2shift Gnew g m n x p1new p2new p1old p2old Gsum s
pack
% all superfluous variables are removed from the memory
%-------------------------------------------------------------------------

%--------------------- take only with ACF low near origin----------------------
p=1;
for s=1:257
        Gshift(s,1)=G(s,511);
        Gshift(s,2:511)=G(s,1:510);
        % Gshift equals sequence s shifted one position
        Eii(s)=Gshift(s,:)*G(s,:)';
        % Eii equals the auto correlation value next to the origin
        if Eii(s)==-1
                Gnew(p,:)=G(s,:);
                % only sequences with a value of -1 for the autocorrelation
                % value next to the origin are selected
                p=p+1;
        end
end
clear G Gshift p s Eii
% all superfluous variables are removed from the memory
G=Gnew;
% This reduced Gold code set becomes the new set
clear Gnew
pack

save g511set G
% the reduced Gold code set is saved in g511set
```

C.2 Main511.m

```
% Main511.m is a program that calculates the cumulative signals from all users
% and multipaths and also calculates the received signal after a correlator and
% optionally a RAKE receiver. All signals and codes are fit into matrixes,
% which made it necessary to grid the signals into equidistant intervals Tc/10.

% path(path,'G:\matlab');
% enlarging the path used by matlab

%------------------ input variables ----------------------------------------
% defining several configuration variables
Tc=input('chip time (ns): ');
Tc=Tc*1e-9;
% normalising the chip period to nanoseconds
K=input('amount of users: ');
% the amount of simultaneous users
R=input('whished user: ');
% user signal which is goiing to be detected
M=input('Maximum amount of paths: ');
% maximal amount of multipaths
global rmax Tc
% making these variables global within functions
rmax=M;
% maximal amount of rays is equal to M
RA=input('RAKE receiver? y/n: ','s');
% variable indicating the use of a RAKE receiver (y/n)
M2=1;
% initialising the number of RAKE taps to one
if RA=='y'
        M2=input('number of RAKE taps: ');
        RAK=menu('Choose type of RAKE receiver', 'Only the strongest signal is taken','The two strongest signals are added','Signals with
level >30% of strongest are added','Maximum ratio combining');
        % if using a RAKE receiver then the type of RAKE receiver and its
        % number of taps are to be defined
end
%-------------------------------------------------------------------------

%------------------ calculating or loading of gold code set in matrix G ------
laden=input('Load or calculate gold code set? l/c: ','s');
% variable indicating to load or calculate the Gold code set
% when the Gold code set has been calculated before, then the set can be loaded
if laden=='c'
        gold511
        save g511set G
        % calculating and saving the Gold code set
else
        load g511set
        % loading the Gold code set
end
clear laden
% removing the variable laden from the memory
%-------------------------------------------------------------------------

% ------------------ Adding datapattern ------------------------------------
% A datapattern of five databits will be added using the sequences from the
% Gold code set.
data511
% ------------------------------------------------------------------------

%------------------ Determination of PDP for K users -----------------------
% Multipath profiles for all K users will be calculated according to a model,
% which has been defined on the basis of the measurements.
```

```
for k=1:K
        usernumber=k;
        model
        % the program model will calculate the multipath profile
end
%-------------------------------------------------------------------------

%----------------------------- Applying impulse delay times -----------------
% Applying the multipath Poisson distributed time delays rounded to Tc/10 to
% the the data sequences.
k=1;m=1;
% k indicates the user number and m indicates the path number
for k=1:K
        for m=1:M
                tlk(m,k)=(round(tlk(m,k)/(Tc/10)))*Tc/10;
                % The Poisson distributed tlk is rounded to Tc/10 to make tlk
                % applicable to the data sequences.
                llk(m,k)=tlk(m,k)/(Tc/10);
                % llk is an index used in matrixes
        end
end

G20old=G20dat;
% The original matrix without multipath, containing spreaded data sequences for
% K users.
k=1;
while k <= K
% summing for K users
        m=1;
        while m <=M
        % summing over M multipath paths
                l=llk(m,k);
                % path delay for user k and path m
                G20dat(k,l+1:25550)=G20dat(k,1:25550-l);
                if l>=1
                G20dat(k,1:l)=G20old(k,25551-l:25550);
                end
                % shifting the spreaded data sequence for user k with path delay
                % llk(m,k)
                if m == 1
                        G20datot = G20dat(k,:)*Blk(m,k);
                else
                        G20datot = G20datot + G20dat(k,:)*Blk(m,k);
                end
                % Adding delayed spreaded data sequence for user k to the
                % cumulative multipath signal for user k
                m=m+1;
        end
        G20dat(k,:)=G20datot;
        % The cumulative multipath signal for all users are stored in vectors
        % of G20dat
k=k+1;
end
clear G20datot G20old
%-------------------------------------------------------------------------

%------------------- Adding the codes of the K active users -------------------
% The cumulative spreaded multipath signals for all users will be cumulated in
% G20tot
k=1; G20tot = G20dat(k,:);k=k+1;
while k <= K
        G20tot = G20tot + G20dat(k,:);
        % Cumulating all K multipath signals
```

```
        k=k+1;
end
%figure
%plot(Tc/10:Tc/10:5110*Tc,real(G20tot(1:5110)))
% Plotting the total cumulative transmitted signals as a function of the time
%-------------------------------------------------------------------------------

%-------------------- Receiving the signal-------------------------------------
if RA=='y'
        % if the variable indicating the use of a RAKE receiver (y/n) is "y"
        % then a RAKE receiver will be applied
        rake

elseif RA=='n'
        % if not then no RAKE receiver will be applied
        norake
end
%-------------------------------------------------------------------------------
```

C.3 Model.m

```
% model generates multipath profiles for all users according to a model
% containing Rayleigh distributed amplitudes, Poisson distributed path
% delays and uniformly distributed phase.

% ---------- Determination poison distributed arrival time ----------
% In this routine, a poisson distributed interarrival times will be determined
% to result in the multipath path delay values.
usernumber
% prints the number of user
lambda=1/input('Mean arrival time: ');
% lambda equals the mean arrival rate
% rmax=input('maximum amount of rays: ');
% rmax has been equaled to M in main511, which is the maximum amount of paths
global corrfact
% the variable corrfact, which will be used in the functions fpois and frayl
% is defined as a global variable.
tlk(1,k)=0;
% All first path delays of the profiles are defined zero, because the initial
% path delay is given in tk

poison=fpois(lambda);
% Poison represents a vector of length 100 containing a poisson process based
% on the mean arrival rate lambda.
% The Poisson process is given by a function that converge to the 1 on the y-axis
% for large values on the x-axis.
for m=2:rmax
        x=rand(1);
        % x represents a uniformly distributed variable between zero and one
        % This loop finds the x-value to the y-value rand(1), according
        % to a Poisson process. This x-value represents the basis for the
        % Poisson distributed interarrival time.
        t=1;
        if x<poison(1)
                x=poison(1);
                % When the randomly found value is smaller than the smallest value
                % in poison, then the randomly found value becomes poison(1), which
                % is near zero.
        end
        if x>poison(100)
                x=poison(100);
                % When the randomly found value is larger than the largest value
                % in poison, then the randomly found value becomes poison(100), which
                % is near one.
        end
        while poison(t)<x
                t=t+1;
        end
        % The poison distributed value t is the basis for the pathdelay
        tlk(m,k)=tlk(m-1,k)+t*1e-9/corrfact;
        % The pathdelay can be calculated by applying a correction factor and
        % cummulating the interarrival times.
end
%figure
%plot(tlk(1:rmax),ones(1,rmax),'c.')
%-------------------------------------------------------------------------

% ---------- Average arrival power ----------
Blkpow(1,k)=input('power level of first ray [dB]: ');
%Blkpow equals the power level of multipath rays for all users in dB

        %Rdb=input('Rdb [dB]: ');
```

```
dlos=input('delta power los [dB]: ');
% dlos equals the power loss for rays (not LOS) compared to the LOS
tl=input('tl [ns]: ');tl=tl*1e-9;
% tl represtents the moment in multipath model when Blkpow starts to diminish
A=input('A [dB/ns]: ');
% A represents the coefficient of the diminishing of Blkpow in dB/ns
t=1;
while tlk(t,k)<tl
% the tlk approximating tl is found by taking the maximal tlk smaller than tl
        t=t+1;
end
ttl=t;
% ttl represents the delay index, with tlk(ttl,k) the maximal tlk < tl
        %Btl=sqrt(Blk(1,k)^2+10^(Rdb/10));
Btlpow=Blkpow(1,k) - dlos;
% Btlpow represents the power level of multipath rays from LOS to moment tl

for n=2:ttl-1
        Blkpow(n,k)=Btlpow;
        % from LOS to moment tl, the vector Blkpow equals Btlpow
end
n=1;
for n=ttl:rmax
        Blkpow(n,k)=Btlpow + A*(tlk(n,k)-tl)*1e9;
        % from tl to rmax, Blkpow equals Btlpow minus A multiplied
        % by the additoinal time
end

%plot(tlk(1:rmax,k),Blkpow(1:rmax,k),'c.')

% Below is the transformation to linear scale of Blkpow
%n=1;
%for n=1:rmax
%       Blk(n,k)=10^(Blkpow(n,k)/20);
%end
%figure
%plot(tlk(1:rmax,k),Blk(1:rmax,k),'c.')
%-------------------------------------------------------------------------


% ------------Rayleigh distrubution-----------------------------------------
% In this routine, Rayleigh distributed ray amplitudes will be calculated, with
% an average power level of Blkpow.
% Thus input to this routine is the average power profile of B in dB and the
% output is the Rayleigh distribution of the ray amplitudes (not in dB)

Blk(1,k)=sqrt(10^(Blkpow(1,k)/10));
% The ray amplitude of the LOS can be calculated with the average
% power Blkpow(1,k)
m=2;
for m=2:ttl-1
% for paths till moment ttl, the Rayleigh process will be applied
        rayleigh=frayl(Blkpow(m,k));
        % rayleigh is a vector of length 100 containing a Rayleigh process
        % The Rayleigh process is given by a function that converge to 1 on
        % the y-axis for large values on the x-axis.

        x=rand(1);
        % x represents a uniformly distributed variable between zero and one
        % This loop finds the x-value to the y-value rand(1), according
        % to a Rayleigh process. This x-value represents the basis for the
        % calculation of the Rayleigh distributed ray amplitudes.
        t=1;
```

```
        if x<rayleigh(1)
                x=rayleigh(1);
                x=poison(1);
                % When the randomly found value is smaller than the smallest value
                % in rayleigh, then the randomly found value becomes rayleigh(1), which
                % is near zero.
        end
        if x>rayleigh(100)
                x=rayleigh(100);
                % When the randomly found value is larger than the largest value
                % in Rayleigh, then the randomly found value becomes rayleigh(100), which
                % is near one.
        end
        while rayleigh(t)<x
                t=t+1;
        end
        % The Rayleigh distributed value t is the basis for the ray amplitude
        ph(m,k)=(2*rand(1)-1)*pi;
        % The phase is uniformly distributed in [-pi,pi]
        Blk(m,k)=(t/corrfact)*exp(i*ph(m,k));
        % Blk is calculated using t, the correction factor and the random phase ph
end

for m=tt1:rmax
% for paths from tt1 till the maximum amount of paths uses the same rayleigh process
        rayleigh=frayl(Blkpow(m,k));
        x=rand(1);
        t=1;

        if x<rayleigh(1)
                x=rayleigh(1);
        end

        if x>rayleigh(100)
                x=rayleigh(100);
        end

        while rayleigh(t)<x
                t=t+1;
        end
        ph(m,k)=(2*rand(1)-1)*pi;
        Blk(m,k)=(t/corrfact)*exp(i*ph(m,k));
end

for k=2:K
        tk(k)=rand(1)*Tc;
        % The initial pathdelay for all users is uniformly random over [0,Tc]
        phc(k)=rand(1)*2*pi;
        % The carrier phase is uniformly random over [0,2*pi]
end

%figure
%plot(tlk(1:rmax,k),real(Blk(1:rmax,k)),'c.')
%xlabel('t')
%ylabel('Beta(l,k)')
%title('1/lambda=, rays, [B(0)]dB=dB,delta =, t1=ns, A=')

%figure
%plot(tlk(1:rmax,k),10*log10(real(Blk(1:rmax,k))),'c.')
%xlabel('t')
%ylabel('10log(Beta(l,k))')
%title('1/lambda=, rays, [B(0)]dB=dB,delta =, t1=ns, A=')
```

Appendix D Performance simulation Matlab program

D.1 Perform.m

```
% Perform calculates the BER using the multipath and muti-user properties of
% the configuration
N=511;
% N represents the sequence length
wc=(2*pi/(N*Tc))*round((60e9)*N*Tc/(2*pi));
% The carrier frequency is calculated as 2*pi*60e9, but then rounded to an
% integer number*2*pi/(N*Tc)
W=1/Tc;
% The available bandwidth W is the reciprocal of the chip time Tc

%---------- defining desired user code----------------------------------------
% The symbol used by user 1 to be detected will be calculated
% including the waveform
for p=1:511
        q(p,:)=G(seq(R),p)*y;
end
r(:)=reshape(q',1,5110);
%--------------------------------------------------------------------------

%-------- Cross correlation according to Welch lower bound--------------------
% The variance of the auto- and cross correlation function of the pseudonoise
% sequence can be determined using the Welch lower bound. Instead of using this
% Welch lower bound approximation other Code sets could be implemented by using
% its correlation properties
for l=1:511
        v1(l)=N-l+1;
        % v1 gives the variance of the auto correlation
        v2(l)=N-l+1;
        % v2 gives the variance of the cross correlation of two different
        % sequences of two different users
        v3(l)=N-l+1;
        % v2 gives the variance of the cross correlation of two different
        % sequences of two different users
end
v1(1)=0;
v3(1)=0;
for l=512:1022
% Also values will be defined for shifting of the codes more than the sequence
% length
        v1(l)=0;
        v2(l)=0;
        v3(l)=0;
end
%--------------------------------------------------------------------------

% ---------Defenition of RAKE met F=amount of taps +1-------------------------
% A RAKE receiver can optionally be implemented according to the analytic theory
% given in the report.
RAKE=input('Applying RAKE receiver in performance calculations? y/n : ','s');
% RAKE is the variable giving the presence of the RAKE receiver
if RAKE=='y'
        F=input('amount of RAKE taps: ');
        % F gives the amount of RAKE taps
        for f=1:F
                af(f)=0;
```

```
                phf(f)=0;
                tapgain(f)=0;
                for l=1:M
                % The expectation of the correlation function R will be determined
                % and will be used in the calculation of the RAKE coefficients
                        if ((tlk(l,R)-(f-1)/W)/Tc)>=0
                                ll=floor((tlk(l,R)-(f-1)/W)/Tc);
                        else
                                ll=ceil((tlk(l,R)-(f-1)/W)/Tc);
                        end
                        if ll==0
                                T1=N*(Tc-tlk(l,R)+(f-1)/W);
                        elseif ll==-1
                                T1=N*(Tc+tlk(l,R)-(f-1)/W);
                        else
                                T1=0;
                        end
                tapgain(f)=tapgain(f) + Blk(l,R)*T1*exp(-j*wc*tlk(l,R));
                end
        af(f)=abs(tapgain(f));
        phf(f)=angle(tapgain(f));
        % The amplitude and phase coefficients for the RAKE
        % receiver are calculated according the theory
        end


else
% If no RAKE receiver is present, than the coefficients will be one, to omit
% its influence
        F=1;
        af(1)=1;
        phf(1)=0;
end


%-------------------------------------------------------------------------


%------------ Power levels ----------------------------------------------
P=0.05;
% The transmitted power equals 50 mW
EboverN0=input(' Eb/N0 at receiver [dB]: ');
% This Eb/No at the receiver is a commonly used parameter on the x-axis
% of a plot of the BER.

Eb=P*N*Tc;
% Eb represents the transmitted energy per bit
% This equation is valid for binary signalling, otherwise Eb=P*N*Tc/log2(M),
% with M representing M-ary signalling

%[ma,ix]=max(Blk(:,R));

N01=0;
N02=0;
for l=1:M
%       N01=N01+abs(Blk(l,R))^2;
        % N01 represents the sum of the Blk^2 for user R and all paths
        % The received energy per bit is now N01* transmitted energy per bit

        N01=N01+10^(Blkpow(l,R)/10);
        % N01 calculated as M*E(Blk^2)
end
for f=1:F
```

```
        N02=N02+ (abs(af(f)))^2;
        % N02 represents the noise introduced by the RAKE taps, which can
        % be calculated by the sum of the quadratures of the tap coefficients
end
N02=1;
N0=Eb*N01/(N02*10^(EboverN0/10));
% This N0 before transmitted over the channel will be used in following equations
% and is calculated using the Eb/N0 at the receiver and values for the
% gain of the path and the noise by the RAKE receiver
%-------------------------------------------------------------------------------


%------------------- Calculation of the self interference and signal ---------------------------
verw=input('Expectation of R in SNR? y/n : ','s');
% This variable is used to give the option of taking an expectation of R in
% the SNR the BER formula. It was not clear in Chase whether to take the
% expectation or not.
NSI=0;
T=0;
for f=1:F
        for m=1:M
                if ((tlk(l,R)-(f-1)/W)/Tc)>=0
                        l1=floor((tlk(l,R)-(f-1)/W)/Tc);
                else
                        l1=ceil((tlk(l,R)-(f-1)/W)/Tc);
                end
        % l1 is determined by rounding the delay "tlk(l,R)-(f-1)/W"
        % ( down for delay>0 and up for delay<0 ) to the nearest l1*Tc.
        NSI1=af(f)*abs(Blk(l,R))*cos(angle(Blk(l,R))-wc*tlk(l,R)-phf(f));
        NSI2=(tlk(l,R)-l1*Tc-(f-1)/W)^2*(2*v3(1+abs(l1-N+1)) + v3(1+abs(l1+1))+v1(1+abs(l1+1)));
        NSI3=(Tc-tlk(l,R)+l1*Tc+(f-1)/W)^2;
        NSI4= v3(1+abs(l1))  + 2 * v3(1+abs(l1-N)) + v1(1+abs(l1));
        NSI=NSI+(2*P)*(NSI1^2)*(NSI2+NSI3*NSI4);
        % The self-interference term can be calculated according to the
        % analytic representation in the report.
        if verw=='n'
                T1= Tc*c12(r,-r,l1-N)+(tlk(l,R)-(f-1)/W - l1*Tc)*(c12(r,-r,l1+1-N)-c12(r,-r,l1-N));
                T2= Tc*c11(r,l1) + (tlk(l,R)-(f-1)/W - l1*Tc)*(c11(r,l1+1)-c11(r,l1));
                % The terms of the sommation in the nominator of SNR (thus containing the signal
                % information) has been calculated by using the definition of correlation function R
        else
                if l1==0
                        T1=N*(Tc-tlk(l,R)+(f-1)/W);
                elseif l1==-1
                        T1=N*(Tc+tlk(l,R)-(f-1)/W);
                else
                T1=0;
                end
                T2=0;
                % The terms of the sommation in the nominator of SNR (thus containing the signal
                % information) has been calculated by using the expectation of the correlation function R
        end
        T=T+(sqrt(2*P))*af(f)*abs(Blk(l,R))*(T1+T2)*cos(angle(Blk(l,R))-wc*tlk(l,R)-phf(f));
        % The nominator follows by summing all the components
        end
end
%-------------------------------------------------------------------------


%------------------- Calculation of Multiple user interference----------------
NMItot=0;

for k=1:R-1
NMI(k)=0;
```

```
% The multiple user noise caused by all other users can be determined according to the formulas
% of the report
        for l=1:M
                for f=1:F
                if ((tlk(l,k)+tk(k)-(f-1)/W)/Tc)>=0
                        l2=floor((tlk(l,k)+tk(k)-(f-1)/W)/Tc);
                else
                        l2=ceil((tlk(l,k)+tk(k)-(f-1)/W)/Tc);
                end
                NMI1=af(f)*abs(Blk(l,k))*cos(angle(Blk(l,k))-wc*tlk(l,k)-phf(f)+phc(k)-phc(1));
                NMI2=( (tlk(l,k)-l2*Tc-(f-1)/W)^2 + Tc*(Tc/3+tlk(l,k)-(f-1)/W -l2*Tc) )*(v2(1+abs(l2+1)) + v2(1+abs(l2-N+1)));
                NMI3=( ((1+l2)*Tc-tlk(l,k)-(f-1)/W)^2 + Tc*(Tc/3+tlk(l,k)-(f-1)/W-(1+l2)*Tc) )*( v2(1+abs(l2)) + v2(1+abs(l2-N)) );
                NMI(k)=NMI(k)+(2*P)*(NMI1^2)*2*(NMI2+NMI3);
                % The multiple user interference of all paths of user k is summated in NMI(k)
                end
        end
NMItot=NMItot+NMI(k);
% The multiple user interference of all paths of all users is summated in NMItot
end

for k=R+1:K
NMI(k)=0;
% The multiple user noise caused by all other users can be determined according to the formulas
% of the report
        for l=1:M
                for f=1:F
                if ((tlk(l,k)+tk(k)-(f-1)/W)/Tc)>=0
                        l2=floor((tlk(l,k)+tk(k)-(f-1)/W)/Tc);
                else
                        l2=ceil((tlk(l,k)+tk(k)-(f-1)/W)/Tc);
                end
                NMI1=af(f)*abs(Blk(l,k))*cos(angle(Blk(l,k))-wc*tlk(l,k)-phf(f)+phc(k)-phc(1));
                NMI2=( (tlk(l,k)-l2*Tc-(f-1)/W)^2 + Tc*(Tc/3+tlk(l,k)-(f-1)/W -l2*Tc) )*(v2(1+abs(l2+1)) + v2(1+abs(l2-N+1)));
                NMI3=( ((1+l2)*Tc-tlk(l,k)-(f-1)/W)^2 + Tc*(Tc/3+tlk(l,k)-(f-1)/W-(1+l2)*Tc) )*( v2(1+abs(l2)) + v2(1+abs(l2-N)) );
                NMI(k)=NMI(k)+(2*P)*(NMI1^2)*2*(NMI2+NMI3);
                % The multiple user interference of all paths of user k is summated in NMI(k)
                end
        end
NMItot=NMItot+NMI(k);
% The multiple user interference of all paths of all users is summated in NMItot
end

%-------------------------------------------------------------------------

%---------- Calculation of thermal noise----------
NI=0;
for f=1:F
        NI=NI+N0*N*Tc*(abs(af(f)))^2;
        % The thermal noise term can be calculated as a function as given in the report
end
%-------------------------------------------------------------------------

%---------- Calculation of SNR and BER----------
SNR=(T^2)/(NSI+NMItot+NI);
% Now the SNR can be calculated using above calculations
Pr=1/2*erfc(sqrt(SNR/2));
% The BER can be calculated using the Gaussian assumption
SNR
Pr
%-------------------------------------------------------------------------
```

Appendix E Simulated multipath model

E.1 Rayleigh distributed path amplitude, presented as $B_{lk}(l,k)$ and $|B_{lk}(l,k)|$, as function of the Poisson distributed arrival time

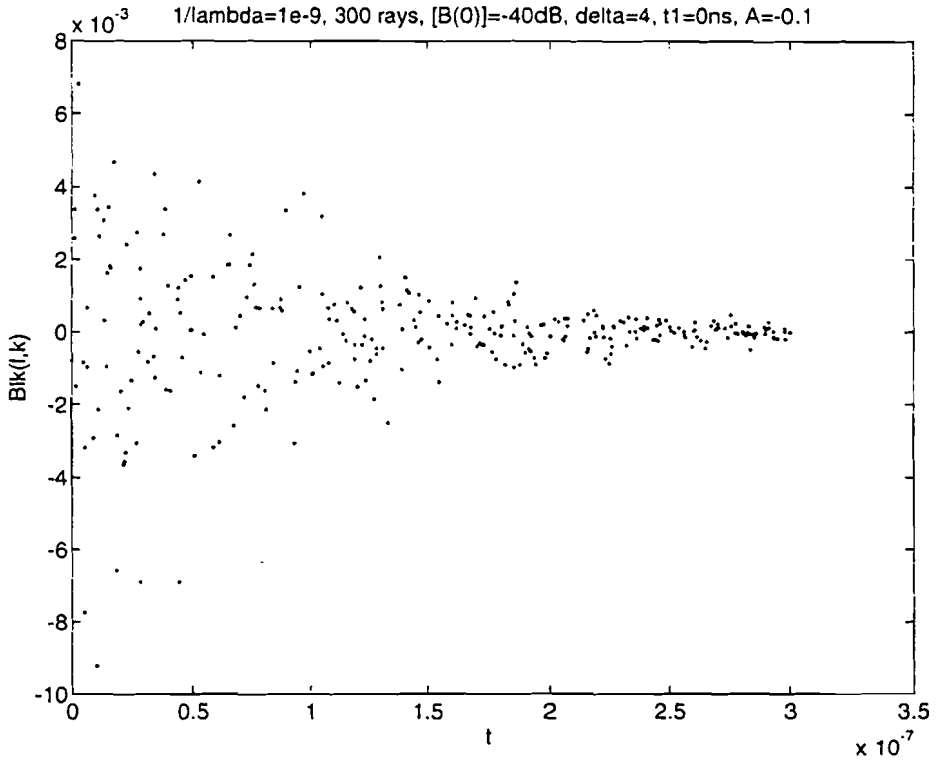

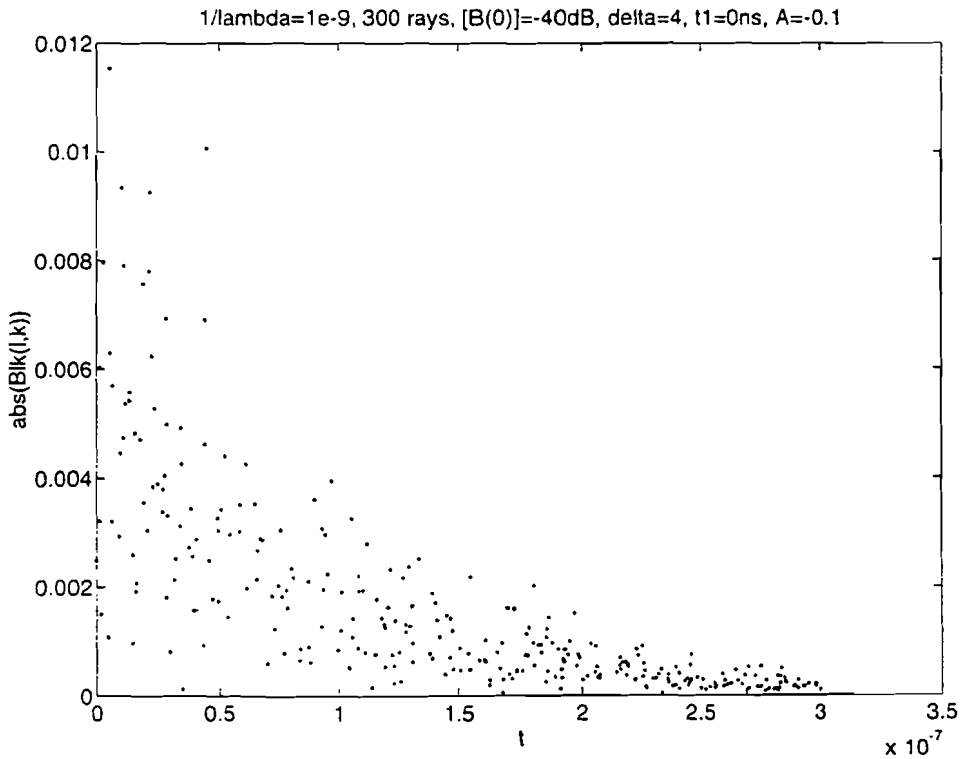

E.2 Rayleigh distributed path amplitude, presented as $10 \cdot {}^{10}\log(|B_{lk}(l,k)|)$, as function of the Poisson distributed arrival time

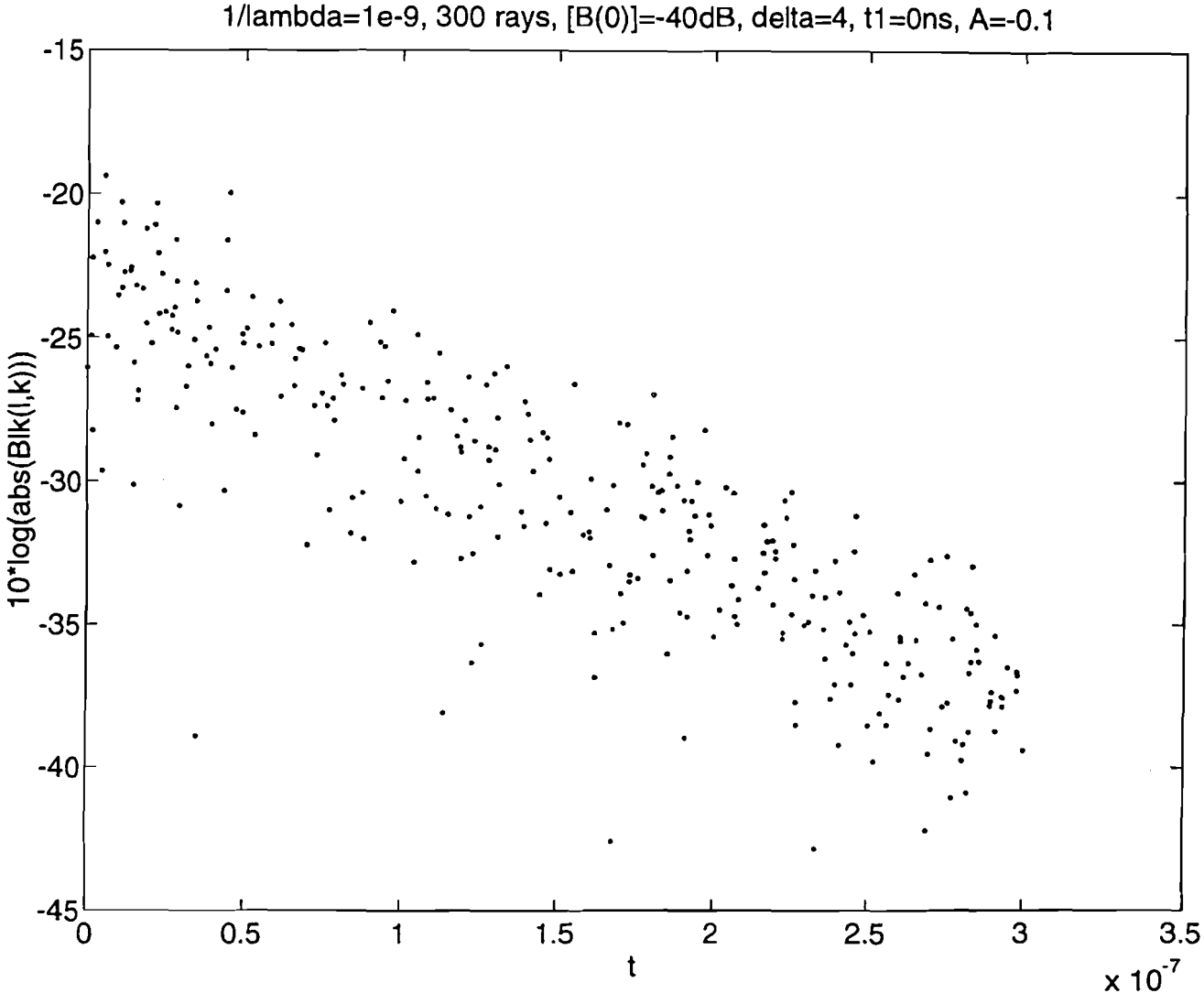

E.3 Rayleigh distributed path amplitude, presented as $|B_{lk}(l,k)|$, as function of the rounded to 1e-9 Poisson distributed arrival time

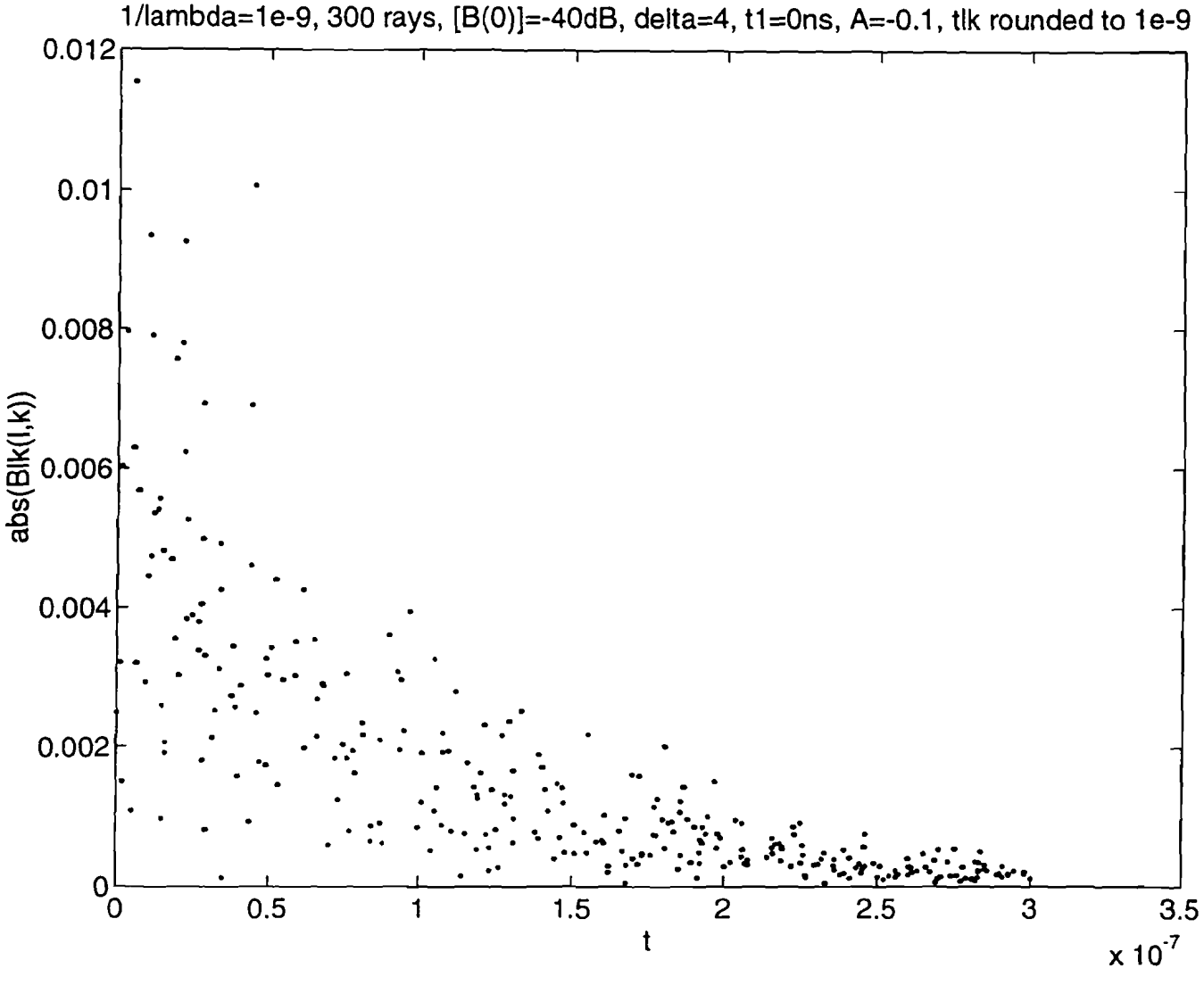

Appendix F Results signal simulations

F.1 Signal simulations for single path and varying amount of users

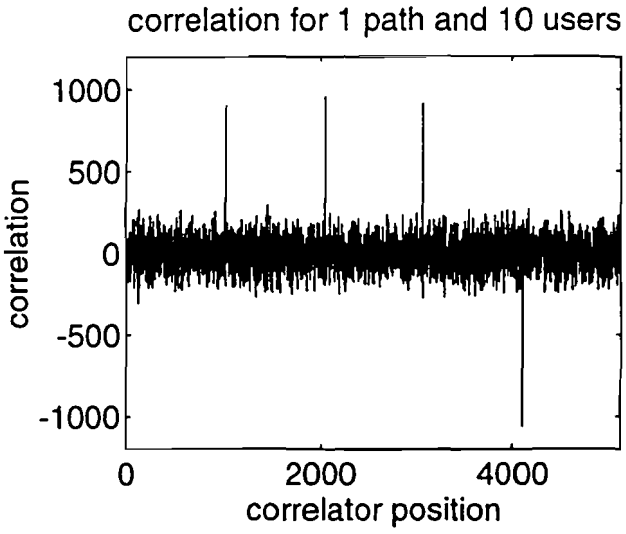

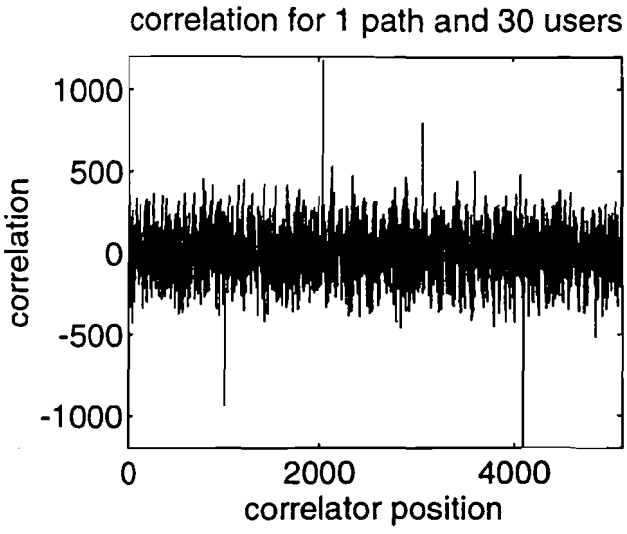

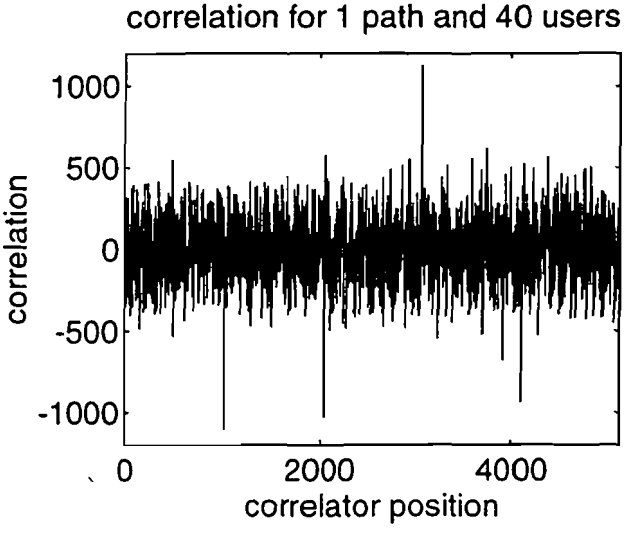

F.2 Signal simulations for ten users and varying amount of paths

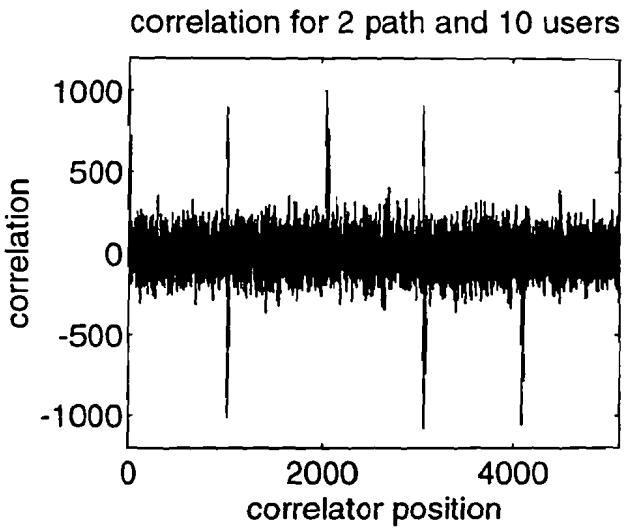

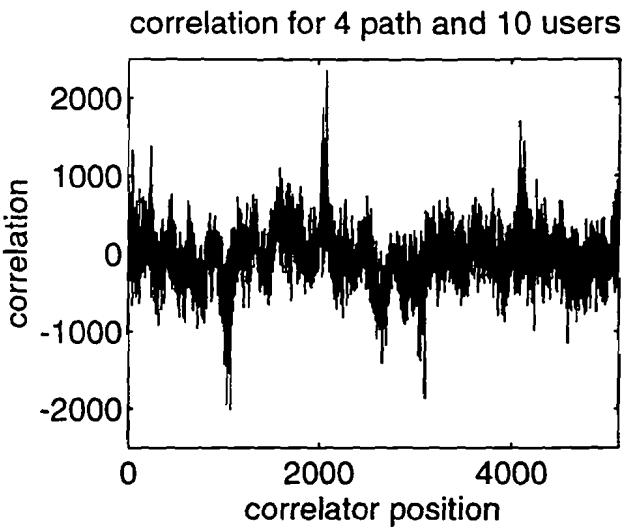

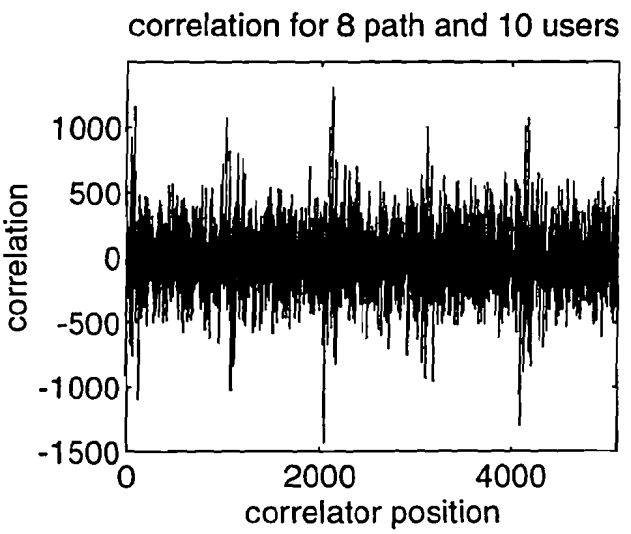

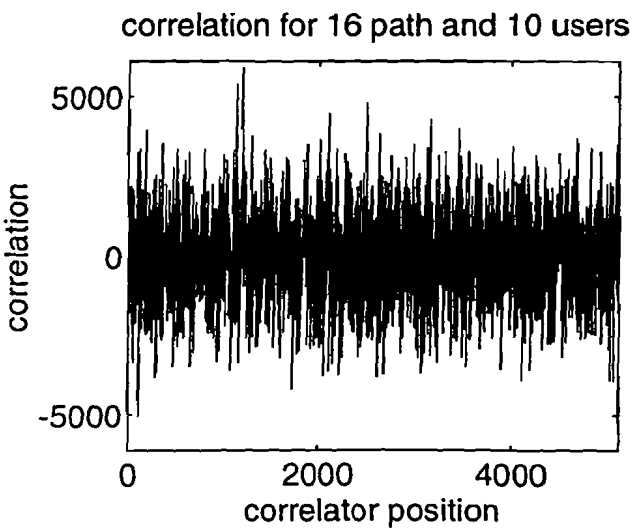

F.3 Signal simulations for ten users, two paths for a combining receiver with one and two taps

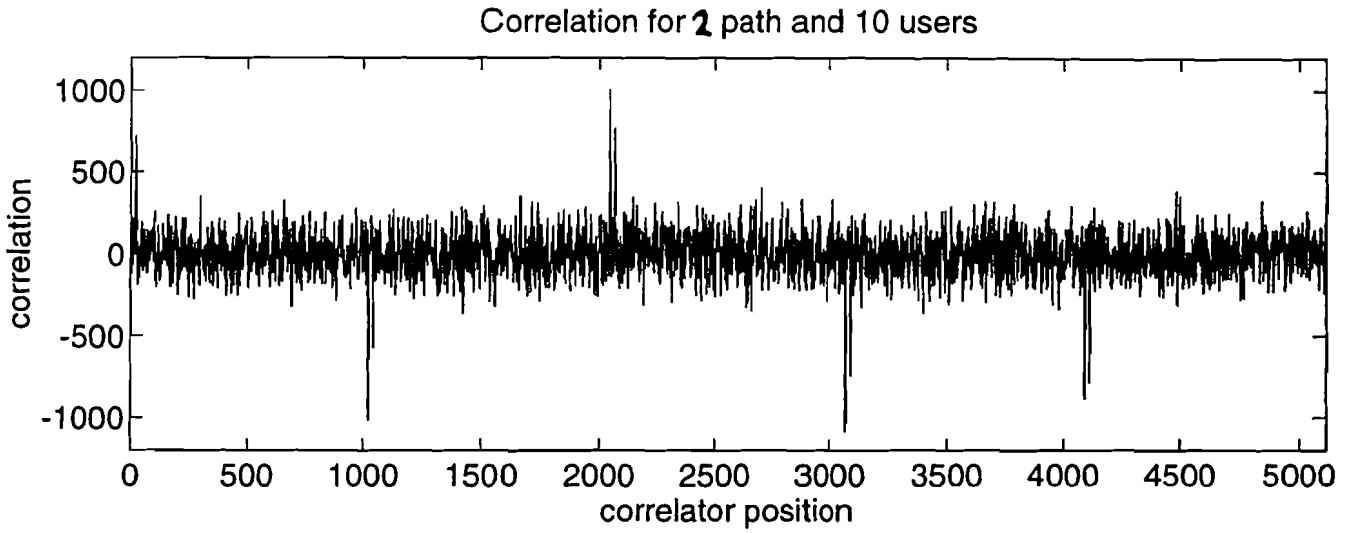

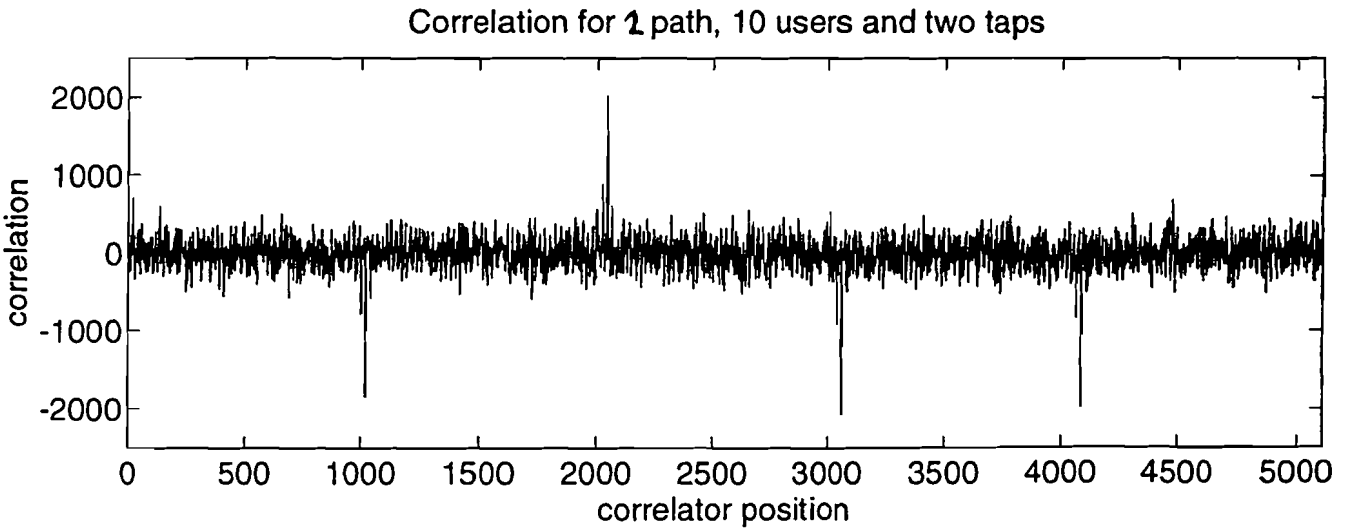

F.4 Simulations for 5 users, the multipath model with 200 rays, without RAKE receiver and with four types of RAKE receivers

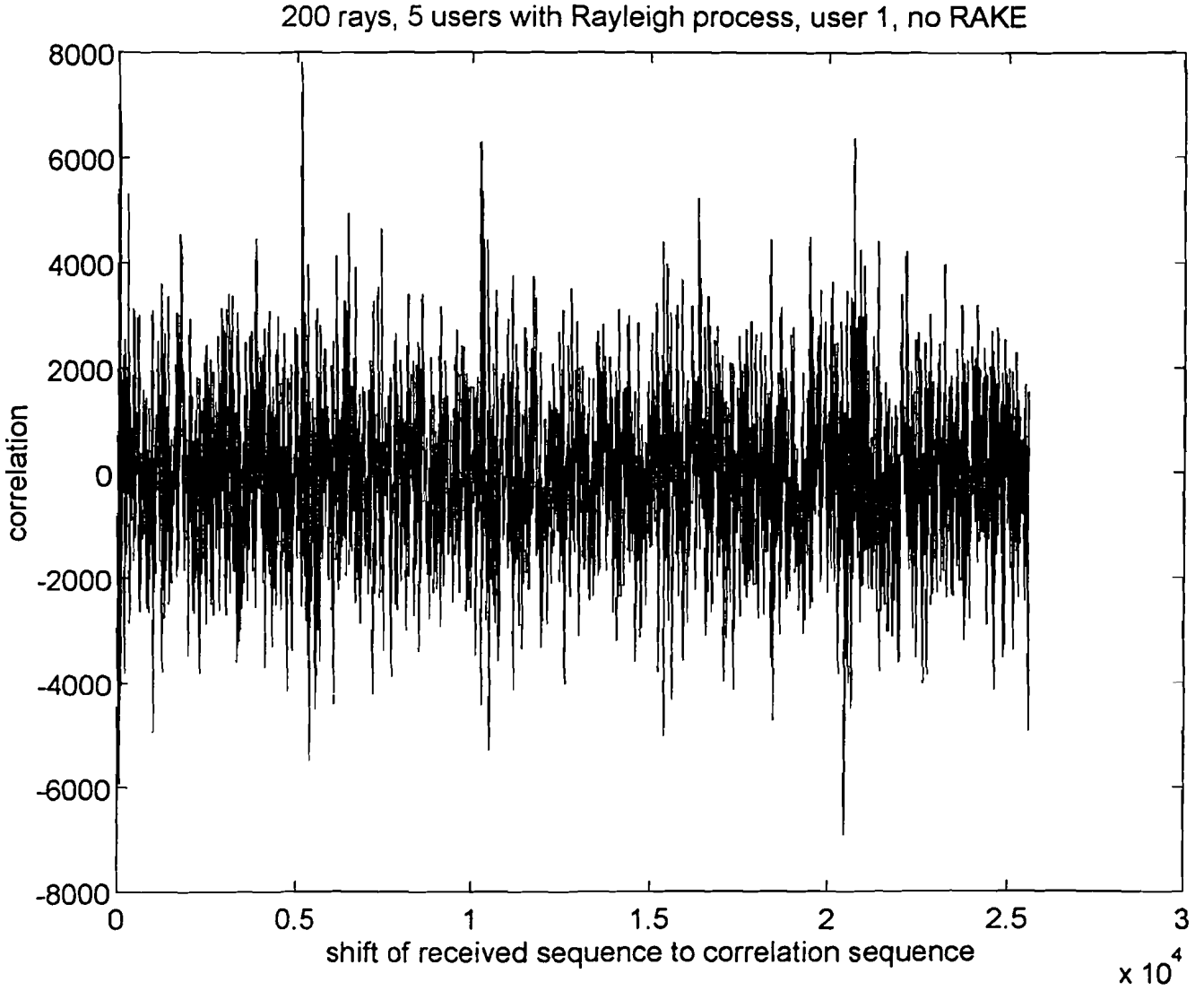

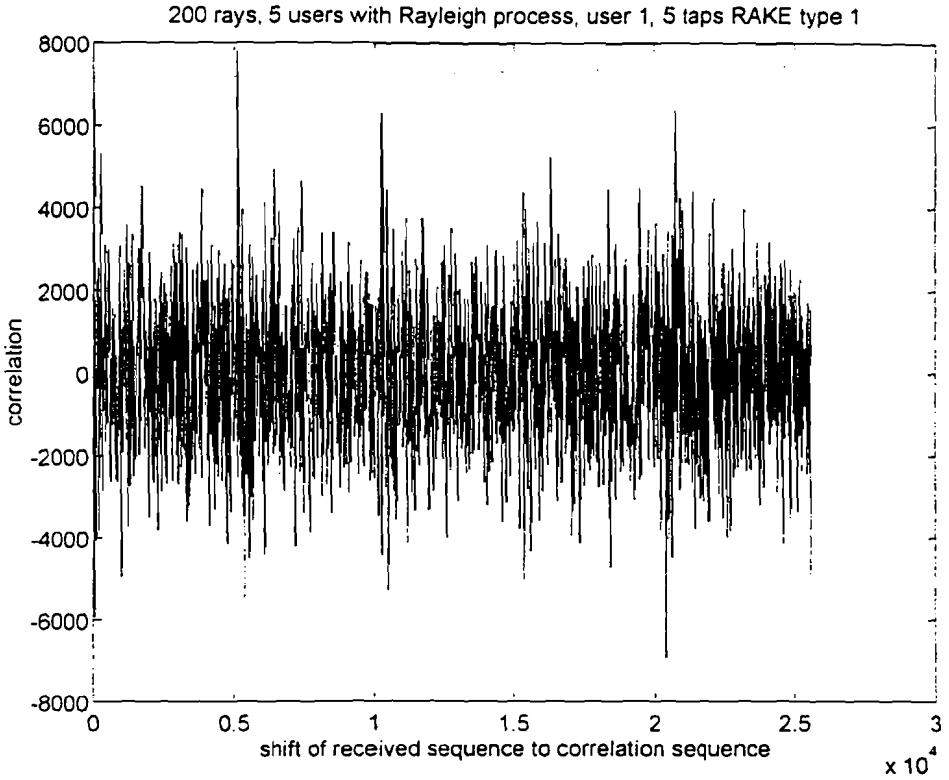
200 rays, 5 users with Rayleigh process, user 1, 5 taps RAKE type 1
correlation
8000
6000
4000
2000
0
-2000
-4000
-6000
-8000
0
0.5
1
1.5
2
2.5
3
shift of received sequence to correlation sequence
x 10^4

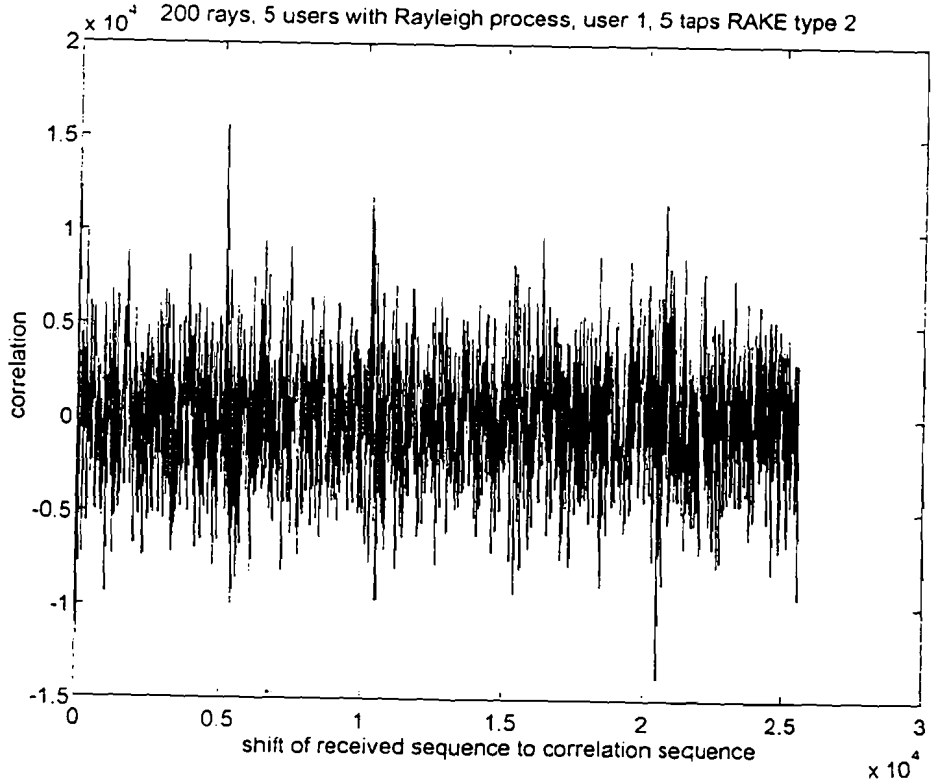
x 10^4
200 rays, 5 users with Rayleigh process, user 1, 5 taps RAKE type 2
correlation
2
1.5
1
0.5
0
-0.5
-1
-1.5
0
0.5
1
1.5
2
2.5
3
shift of received sequence to correlation sequence
x 10^4

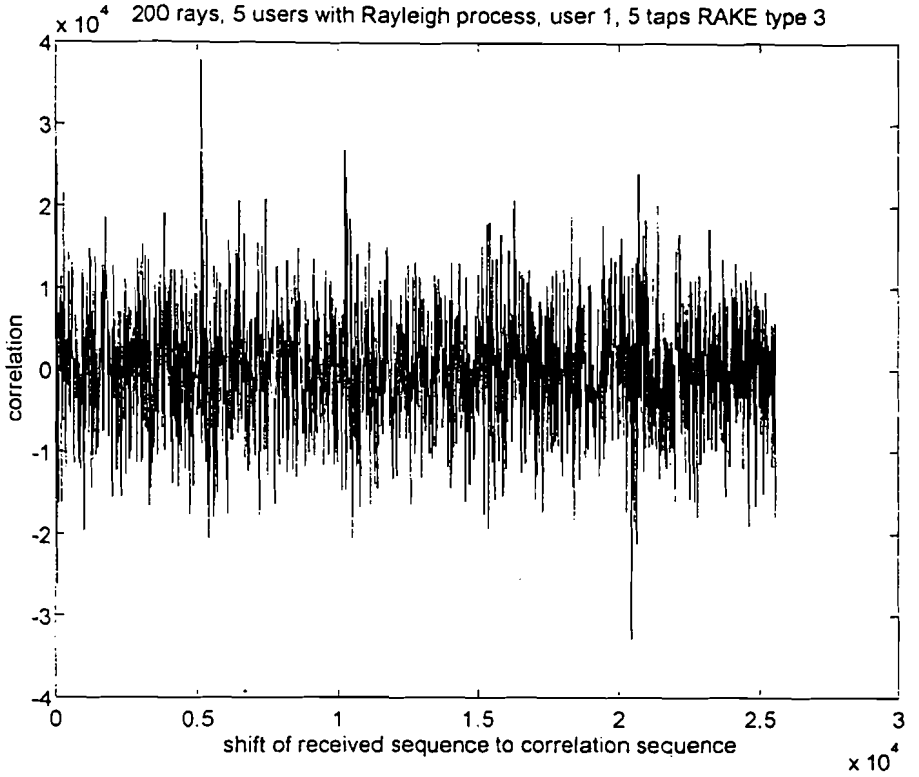
x 10^4
200 rays, 5 users with Rayleigh process, user 1, 5 taps RAKE type 3
correlation
shift of received sequence to correlation sequence
x 10^4

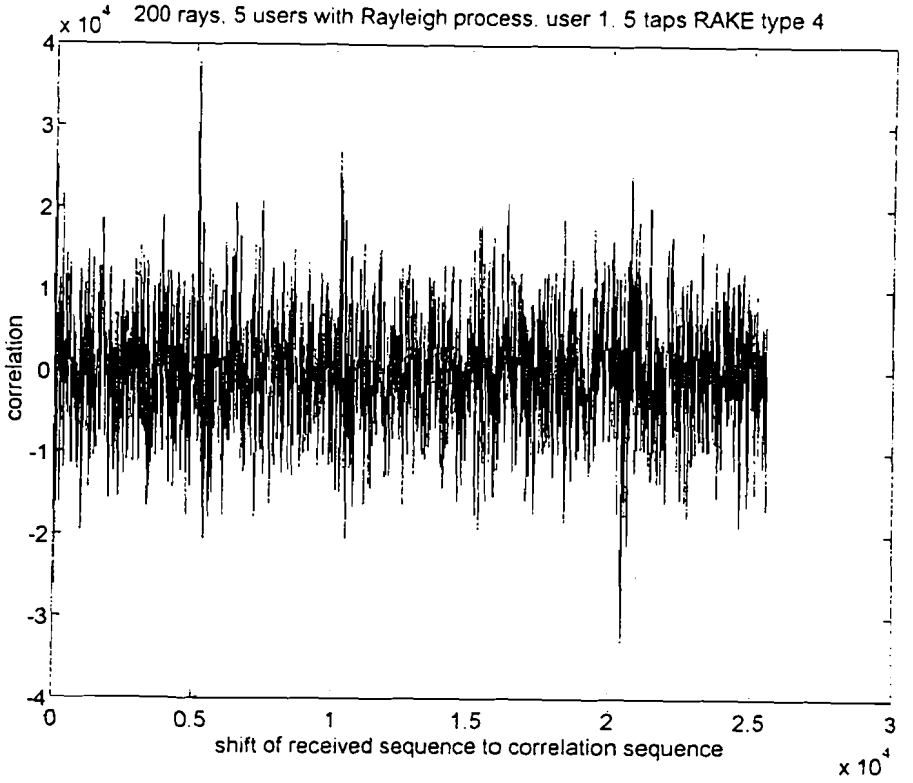
x 10^4
200 rays, 5 users with Rayleigh process, user 1, 5 taps RAKE type 4
correlation
shift of received sequence to correlation sequence
x 10^4